Bauxite Residue Disposal and the Environmental Benefit of Açaí, Soil and Gypsum Amendments

A case of study of geochemical processes and modeling in Pará, Brazil

Jorge Felipe Torres Ortiz

Master Thesis in Geoscience
Environmental Geoscience
60 credits

Department of Geoscience
Faculty of Mathematics and Natural Sciences

UNIVERSITY OF OSLO

June 2021

Bauxite Residue Disposal and the Environmental Benefit of Açaí, Soil and Gypsum Amendments

A case of study of geochemical processes and modeling in Pará, Brazil

2021

Bauxite Residue Disposal and the Environmental Benefit of Açaí, Soil and Gypsum Amendments
Jorge Felipe Torres Ortiz

http://www.duo.uio.no/

Print: Reprosentralen, University of Oslo

Abstract

Production of alumina from bauxite results in a large amount of bauxite residue. The accumulation of this hazardous material has unfavorable properties for plant growth and the closure of disposal areas is challenging. The recovery of bauxite residue disposal sites (BRDA) requires the addition of suitable amendments to achieve environmental improvement. One of the possible approaches is the application of açaí, soil, or gypsum amendments. This study focusses on a case study site in Pará—a state located in northeastern Brazil.

This thesis analyzes the leaching behavior of dissolved inorganic elements of four types of samples: bauxite residue (red mud) without amendments, and with three different amendments—açaí, soil, and gypsum in a proportion of 10%. The leaching pattern of major and minor elements, pH, electrical conductivity (EC), and acid buffering capacity were analyzed in the four types of samples in a sequential batch leaching test comprised of five steps that correspond to a cumulative liquid to solid ratio of 50:1. (i.e., 3.9 g bauxite residue, 0.03 g of amendment for 44 ml of water solution). The analytical data obtained in the batch leaching test was modelled using the PHREEQC geochemical modelling software to assess mineral equilibria and the influence of carbon dioxide on the pH and formation of secondary minerals.

The Electrical Conductivity (EC), Exchangeable Sodium Percentage (ESP), and Sodium Absorption Ratio (SAR) measurements suggest that these parameters will decrease (EC: 3.290 to 577, ESP: 19.29 to 1.52, and SAR: 17.06 to 1.90) after the 5-step sequential batch test and differ with each type of amendment. The initial and final batch leaching test results show that each of the four types of samples generally decrease the pH in a range from 11.98 to 10.92. These results imply that the high alkalinity and pH will continue under field conditions if no further actions are taken.

The dissolved fraction of Al present in this study demonstrates that in BRDA, highly mobile Al-hydroxide species are available (20 mg/l) and should be addressed for successful remediation. This is important to consider in the implementation of sustainable alternatives of bauxite residue amelioration. The pH does not need to be reduced to neutral pH, values below 9 are acceptable since the concentration of negative Al-hydroxides will be considerably reduced.

The geochemical modelling shows that the reaction of bauxite residue with carbon dioxide in the atmosphere can reduce the initial pH from 11.5 to 9.1 (these values are the average of both the first and the final batch tests with and without amendments) and with a higher concentration of carbon dioxide, usually found in the soil, pH values near 7.2 can be reached. Thus, when the formation of carbonates is taken into account, the reaction with atmospheric carbon dioxide can lead to a higher precipitation of carbonates such as calcite, dolomite, and hydrozincite when compared with the formation of carbonates caused by the reaction of carbon dioxide in the soil. These can provide a way to improve the poor environmental conditions of bauxite residue and lead to a feasible rehabilitation of the area.

Determination of the minor element composition by XRF method reveals that bauxite residue samples form Barcarena, Pará, Brazil, showed a high concentration of chromium and vanadium, 290 mg/kg and 536 mg/kg respectively. These amounts are present in the solid phase with or without amendments, representing a potential detrimental effect on plant growth in BRDAs.

Acknowledgements

I would like to acknowledge the help of my supervisor Prof. Gijsbert Breedveld and co-supervisor Dr. Sc Clara Sena for their support, knowledge, kindness, and professionalism. The zoom meetings helped me greatly, not only to study but also to add some order and structure to the working weeks. I would also like to express my gratitude to Mufak Said Naoroz and Magnus Kristoffersen who explained the details of all the lab equipment I had to use carefully and patiently. They also taught me how many skills are gained with experience and cannot be learned by reading the manual of the machines used. In addition, I wish to extend my special thanks to NGI-Hydro-UIO and NMBU for the opportunity to work collaboratively on this thesis.

None of this 2 year master's program would be possible without the unconditional support of my family members—it is completely naive to think I could do this without them. I know that maintaining a physical distance of over 9,275 km (Oslo - Bogotá) is enough for them to feel that I was not present for them, but they were always in my thoughts and whatever they needed, I would do anything for them despite living abroad in the middle of the COVID - 19 pandemic.

The idea of a scientist working alone is no longer valid. In modern scientific disciplines, such as earth sciences, the experiences of a master's program in natural sciences would not be as enriching without sharing academic achievements and defeats with my colleagues and friends from MOG (miljøgeologi) and all the people I had the privilege to meet at this time of my life. The successful completion of this master's thesis would probably not be possible without the support of Lianna Stewart who makes the international master's experience more enjoyable. Her kindness never goes unnoticed, especially in the dark and long winter days she has been ever present and has been my Norwegian sunshine ☼.

This thesis is just the beginning of a journey as an environmental geoscientist and the possibility to make a change in the interaction of humans and nature, working for the benefit of social solutions. With many more things to say but not enough space, I just want to express to each of them—I will be forever indebted to all of you.

Abbreviations

BRDA	- Bauxite residue disposal areas
CCV	- Continuing calibration verification
CEC	- Cation exchange capacity
CFA	- Continuous Flow Analysis
DOM	- Dissolved organic matter
DSP	- Desilication product
EC	- Electrical Conductivity
ESP	- Exchangeable Sodium percentage
IC	- Ion Chromatography
ICP-MS	- Inductively Coupled Plasma Mass Spectrometry
LOD	- Limit of Detection
Mt	- Unit of weight equivalent to 1000 kilograms
OC	- Organic Carbon
QC	- Quality Control
SAR	- Sodium Absorption Ratio
TOC	- Total Organic Carbon
WHO	- World Health Organization
XRF	- X-ray fluorescence

Table of contents

Table of figures

Table of tables

1 Introduction

The mining industry generates a large amount of waste that results in the destruction and degradation of huge areas of landscapes in vast geographic locations, such as those produced by aluminum mining around the world (e.g., United States, Australia, Brazil, Guyana, Jamaica, India, Venezuela, Suriname, and China) (Meyer, 2004; Moors, 2006). An acceptable metallurgical plant operation always contemplates the rehabilitation of industrial waste, which is fundamental for a good practice of a company that accepts responsibility for the environment and the communities it affects.

For the production of aluminum, the bauxite ore is processed using the Bayer process where sodium hydroxide (NaOH) is added at a high temperature (100-250˚C) and pressure (≈3.45 MPa). This results in the production of alumina (Al_2O_3) and the recrystallization of various minerals that end up in a bauxite residue—commonly known as red mud (Jones and Haynes, 2011). Alumina produced after the Bayer process can create approximately 0.5 to 2 tons of waste for every ton of alumina produced (Evans, 2016; Gräfe et al., 2011).

Globally, an estimated 3 to 4 billion tonnes (Bt) of bauxite waste is stored in large disposal areas with few sites that have been successfully remediated. In addition, bauxite residue waste increases continuously by 120 million tonnes (Mt) each year (Gräfe et al., 2011).

The management of bauxite residue is a challenging problem that causes a major concern for alumina refineries (Kong, et al., 2018). The chemical composition of bauxite residue can differ substantially. This is determined primarily by the composition of the parent rock and the subsequent refinery processing operations. The main minerals in the residue consist of iron and aluminum oxides (boehmite, gibbsite, hematite, and goethite), Na- and Ca-aluminosilicate phases (e.g., sodalite, cancrinite), and titanium oxides. Their presence is related to the inherent physicochemical properties of the bauxite residue—especially its alkalinity, alkaline groups, salinity, sodicity, and low hydraulic conductivity (Jones and Haynes, 2011). These properties limit the potential for soil formation and prospects for site closure and revegetation with native plant species at bauxite residue disposal area (BRDA).

The goal of natural environmental restoration is to reduce and neutralize the excess pH, EC, and alkalinity of the bauxite tailings. In order to achieve this, it is important to understand the

influence of the physicochemical properties of bauxite residues and the potential beneficial effect of application of different amendments to overcome the environmental risks at BRDA sites.

1.1 The present research

The main objective of this master's thesis project is to understand the effect of different amendments on bauxite residue as possible remediation methods. These techniques may improve the chemical stability of bauxite tailings and allow the material to be used as a top cover on bauxite residue sites. The focus for this study has been the site belonging to Hydro Alunorte located in northeastern Brazil.

The aim of this thesis is to contribute to a better understanding of the changes in the geochemical composition of bauxite residue that can support the potential for plant growth in the study area. Within this aim, the specific objectives of the present work are to:

I. Investigate the effects of açaí, soil, and gypsum as potential amendments of bauxite residue through a batch leaching test.

II. Understand how the characteristics of pH, Electrical Conductivity (EC), Exchangeable Sodium Percentage (ESP), Sodium Absorption Ratio (SAR), acid buffer capacity, and the major chemical composition of the bauxite residue change with amendments.

III. Build geochemical models to assess how the geochemical properties of the amended and non-amended bauxite residue will evolve in contact with carbon dioxide in the atmosphere and the soil environment.

2 Background and theory

2.1 Bauxite ore

Bauxite ore is mined worldwide in order to extract aluminum. The majority of aluminum used today is obtained from bauxite rocks. Bauxite ore is formed when lateritic soils are heavily leached. This promotes silicate weathering as a process of dissolving primary minerals and precipitating secondary minerals (montmorillonite, kaolinite, and gibbsite) normally retaining insoluble Al-hydroxides (Appelo and Postma, 2004).

The precipitation rate and mineral weathering are major factors in determining the formation of gibbsite and other Al-hydroxides. The transition of kaolinite to bauxite is a result of the increased amount of weathering products along with the amount of annual rainfall (Figure 1). This normally occurs in a tropical or humid subtropical climate, such as the one in the northeastern Amazonian Region in Brazil, ending up with the formation of bauxite ore (Appelo and Postma, 2004).

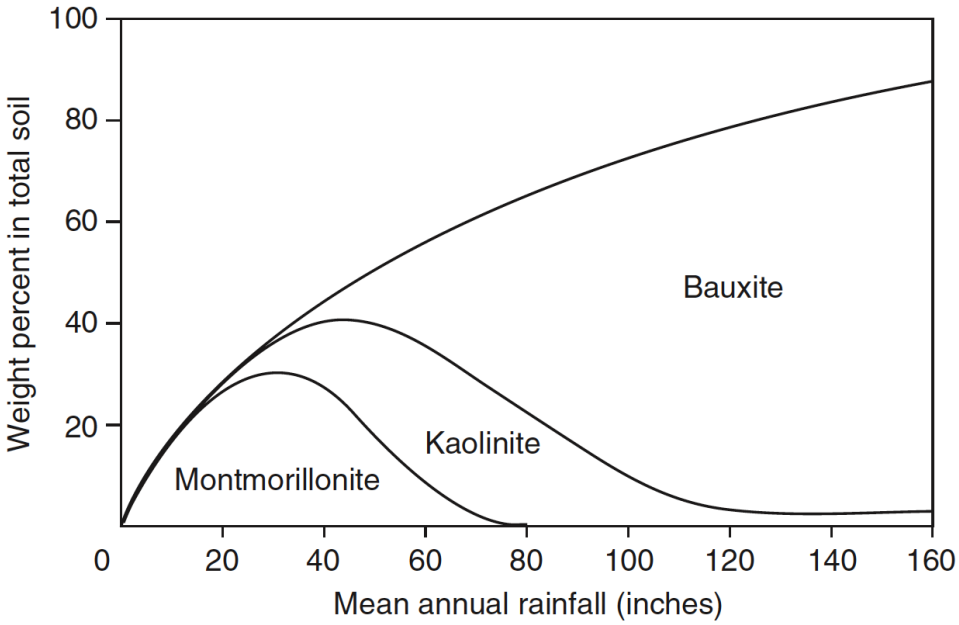

Figure 1. Weathering products on volcanic rock on the island of Hawaii as a function of mean annual rainfall. The increase in annual rainfall (inches) increased the intensity of leaching, removing silica and cations from parental rock. This promotes the concentration of Al-hydroxides mainly in bauxite content. The content of different minerals is plotted cumulatively as weight percent in total soil (Berner, 1971), modified from (Appelo & Postma, 2004).

Brazil is one of the major producers of alumina. It is the fourth largest producer of bauxite ore according to United States Geological Survey (USGS) (Table 1). Aluminum extracted from bauxite is conductive, malleable, durable, resistant to corrosion, strong, lightweight, and easy to recycle (Jones and Haynes, 2011). The demand of this commodity is annually increasing which makes this type of ore more desirable to extract. Some of the main industries that require more aluminum include construction, electronics, transport, energy, and the consumer goods industry.

Table 1. Countries producing over more than 5 million metric tons of bauxite in 2017, data from the USGS Mineral commodity, modified from (King, 2021).

Country	Bauxite ore thousands of metric tons
Australia	83.000
China	68.000
Guinea	45.000
Brazil	36.000
India	27.000
Jamaica	8.100
Russia	5.600
Kazakhstan	5.000

2.2 Properties of bauxite

2.2.1 Composition

Bauxite is a weathered rock and its composition is influenced by the parental rock. Normally, the most common elements are Fe (20-50%), Al (15-25%), Si (5-15%), Na (5-10%), Ca (5-10%), and Ti in trace amounts (Table 2). Other oxides can vary according to the provenance of the bauxite. In some cases, it is possible to find hydrogarnet, chantalite, hydroxycancrinite, and sodium titanate. The main impurities in bauxite are Si, Ti oxides, Zn, P, Ni, and V found in trace quantities (Paramguru et al., 2005).

Table 2. Mineralogical composition range (%) for bauxite ore and residue modified from (Whittington, 1996 & World Aluminum, 2015).

Mineral	Formula	Bauxite Typical range %	
		Ores	Residue
Gibbsite	$Al(OH)_3$	0 - 71	0 - 5
Boehmite	γ–AlO(OH)	0.4 - 30	0 - 20
Diaspore	α–AlO(OH)	0.2 - 60	0 - 50
Kaolinite	$Al_2O_3 \cdot 2SiO_3 \cdot 2H_2O$	2.3 - 12.7	0 - 5
Quartz	SiO_2	0 - 17.4	3 - 20
Hematite	Fe_2O_3	2.6 - 21	20 - 45
Goethite	FeO(OH)	2.4 - 13.8	10 - 30
Sodalite	$3Na_2O \cdot 3Al_2O_3 \cdot 6SiO_2 \cdot Na_2SO_2$	-	4 - 40
Magnetite	Fe_3O_4	-	0 - 8
Calcium aluminate	$3CaO \cdot Al_2O_3 \cdot 6H_2O$	-	2 - 20
Muscovite	$K_2O \cdot 3Al_2O_3 \cdot 6\ SiO_2 \cdot 2H_2O$	-	0 - 15
Calcite	$CaCO_3$	-	2 - 20
Perovskite	$CaTiO_3$	-	0 - 12
Cancrinite	$Na_6(Al_6Si_6O_{24}) \cdot 2CaCO3$	-	0 - 50
	TiO_2	0 - 6	2 - 20
	CaO	0 - 0.9	0 - 14
	Na_2O	-	2 - 8
	Al_2O_3	-	10 - 22

Note: Silica (SiO_2) contains both crystalline and amorphous phases.

The presence of dissolution-resistant minerals—such as quartz—represent more than 30 wt% in some cases, but iron oxides compromise an important fraction of 35-65 wt%. The mineral phase distribution of bauxite residue is mainly crystalline with around 5-30 wt% of amorphous-unidentified content depending on the source rock, metallurgical refinery treatment, accuracy of the analysis method, and weathering process after deposition (Whittington, 1996).

Similarly, Wik (2020) carried out an experiment using X-ray florescence (XRF) to determine the main compounds present in the bauxite residue of Brazil—approximately Fe_2O_3 (37%), AlO_3 (21%), SiO_2 (17 %), Na_2O (8.1%), and lesser quantities of TiO_2 (5.6%), CaO (1.2%), and ZrO_2 (0.8%).

Some of the physical and chemical characteristics of bauxite residue include a high bulk density ranging from 1.14 - 1.7 g/cm^3, high salinity between 7.7-36 dS/m, low hydraulic conductivity 1.49 10^{-6} m/s, water holding capacity 224 g/kg, low micronutrient content, and

availability of toxic element for plant growth (Al, As, Cr, Ni, Pb, Mo, and V) (Jones and Haynes, 2011; Wong and Ho, 1994).

Van der Sloot and Kosson (2010) and Gräfe et al. (2011) studied the porosity of bauxite residue and reported a value around 0.64. The incremental loading test performed by Schneider (2020), with the same bauxite residue sample as the one used in this work, showed a porosity range between 0.53-0.63 which is similar to the previously reported value.

Sediment textural classification, according to Wentworth (1922), categorizes bauxite residue as a silty clay loam with approximately 55% silt, 37% clay, and 8% sand (Schneider, 2020).

2.3 Bayer process

Bauxite rock is treated in a refinery using the Bayer process to extract the alumina. The Bayer process has been in use for over 130 years and only 2-3% of the annual bauxite residue is used in beneficial applications (Evans, 2015). The process contains five steps: grinding, digestion, clarification, precipitation of alumina hydrate, and calcination until it reaches the extraction of alumina. After these steps, the processing residue is placed in the bauxite residue disposal area. The following subsections are used to briefly describe each step of the Bayer process.

2.3.1 Grinding

The first step is to wash the bauxite material to eliminate any trace of contamination that can disturb the efficiency of the industrial refining process. The bauxite will then be crushed to increase the surface area. Then, when the bauxite is added to the hot sodium hydroxide, the reaction speed increases. Afterwards, the mixture is stored and the silica is partially separated from sodium hydroxide prior to digestion.

2.3.2 Digestion

In this stage, more sodium hydroxide is added and heated in an industrial digester. The goal of the digestion step is to extract the alumina. In order to achieve this, the insoluble oxides containing aluminum are separated by the reaction with sodium hydroxide. The refinery treats the bauxite mixture with temperatures ranging between 100-250˚C to dissolve gibbsite, boehmite, and diaspore—each respective mineral requiring an increasingly high temperature. The order of dissolution of these minerals differs by the strength of each mineral’s hydrogen

bond. In this procedure, is vital to reduce the amount of impurities since they may lead to less cost-efficient processes.

When soluble sodium silicates form, they react with the sodium aluminate solution and form insoluble sodium aluminum silicate. This creates a desilication product (DSP). The DSP blocks the pipes in the Bayer process and contaminates the alumina extraction. To prevent this, the refinery normally precipitates DSP before the clarification step (Jones and Haynes, 2011).

The sodium hydroxide is removed when DSP precipitates. In an effort to restrain the cost, lime is added to reduce the loss of sodium hydroxide which represents 20% of the cost of production. Then, the hydrated lime reacts with sodium carbonate and forms calcium carbonate and sodium hydroxide. Aluminosilicates are present in the digestion step, normally dominated by sodalite ($Na_8(Al_6Si_6O_{24})Cl_2$) and cancrinite ($Na_8(Al_6Si_6O_{24})\cdot 2(CaCO_3)$) (Freire et al., 2012; Pan et al., 2015).

2.3.3 Clarification

The bauxite residue is detached from the other dissolved compounds by supersaturated sodium aluminate in the sodium hydroxide solution. The first step separates the coarse particles simply by gravitational force. In the second step, the major amount of hydroxide solution is recycled.

The residual mud that is transported to the disposal storage area contains significant amounts of DSP, non-reactive silicate, Fe-Ti Oxides, and traces of heavy metals. But, due to the high alkalinity, some of the heavy metals are in mobile form (V, Cr, and As).

2.3.4 Precipitation

The bauxite with sodium hydroxide and lime is mixed with small amounts of aluminum trihydrate ($Al_2O_3 3H_2O$) to produce precipitation of alumina. This catalyzes crystallization and growth of aluminum minerals. In the precipitation process, the course fraction is separated and sent to the next step (calcination) and the fine particles are reused to increase the effectiveness of alumina extraction.

2.3.5 Calcination

In this step, the drying hydroxide alumina is removed. Then, water is added and heated to around 1100˚C to extract the alumina (Eq.1) with a mineral texture of sand. This is the main ingredient for aluminum smelters.

$$2Al(OH)_3 \rightarrow AL_2O_3 + 3H_2 \qquad (Eq.1)$$

Some elements do not dissolve and remain present in the red mud while others are soluble in the Bayer process and interact with the aluminum hydroxide and lime in the refinery. The final concentration may vary depending on the temperature and pressure used, increasing or decreasing in the bauxite residue (Table 2).

2.3.6 Bauxite residue disposal and storage

In the aluminum industry, one of the main concerns is the treatment and use of bauxite residue. Normally, there are not many economically viable uses for this material. The disposal contributes to approximately 5% of the operations of alumina refinery costs and around 45% of the operations are directly related to the disposal and storage (Kumar et al. 2006).

Bauxite processing generates a residue—known as red mud—approximately 0.5-2 tons per ton of alumina produced (Al_2O_3) (Kong, et al., 2018). Management of this residue provides a tremendous environmental risk associated with the land-based bauxite residue disposal areas (BRDAs). This includes contaminated run-off water, dispersal of alkaline dust by wind, absence of any kind of vegetation, and degraded esthetic visual landscape.

There are several specific disposal procedures and storage methods. Environmental regulations, available space, and economic profitability for the company are all determining factors for choosing an effective method.

The main disposal procedures are dependent on whether the transport is wet or dry and which technology is used by the refinery.

In the case of wet transport, various techniques can be found:

- Abandonment of waste: The aluminum refineries dispose the bauxite residue on land and abandon it without any treatment to reduce the risk of potential contamination in the groundwater and surroundings.

- Solar drying: The wet red mud is deposited on slopes with a low inclination near to 5% and it is dried by the continuous solar radiation which is useful in a hot dry climate without rainy periods.

- Conventional method: The bauxite waste is thickened by the extraction of the remaining sodium hydroxide and the remaining diluted slurry is deposited in an impoundment area (a dam with a clay seal to avoid leakage of hazardous contaminates) (Nguyen and Boger, 1998).

- Drained method: Similar to the conventional method, this method uses a consolidated fast material which reduces the groundwater contamination and improves the area in which the bauxite residue needs to be deposited.

In the case of dry transport, the method of dry residue disposal is used. Highlighted in this case study, Alumina do Norte do Brazil implements the dry cake disposal method to dewater residue mud by filter presses and produces a thickened cake (Cooling, 2007; Nguyen and Boger, 1998). The thickened cake is transported by belt to be dried and packed in the BRDA, reducing the spaces required and possibility of leaching into groundwater. One of the limitations of this method is that the environmental conditions need to be optimal to dry each layer before the next cake layer is deposited (Cooling, 2007; Witt and Schönhardt, 2004). In this region of Brazil, the annual precipitation in Belém is around 3084 mm (INMET, 2020) which are not beneficial conditions for successfully operating a residue disposal area. This will be discussed in further detail in the section 3: The study site.

2.4 The remediation of bauxite residue disposal area

If bauxite residue is not treated, the following environmental circumstances occur (Bray et al., 2018; Jones and Haynes, 2011):

- High alkalinity conditions with pH between 10-12.5

- Low porosity
- Elevated salinity (EC=30-60 dSm^{-1})
- High sodicity (ESP%=50-90)
- High electrical conductivity (EC=60-50 mS/cm)
- Lack of bioprocesses (Organic Carbon (OC) less than 0.3%)
- Elevated concentration of toxic elements for plants (V, Cr, As, and Al).

These side effects of BRDAs can persist for more than 30 years. This demonstrates the importance of addressing the physio-chemical properties of the disposal areas in the production of alumina. Remediating affected sites on a global scale reinforces the necessary conditions for suitable plant growth. This is vital for a sustainable extraction of aluminum that all humans are responsible for.

The most significant barrier to remediate a BRDA is the high alkalinity. Scientists are focusing their efforts on different techniques to reduce the pH from a range of 11-12. The goal is to eventually achieve a pH below 9. If this goal is achieved, plants can grow without being hindered by the unfavorable conditions listed above. According to several studies, the main remediation pathway would be bioremediation which aims to reduce the sodic content of the bauxite residue in the upper layers of the BRDAs. A reduction will improve the chemical and physical stability in the short and long term (World Aluminum, 2015).

2.4.1 Amendments for bauxite residue

During several decades of extraction of alumina from bauxite ore, the industry has established the need of direct revegetation of the bauxite residue. This can be achieved with different rehabilitation methods to guarantee the growth medium for sustainable microbial and vegetation.

In this thesis, the in-situ remediation strategies could be implemented using possible viable materials. The implementation of açaí seed (e.g., increase the OC), soil (e.g., reduced dust and waterlogging), and gypsum (e.g., extracted Na concentration) will aid in reducing the high alkalinity (pH between 10-12.5) to reach values under 9, EC <4000µS/cm, salinity, and sodicity.

2.4.2 Salinity and sodicity

Salinity refers to the amount of dissolved salt content in water, such as the total dissolved solids (e.g., Na, Mg, K, Ca, Si, Cl, F, Br, SO4, and NO_3). If the concentration is too high, it can negatively affect the root zone which restricts plant growth. In extreme conditions, excess salt in the root zone makes it difficult to extract water from the soil regardless of the amount of water in present in this zone (Seilsepour et al,. 2009).

The electrical conductivity (EC) is the ability of a material to transmit electrical current in dissolved ions. This measurement is directly related to the concentration of salt in the soil solution. Therefore, soil salinity can be determined by measuring EC.

Sodicity is determined by the amount of Na present in a solution and can be categorized by the exchangeable sodium percentage (ESP) and the sodium adsorption ratio (SAR). The SAR is used to estimate the ESP without the need to determine the total cation exchange capacity (CEC). Both empirical formulas measure the sodium content in relation to the major ions, calcium, and magnesium in meq/l (Eq. 2 - 3). Normally, there is a relationship between ESP and SAR, but it is not always constant and should ideally be determined directly for the specific soil that is studied (Seilsepour et al., 2009).

$$SAR = \frac{[Na^+]}{\sqrt{([Ca^{2+}] + [Mg^{2+}])/2}} \qquad (Eq. 2)$$

$$ESP = \frac{[100 \cdot (-0.0126 + 0.01475 \cdot SAR]}{[1 + (-0.0126 + 0.01475 \cdot SAR]} \qquad (Eq. 3)$$

Saline soils are classified using the U.S. Salinity Laboratory Staff system (1954) (Table 3). Sodic soils are low in total soluble salts but high in ESP, which means that soil particles are dispersed and ultimately destroy the soil structure vital for plant growth (Franzen and Wick, 2021). The most basic solution to address these detrimental soil conditions is to increase the drainage capacity so that salts can leach out of the soil system (Seelig, 2000).

Table 3. U.S. Salinity classification system 1954. Modified from (Franzen and Wick, 2021).

Classification	EC (µS/cm)	SAR	ESP (%)	pH	Soil Physical Condition
Sodic	< 4000	> 13	> 15	> 8.5	Poor
Saline	> 4000	< 13	< 15	< 8.5	Normal
Saline-Sodic	> 4000	> 13	> 15	< 8.5	Normal

In a study conducted by Gräfe et al. (2011), it was shown that ESP% and SAR values in bauxite residue are between 32-91 and 31-673 respectively. Regarding management techniques for sodic soils, such as red mud, it is necessary to replace the excess sodium in the CEC with a significant amount of calcium (usually with the use of gypsum) before starting the leaching process. Both saline and sodic soils require good soil drainage and a low groundwater level. When Na^+ is replaced by Ca^{2+} at cation exchange sites, Na^+ reacts and forms sodium sulfate (Na_2SO_4) which is subsequently leached (Seelig, 2000).

3 The study site

3.1 Provenance of the bauxite

Located in the northeast part of the state of Pará, Brazil, the bauxitic province of Paragominas has a size of approximately 50.000 km^2, making it one of the most extended bauxite deposits in the Amazon in Brazil (Figure 2). Due to the large extension, it can contain the metallurgic reserves of more than 20.000 Mt (Kotschoubey et al., 2005). Because of the elevated demand of aluminum in the world market, Brazil has the commodities to provide this essential metal supply. However, the extraction of aluminum disrupts the landscape and natural environment. This is exemplified in Figure 2, which shows a bauxite deposit extraction of approximately 12 km^2.

Figure 2. Mineração Rio do Norte (MRN) has 22 bauxite deposits, sand tailings, and dams. The companies still intend to expand their extraction areas (>12 km^2). Hydro has 5% of this bauxite mining in Oriximaná, Pará, Brazil. -Photo: Carlos Penteado, coordinates 1°40'52.2"S 56°26'28.7"W.

These bauxitic deposits are situated on top of silicate clastic rocks with two differentiating horizontal profiles. The first one is a gibbsitic horizon and the other horizon is rich in iron. These distinctive horizons show the dynamic evolution of a more developed residual layer.

Due to long lasting physical-chemical processes (weathering and precipitation), the dissolution of kaolinite produces a migration of Fe and Al resulting in the enrichment of the Al-hydroxides present in the bauxite rock (Kotschoubey et al., 2005).

According to various geological and geochemical studies, a 5-stage polygenetic model of bauxite formation is determined:

1. Laterization of saprolite.
2. Iron-aluminum crusting formation.
3. First phase of gibbsite formation.
4. Second phase rework of the crust and formation of ferruginous gravel.
5. Second phase of gibbsite formation and bauxite of the upper part of the crust.

3.2 Paragominas-Capim (Pará)

Mature bauxite, which contains well-defined and varied horizons, is present in the Amazonian laterites. This mature bauxite consists of reddish sandstones (high iron content) and yellowish argillaceous sandstones (high clay content). These two types of sandstone are autochthonous and allochthonous, both from the parental rock that belongs to the Alter do Chão and Itapecuru Formation. Rocks of these types belong to the Cretaceous period.

A distinctive range of minerals are formed in mature bauxite including: hematite, goethite, goethite with aluminum and maghemite, kaolinite, gibbsite, smectite, illite and Mn hydroxides with different textures such as concretions, ferrous nodules, and iron horizons (Costa, 1991).

Bauxite is extracted from laterite deposits, in this case, from Paragominas-Capim (Pará). Normally, the superficial layers (5 meters beneath the ground) of the deposit are mined in the Trombetas and Paragominas mines. The method of transport to the refinery is different for both locations. For the Trombetas site, the bauxite is shipped by boat and processed in the refinery following rigorous steps (Bayer process). In the case of the Paragominas site, the bauxite is ground and mixed with water; it then travels through an approximately 200 km-long pipeline to the Hydro Alunorte refinery (Figure 3).

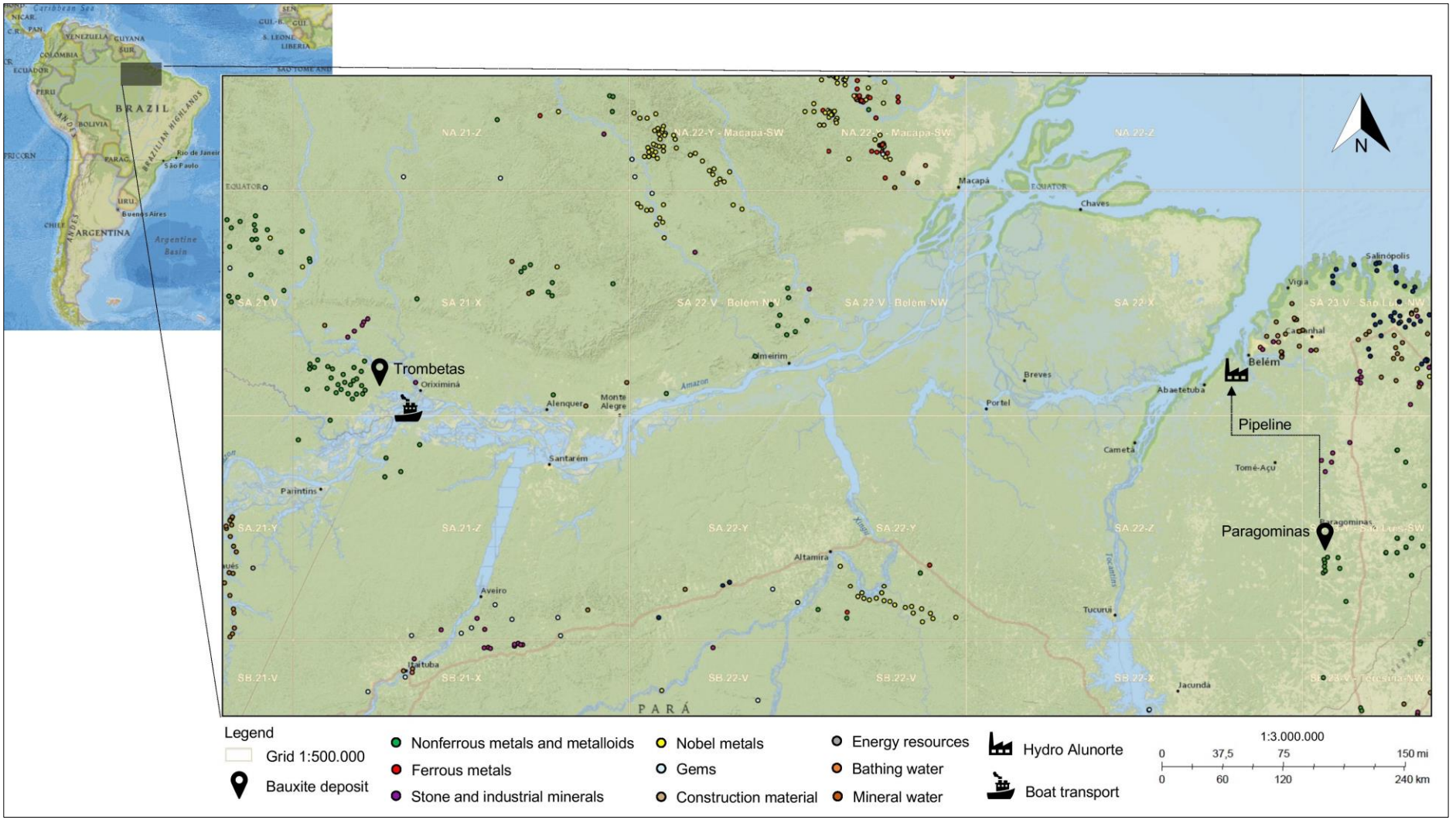

Figure 3. Laterites ore such as bauxite are included in nonferrous metal and metalloids legend, Serviço Geológico do Brasil -SGB-CPRM; National Geographic, Esri, Gamin, HERE, UNEP-WCMC, USGS, NASA, ESA, METI, NRCAN, GEBCO, NOAA increment P corp, 2021

3.3 The geographic location of samples

The alumina refinery is located in northeastern Brazil, situated in the state of Pará. It is 25 km from the state capital, Belém, with an annual average temperature of 27˚C, and precipitation of 3084 mm (Medeiros et al., 2017; INMET, 2020). This refinery incorporates a red mud (the by-product of alumina production) disposal area of approximately 2 km^2 (Figure 4). Prior to deposition, the bauxite residue is dewatered with a filter press to reduce the moisture content. It is then transported by an industrial belt or truck. Finally, it is deposited in the bauxite residue disposal area (BRDA). Figure 5 shows the location where the samples were extracted at the end of the filter press from the bauxite residue material used for the experiment of this study. In addition, it is possible to see the size of the first BRDA (about 2 km^2) that has reached the maximum storage capacity and the formation of a second BRDA.

In the municipality of Barcarena, possible environmental contamination is found near the multinational mining industry. One of these companies apart of the mining industry is Hydro Alunorte. Environmental challenges could lead to legal actions against mining companies in the city of Barcarena, state of Pará (MA-PA/MPF-PA, 2015).

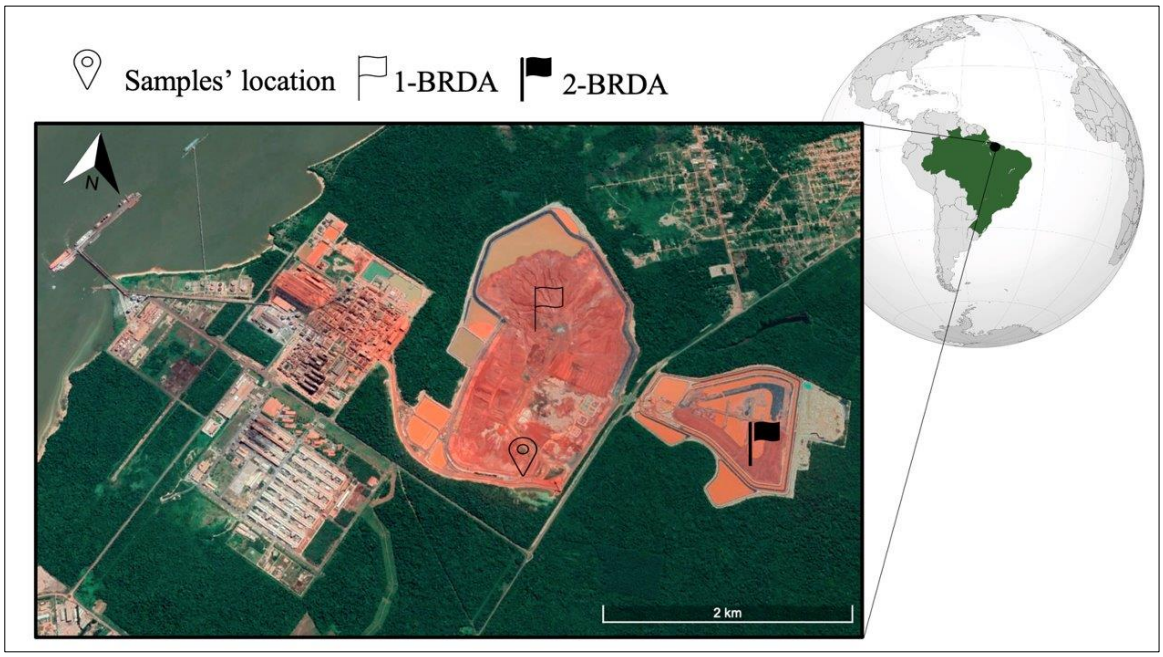

Figure 4. The alumina refinery: Alunorte Barcarena located in the northeast of Pará, Brazil showing the bauxite residue disposal area (BRDA) and location of the extraction samples with the coordinates 1°33'04.2"S 48°42'58.6"W, modified from Image 2020 © 2020 Maxar Technologies & Terra Metrics with Natural Earth Data.

4 Materials and methods

4.1 Materials

4.1.1 Bauxite residue and amendments

In 2019, new bauxite residue was sampled and used in this thesis. The material comes from the end of the pumping pipeline of the filter press prior to its passage through the disposal area. About 20 kg of bauxite residue was shipped to Oslo, Norway and a portion was stored in plastic containers and refrigerated at 6 C° at the Department of Geosciences at the University of Oslo. The physicochemical characterization of the same bauxite residue without amendments was also used in the works by Schneider (2020) and Wik (2020). This previous studies determined the basic knowledge of the red mud and, in this thesis, their findings will be useful in understanding the behavior of red mud with the inclusion of amendments.

The amendment materials used in this work (Table 4) were obtained at the Norwegian University of Life Sciences (NMBU) in collaboration with Hydro and the Norwegian Geotechnical Institute (NGI). Soil and açaí, originally obtained in the state of Pará, were chosen due to their availability in the vicinity of the refinery plant in Barcarena. Despite its inexistence nearby, a third amendment material (gypsum) was chosen due to its wide application in Ireland and Australia (Bray et al., 2018).

Table 4. Characteristics of pH, EC, total carbon, total nitrogen, and carbon/nitrogen ratio of amendments and Alunorte bauxite residue used in this study.

Materials	pH	EC (mS/Cm)	Tot. C (%)	Tot. N (%)	C/N (%)
Açaí seed	5.37	1.39	46.22	1.04	44.53
Soil	6.61	2.68	0.73	0.06	11.71
Gypsum	7.35	2.15	-	-	-
Bauxite Residue	12.31	3.45	-	-	-

This material was used to perform a sequential batch leaching test and subsequent geochemical analyses. The sample codes used are bauxite residue (BR), açaí (A), soil (S), and gypsum (G) for the respective analyses. Prior to explaining the batch test and geochemical model, the next subsections provide a brief description of each amendment used in this study.

4.1.2 Açaí seed

Euterpe oleracea is a type of palm tree known as açaí that produces a tropical fruit widely consumed in the Amazon region. The extraction processes of açaí pulp produces a large volume of waste, mainly composed of seeds rich in lipids, fibers, and fatty acids (Melo et al., 2021).

Açaí seed can be used to ameliorate the BRDA. This is because it is a green waste and it is affordable to produce in large quantities. Bauxite residue not only presents toxic levels for plant growth with Al, but it also contains nutrient deficiencies (P, K, Mn, Zn, and N) essential for plant growth (Table 5). The açaí seed waste is rich in organic matter which aids in rehabilitation strategies. When açaí seed is compared to bauxite residue, it presents lower concentrations of minor elements such as Cr and Pb that have potential to be toxic for restoring BRDAs (Table 6).

Table 5. Major elements of bauxite residue, açaí, and soil composition. Modified from (Y. Silveira 2020 unpublished).

Materials (g/Kg)	Na	Mg	Al	P	K	Ca	Mn	Fe	Zn
Açaí seed	0.04	0.42	0.25	0.78	3.1	0.6	0.14	0.26	10
Soil	0.11	0.13	49	0.04	0.2	0.38	0.03	10	8.85
Bauxite Residue	63	0.12	94	0.23	0.14	7.7	0.07	190	0

Table 6. Minor elements of bauxite residue, açaí, and soil composition. Modified from (Y. Silveira 2020 unpublished).

Materials (mg/Kg)	B	Cr	Cu	Cd	Hg	Pb
Açaí seed	7.05	3.25	8.6	0.03	<LOD	0.15
Soil	3.75	39.5	2.3	<LOD	0.12	6.1
Bauxite Residue	4.6	200	4.9	<LOD	0.94	64

Note: limit of detection (LOD)

These natural characteristics create and maintain a suitable soil structure with organic matter accumulation, enhance soil formation, and create nutrient release/fixation. Additionally, the higher concentration of Mg in açaí (compared with bauxite residue) can displace exchangeable Na, decreasing the ESP which increases the cation exchange capacity (CEC) (Hue, 1995).

4.1.3 Soil

Aligned with Hydro's objective of sustainability and profitability, in-situ soil is one of the most cost-effective rehabilitation designs as it reduces dust generation, water pollution, improves visual impact, and increases macro and micronutrients retention capacity. Nevertheless, due to the geographical location of the refinery (Figure 5), the soil's actual availability has to be taken into account. In this specific location, it is a challenging method of rehabilitation because obtaining the in-situ soil changes the natural conditions of the extraction site. However, without the soil surface cover, it can generate long term problems of dust and water infiltration among other difficulties. In theory, this is considered to be a cost effective method, but previous studies estimate for BRDA 100K €/ha in the EU, making for an additional challenge (Bray et al., 2018).

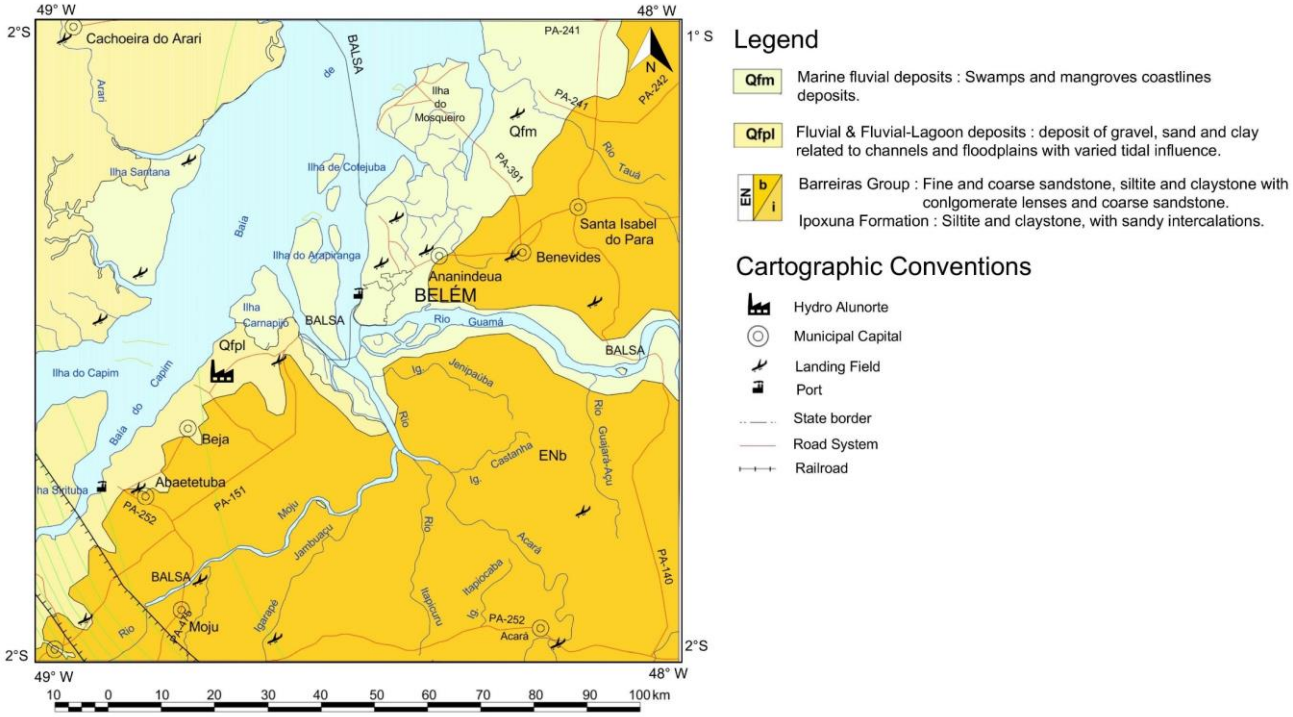

Figure 5. Map of Quaternary deposits that includes Hydro Alunorte aluminium refinery, modified from; Serviço Geológico do Brasil -SGB-CPRM; NOAA increment P corp, 2021.

The re-vegetation strategies for bauxite residue include implementing a soil layer over the red mud deposits which could reduce the water holding capacity. This promotes environmental conditions for a sustainable ecosystem. A soil cover protects the tailings from wind and water erosion and provides a cleaner surface capable of supporting microorganisms (Jones and Haynes, 2011).

Depending on the depth of the soil, the vegetation can vary. For example, a shallow soil (20 cm) can primarily support grass cover, while a deep soil (200 cm) cover can support a more varied and diverse vegetation composed of trees, bushes, and grasses. However, this requires considerable amounts of transport and there is a limited availability of the soil (Wehr et al., 2005, 2006; Wong and Ho, 1991).

4.1.4 Gypsum

In an ideal case of study, one of the best chemical amendments would be the use of gypsum ($CaSO_4 \cdot 2H_2O$) powder. Gypsum can decrease exchangeable sodium concentration, leaching the Na concentration, and release Ca^{2+} ions that will precipitate with carbonate to form possible calcite mineralization. These reactions can reduce the pH and, in turn, reduce the availability of Al in solution. Due to the low economic feasibility of this material in Hydro Pará, it is necessary to consider other, more practical solutions like açaí seed and in-situ soil. Nevertheless, it is valuable to obtain the amendment information and compare it with the other amendments selected for this study.

This study contributes to the development of feasible amendments of bauxite residue disposal areas. Integrating the knowledge of previous studies and the implementation of new techniques that will ameliorate the poor quality of BRDAs.

4.2 Batch test

The batch procedure is performed according to the guidance regulations of the United States Environmental Agency (U.S.-EPA) method—liquid-solid partitioning as a function of liquid-to-solid ratio in solid materials. This experiment follows the quality control (QC) acceptance criteria of the chemistry laboratory at the Geology department of the University of Oslo.

This method is intended to provide the pH, EC, acid buffer capacity, and chemical equilibrium distribution achieved in the liquid to solid (L/S) ratio. Changes using natural amendments are considered as part of the assessment of both environmental leaching and the effectiveness of site treatment and remediation.

In this case, there is no need for a particle size reduction procedure due to the type of samples that can approach liquid-solid equilibrium without this procedure. Nevertheless, the moisture content in the bauxite residue and the three amendments need to be measured with the

intention that the liquid-solid ratio is referring to the weight of the dry solid material during the whole experiment (Figure 6).

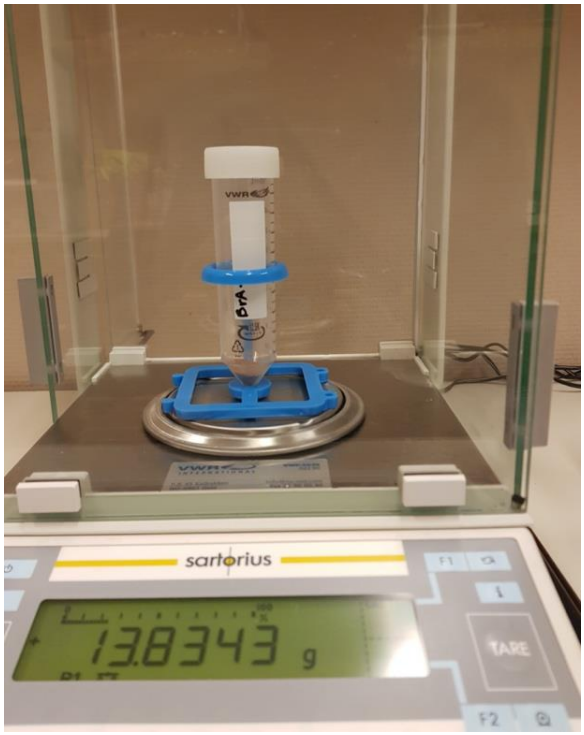

Figure 6. Measuring the weight of bauxite residue to determine the soil moisture content, taking into account the weight of the tube samples.

The moisture content is determined using Eq. 4, three replicates of 5 g of bauxite residue, and duplicates of 2 g of each amendment (Table 7). The samples were dried at 100 C° for 24 hours. Afterwards, the samples of soil and gypsum were sieved until they reached 250 micron meters.

$$Water\ \% = \frac{sample_{wet} - sample_{dry}}{sample_{dry}} \cdot 100 \qquad (Eq.\ 4)$$

Table 7. Water samples content before drying, different from those used in the L/S ratio.

Samples	Wet Weight (g)
BR1	14.06
BR2	14.13
BR3	14.04
Açaí seed 1	10.82
Açaí seed 2	10.83
Gypsum 1 G-250	10.70
Gypsum 2 G-250	10.80
Soil 1 G-250	10.79
Soil 2 G-250	10.78

4.3 Sequential batch leaching test

Five sequential leaching steps were made with triplicates for all samples: bauxite residue without amendments and bauxite residue with each of the three amendments (Table 8). The percentage of amendment used is 10% of the dry weight of the bauxite residue, in this case the initial liquid-solid ratio is 10:1, with 3.9 gr of fresh bauxite residue and 0.4 ± 0.03 gr of amendment (Appendix 1).

Table 8. Leaching steps with their respective amount of days and type of amendments. This table summarizes the calculated L/S ratio for each step. Mean ± standard error values are shown (n=3).

Leaching Step	Days	Amendment	L/S (per week)	L/S (cumulative)
1	7	None	10.05 ± 0.05	10.05 ± 0.05
		Açaí	10.02 ± 0.03	10.02 ± 0.03
		Soil	10.02 ± 0.01	10.02 ± 0.01
		Gypsum	10.02 ± 0.01	10.02 ± 0.01
2	14	None	10.03 ± 0.01	20.07 ± 0.05
		Açaí	10.03 ± 0.04	20.04 ± 0.07
		Soil	10.09 ± 0.04	20.11 ± 0.04
		Gypsum	10.02 ± 0.01	20.03 ± 0.02
3	21	None	10.03 ± 0.03	30.10 ± 0.03
		Açaí	10.04 ± 0.09	30.08 ± 0.15
		Soil	10.02 ± 0.02	30.12 ± 0.03
		Gypsum	10.05 ± 0.04	30.08 ± 0.05
4	28	None	10.03 ± 0.03	40.13 ± 0.03
		Açaí	10.04 ± 0.09	40.11 ± 0.24
		Soil	10.02 ± 0.02	40.14 ± 0.04
		Gypsum	10.05 ± 0.04	40.13 ± 0.09
5	35	None	10.02 ± 0.01	50.15 ± 0.05
		Açaí	10.03 ± 0.03	50.14 ± 0.27
		Soil	10.07 ± 0.06	50.21 ± 0.04
		Gypsum	10.02 ± 0.01	50.14 ± 0.10

Samples were mixed with 44 g of deionized ultrapure Mili-Q water and subsequently shook for 7 days to ensure complete contact between the solid and liquid phase. Then, the suspension was centrifuged at high speed 4.000 rpm for 1 hour and filtered (Figure 7).

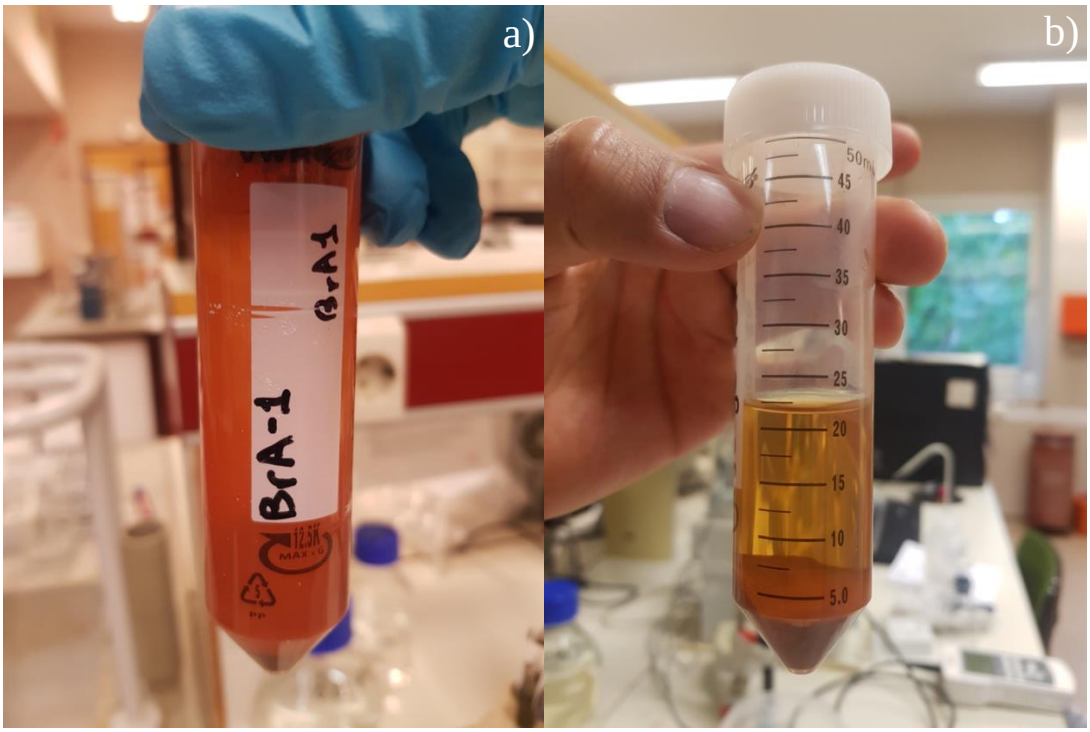

Figure 7. Picture on the left a) sample of bauxite residue with açaí after shaken for 7 days. Picture on the right b) sample after centrifugation for 1 hour.

After the samples are shaken and centrifuged, 10 ml of the eluent unfiltered are extracted to measure the EC, pH, and acid buffer capacity. This eluent is not preserved since the sample cannot be conserved by the destructive method for the acid buffer capacity experiment.

In order to separate the solid in suspension in each extraction, the eluent is filtered through a 0.45-µm pore size membrane using a one-use syringe for all samples. Immediately, it is preserved at 6 C° and the samples of remnant soil and eluate required for chemical analysis were then stored. These chemical analyses include: Ion Chromatography (IC), Ion Chromatography Coupled Plasma Spectrometry (ICP-MS), and Continuous Flow Analysis (CFA).

The remaining solid amount in the first batch of polyethylene tubes is refilled with Mili-Q water to achieve the liquid solid ratio of 10:1. These are mixed for another seven days, centrifuged, and filtered repeatedly using five steps. An outline of how to do the experiment is briefly explained in the diagram (Figure 8).

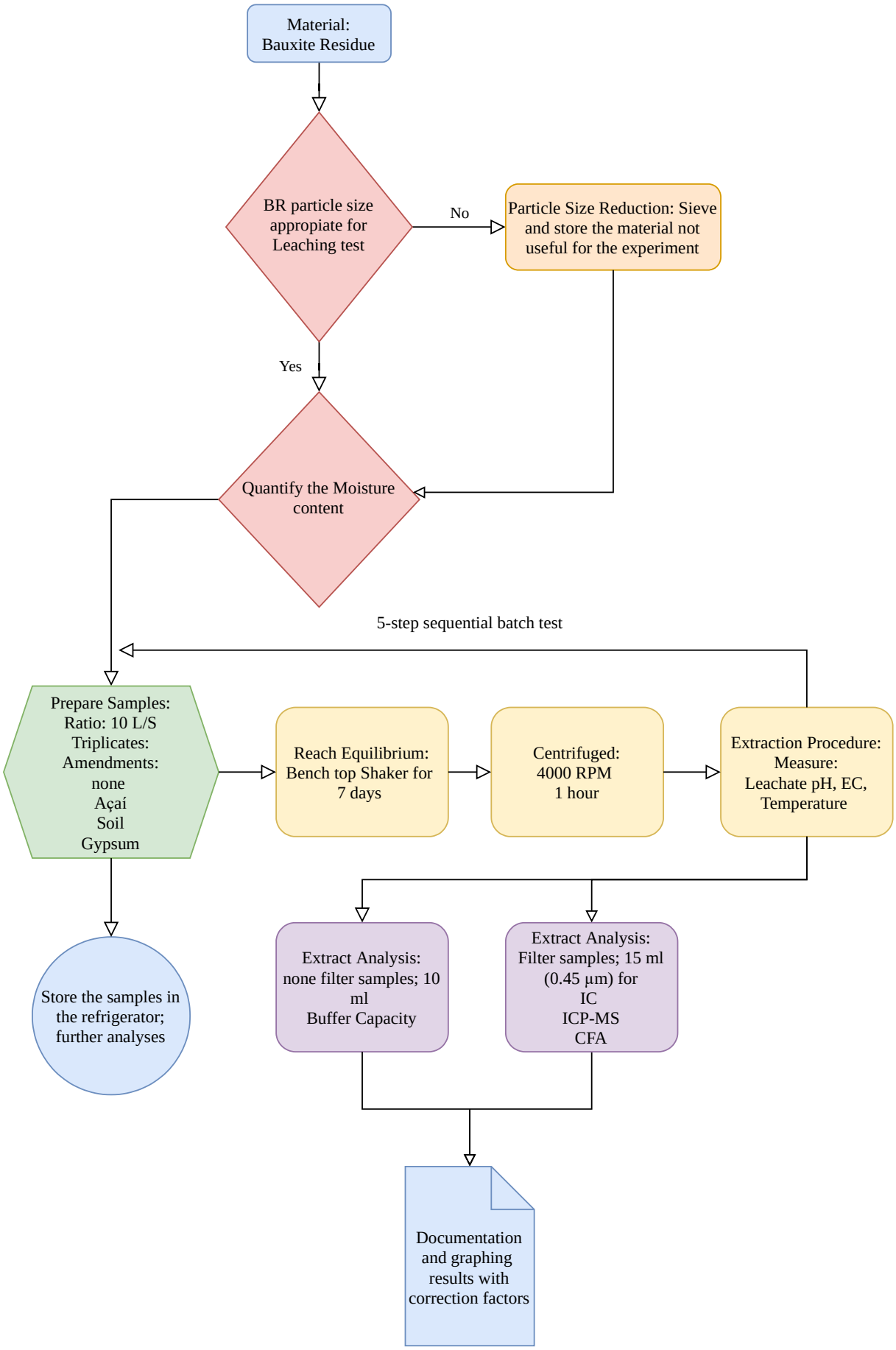

Figure 8. Diagram of essential steps for the sequential batch leaching test of bauxite residue and amendments.

Once the five leaching steps are completed, the solid part of the samples is freeze dried with Christ Alpha 2-4 LDplus and the amount of solid that has been lost after 5 weeks is calculated. After the continuous 32 days of the sequential batch leaching test, the liquid-solid ratio is measured to analyze how much of it is maintained.

4.4 Analyses methods

4.4.1 Electrical conductivity and pH

The measurement machine used for pH is a Metrhohm 702 SM Tirino which is calibrated with a neutral pH of 7 beforehand. To avoid neutralization of the solution, the pH was measured in the 10 ml unfiltered sample within 15 minutes. Due to the exposure to the atmospheric CO_2, this neutralization can happen quite fast particularly with alkaline material.

The EC was measured after the centrifuge was finished without the samples being filtered (Figure 9). A VWR pHenomenal Pc 500 H was used for all 60 samples at 25 C°, previously calibrated at 0.01 M KCL (1355 µS at 23 C°).

Figure 9. Picture on the left a) sample of bauxite residue with açaí before measuring the EC. Picture on the right b) the electrode removing some slight amount of the solid phase.

4.4.2 Acid buffer capacity

The buffer capacity measures the ability of an aqueous solution to resist pH changes by releasing H+ or gaining OH- ions. This refers to the number of moles of an acid needed to change the pH by 1. A buffer solution resists pH changes when a small amount of acid is added. Once the pH is less than 7, it is called an acidic buffer solution (Harris, 2010).

Buffer capacity was determined by a titration experiment. A pH electrode was used to monitor the pH change reaching the flat region of the titration curve (Figure 10). When the pH crosses the equivalence point in the buffer region, the pH changes significantly. To measure the buffer capacity, a titration curve is used with a Metrhohm 702 SM Titrino apparatus. The 10 ml of the initial sample volume is destroyed in the experiment which means that another 10 ml of the same sample without filtration is necessary to replicate the titration curve.

In order to construct the titration curves of each sample, 10 ml of each initial sample is needed with 0.1 ml of weak acid (HCl). The acid concentration strength can vary between 0.0005-0.1 mol/l and the acid is added continuously every 0.1 ml until a pH of 4.5 is reached.

Figure 10. Measurement equipment of pH and titration curved of acid buffer capacity; Metrohm 728 Strirrer analyzing a second leaching step of bauxite residue with açaí sample.

Knowing the volume of acid (ml) near the equivalence point (4.5 pH) and the concentration of HCl (mol/l) permits the calculation of the acid buffer capacity in the aqueous solution with Eq. 5 using the data in Appendix 3.

$$Buffer\ Capacity = \frac{Acid\ Volume(ml) \cdot Concentration\ of\ Acid(mol/l)}{Initial\ sample\ Volume(ml)} = mol/l\ (Eq. 5)$$

4.4.3 Ion chromatography of cations

Cation chromatography of sodium, magnesium, potassium, and calcium is analyzed using suppressed conductivity detection of a liquid eluent. Part of the sample is injected into a stream of eluent of Methane Sulphonic Acid (MSA) and directed into an ion chromatography column. Depending on the cation's exchange affinity, the ions are detached through the column. After this step, the eluent is affected by an anion self-generating suppressor (ASRS Dionex®) to replace the MSA with OH^-. Subsequently, a conductivity detector (SCD) determines the amount of anions in the eluent by electrical conductivity characterization in micro Siemens unit or the area based on EC and time (minutes). Finally, the absolute concentration of the anions in (ppm) is verified with external standards for each anion.

The cation chromatography used in this experiment is the Dionex ICS-100 Ion Chromatography System with a cation separator column (Dionex IonPac CS16 Analytical), Cation self-regeneration suppressor (Dionex CSRS300), and detector (Dionex Conductivity Detector DS6). Five calibration solutions are determined for lithium, sodium, potassium, magnesium, and calcium standards. All calibration solutions were diluted 10 and 100 times with Milli-Q water at 18.2 MΩ.cm with a temperature of 25 C° and TOC of 4 ppb.

The sample amount is 15 ml of filtered eluent (0.45 μm) from the 60 samples in the sequential batch leaching test. All samples were diluted with deionized water by a factor of 10 and 100 times, with a total of 120 samples. The range of the dilution factor is due to the fact that certain elements may be concentrated to a greater extent than others, meaning that some of these elements can be in different calibration ranges of the IC machine, therefore, limiting the use of a single dilution factor.

4.4.4 Ion chromatography of anions

Anion chromatography of fluoride, chloride, nitrate, sulfate, and phosphate is based on the separation on their relative affinities for the corresponding placement inside special columns. These columns are filled with the sample and the eluent with KOH. The separation occurs when each sample's anions pass through a conductivity suppressor that provides continuous suppression of eluent conductivity and enhances the analyte response. Separate anions are identified and quantified with an electrical conductivity chamber and the compounds are classified by their retention time signature and compared with the calibrated standards. The chromatography software transforms the signal strength into a sample concentration (ppm).

The anion chromatography used is the Dionex ICS-2000 Ion Chromatography System (ICS-2000) with an Autosampler Dionex AS40, anion guard column (Dionex AG18), and anion guard column (DionexAG18) through an ASRS suppressor at 70 MA current. The altered level of calibration solution used an Anion Multi Component Standard 2 Aqueous Solution (VWR BDH). All reagents and calibrated standards are prepared with Type 1 deionized water (Milli-Q) at 18.2 2 MΩ.cm with a temperature of 25 C° and TOC of 3 ppb.

The samples are rectified by quality control (QC) for a multi cation standard (VWR, Certipur IC Multi-element std). Results with values between ± 5 % of the calibration method should not be taken into account. If this happens, new standards of elements should be prepared. The samples that have been recalibrated with a higher or lower dilution magnitude need to be rerun to satisfy the continuing calibration verification system (CCV). This QC and CCV are run several times over the process to guarantee accuracy and precision in the final results.

4.4.5 Inductively coupled plasma mass spectrometry (ICP-MS)

ICP-MS is used for ultra-trace elemental analysis. This instrument features a high sensitivity characteristic due to a 90° reflector sampling interface with high-performance 3D ion optics quadrupole. The instrument is operated with a high-performance quadrupole mass analyzer that improves the abundance sensitivity. The sample disintegrates into ions at a temperature of 4726 C° in an argon plasma. The efficiency of the optical ion mirror allows a sensitivity of 1.5 Mcps per ppb in the solution.

The ICP-MS used is a Bruker Aurora Elite M90, the samples are arranged using the ASX-520 CETAC auto-sampler instrument, and one fast sample introduction system into the ICP-MS.

The sample quantity is the same used for the IC of the sequential batch leaching method with 60 samples weighing 0.1 g of sample eluent and 5 g of HNO_3 giving a dilution factor of approximately 50 (Appendix 6). This dilution factor is in the range in which the ICP-MS machine can process the samples with an acceptable detection limit for the standards used for each element. Those analyzed are Na, Mg, Al, K, Ca, Sc, V, Cr, M, Fe, Ni, Cu, Zn, Ga, As, Cd, La, Hf, Pb, and Th. The results are given in µg/l without the dilution factor correction.

4.4.6 Continuous flow analysis (CFA)

Continuous Flow Analysis (CFA) can detect the concentration in mg/l of soluble elements in a solution. The CFA equipment consists of an automatic sampler, a peristaltic pump, a chemistry cartridge collector, a photometric detector, and specialized data acquisition software.

The procedure starts with a light source generated by a wavelength aperture regulator. Then, a monochromatic detector of the selected wave passes through a flow cell, and finally, the detector translates the light energy into an electric current. The concentration of the compound is measured by the light absorbance proportional to the intensity of the color, in this case, silica. The result is compared with an internal standard with the same initial parameters.

To determine the concentration of dissolved silica in the 60 filtered eluent samples, 2 ml were extracted from the batch leaching test tubes and the Seal Auto Analyzer (AA3) was performed (Figure 11).

Figure 11. Sample extraction of eluent is filtered (2ml) for CFA experiment. Notice the lack of color of bauxite residue with gypsum.

4.4.7 X-ray fluorescence

XRF is a cost-effective experiment that ideally analyzes the major and trace elements of a material. XRF works by quantifying the measured fluorescence emitted by the material after being agitated with an X-ray source. Each chemical element contained in the sample produces a characteristic fluorescent feature and allows for the distribution and abundance of various elements to be distinguished (Towett, et al., 2016).

The energy released after the X-ray impact on the material causes the interaction of the atoms with a high-energy source that emits short wavelength radiation (0.003-3 nm). The atom becomes unstable and the electron in the outer orbital replaces the missing inner electron (inner shell). This physical event emits photon energy characteristic to the transition between different electron orbitals in a specific element. It allows for the identification of the elements within the sample (Gill, 2014).

Five samples of approximately 7.2 g were sent to Activation Laboratories (Act-Labs) in Ontario, Canada for XRF trace element analysis. Four of these samples are the solid material left in the polyethylene tubes after the 32-day batch test and one sample is the unaltered bauxite residue.

4.4.8 Geochemical numerical modelling

PHREEQC Version 3 is a computer program initially coded in C++ language made by the United States Geological Survey (USGS). The program is designed to calculate different geochemical processes with capabilities of speciation, saturation-index, batch reaction, and transport calculations including aqueous, mineral, solid-solution, kinetically controlled reactions, and temperature changes among other geochemical processes (Parkhurst & Appelo, 1999).

For this study, two thermodynamic databases were used to calculate the aqueous speciation of the eluates obtained in the sequential batch leaching test—phreeqc.dat and llnl.dat. In addition, the electrical conductivity (designated in PHREEQC as specific conductance), saturation indices of selected minerals, and the partial pressure of gas phases were also calculated and written in the output file given by the PHREEQC program.

The input files include the initial conditions of the measured concentration achieved from IC, ICP-MS, and CFA of each chemical element in the triplicates along with the intermediate pH and temperature (C°). The following four case scenarios with 10% of each amendment and one case-control include:

- Case 1: No amendment (case-control)
- Case 2: Açaí seed waste (affordable organic matter) from the state of Pará, Brazil
- Case 3: Local soil, nearby the rehabilitation area in Barcarena, Brazil
- Case 4: Gypsum powder, from a chemical production facility

An outline of how the geochemical modelling was done is briefly explained in the following flow diagram (Figure 12).

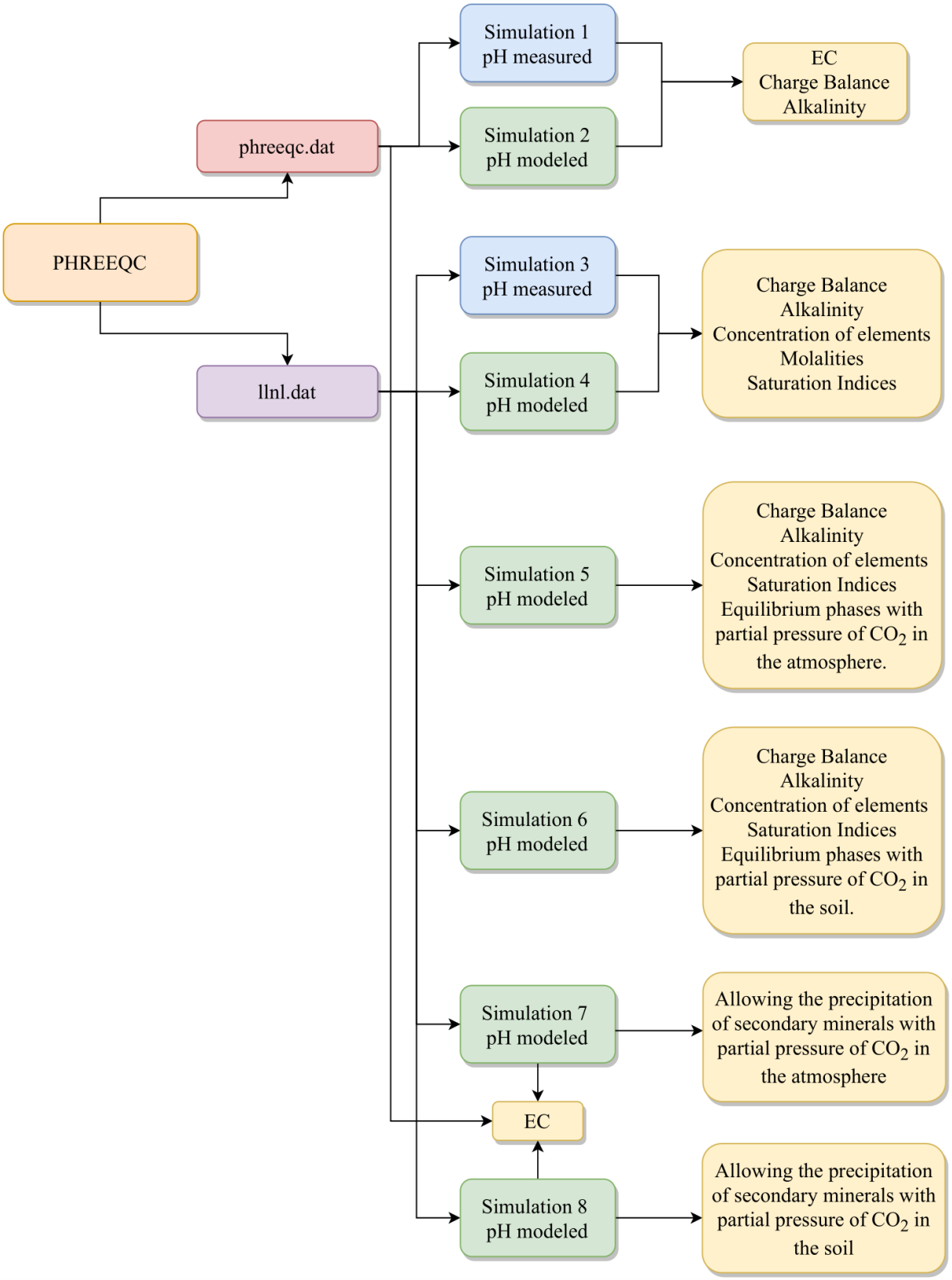

Figure 12. Flow diagram of essential steps for PHREEQC modelling of bauxite residue and amendments with the addition of CO_2 in the samples.

5 Laboratory results

Results obtained are presented in the following order: the first section contains the batch test moisture content of raw bauxite residue and amendments, total loss of solid amount in the batch test, and the sequential batch leaching test. The second segment consists of the electrical conductivity, pH measurements, elemental concentration in the eluates (results obtained by IC, ICP-MS, and CFA), acid buffer capacity, trace elements in the solid phase, and SAR-ESP% ratios. Finally, the third section has the geochemical modelling results with a brief description of the characteristics for simulations 1 through 8.

5.1 Batch test

The calculated moisture content of the raw bauxite residue and amendments are presented in Table 9. The total weight of the samples are measured before and after being dried, and the water content is estimated. Furthermore, the percentage amount of the water content is the partition of the wet weight and the dry weight. The raw bauxite residue presents a water content of 8%, açaí seed 5.56%, gypsum 2.47%, and soil 1.75%.

Table 9. The amount of water present in the raw material before mixing of bauxite residue (BR), açaí seed, gypsum, and soil (G-250 the fraction part below 250 micrometers).

Samples	Wet weight (g)	Dry weight (g)	Water %	Average %	% of amount
BR1	14.06	12.99	8.22	8.22	1.08
BR2	14.13	13.06	8.24		
BR3	14.04	12.98	8.19		
Açaí seed 1	10.82	10.25	5.51	5.56	1.06
Açaí seed 2	10.83	10.25	5.62		
Gypsum 1 G-250	10.70	10.45	2.43	2.47	1.02
Gypsum 2 G-250	10.80	10.54	2.52		
Soil 1 G-250	10.79	10.61	1.70	1.75	1.08
Soil 2 G-250	10.78	10.59	1.79		

The amount of solid in the tubes is weighed before and after the experiment is finished. These measurements identify how much of the solid phase is lost after the completion of the 5-step sequential batch test. Table 10 shows the loss of the solid fraction through the five leaching steps after the last day of the experiment. The values showed an average of 13% for bauxite, 15% for açaí, 9% for soil, and 16% for gypsum. It is important to emphasize that these losses of solid fraction are accumulative for the entire batch test, meaning that the average of loss of

solid per week is 2.69%. The total loss of solid phase is less than 3% which implies that the laboratory methodology used in the batch test is satisfactory.

Table 10. The bauxite residue, açaí, soil, and gypsum solid fraction weight before and after the five leaching steps showing the loss of solid fraction through 32 days, the total average loss of solid is the amount per leaching step.

Sample	Tube + Total Solid (g) Before Dry	Tube + Total Solid (g) After Dry	Remains of Solid (g)	Loss of Solid (%)
BR 1	16.96	16.51	3.15	12.54
BR 2	17.06	16.60	3.13	12.98
BR 3	17.30	16.80	3.10	13.76
Açaí 1	17.49	16.88	3.39	15.15
Açaí 2	17.39	16.79	3.40	15.13
Açaí 3	17.41	16.80	3.39	15.21
Soil 1	17.50	17.12	3.62	9.50
Soil 2	17.52	17.14	3.62	9.53
Soil 3	17.50	17.15	3.65	8.77
Gypsum 1	17.35	16.71	3.36	15.99
Gypsum 2	17.44	16.76	3.32	16.98
Gypsum 3	17.48	16.84	3.36	16.01
			Average loss per week:	2.69

5.2 Sequential batch leaching test

The sequential batch leaching test for 12 samples of bauxite residue was performed over a 5 week period. These contain three replicas for each type of sample (bauxite residue without amendments, açaí, soil, and gypsum). The liquid solid ratio (L/S) achieved is around 10 with a slight mean standard error deviation for each sample (Figure 11). In addition, the EC and pH was measured for each sample with their respective mean standard error. For the EC measurements, bauxite residue with no amendments presented the highest difference in their respective replicas after the first leaching step. According to the pH results, the deviation standard of the samples is considerably low, meaning that the precision of the measurement devices was adequate.

Table 11. Electrical conductivity (EC), pH and liquid solid ratio (L/S) for all leaching steps and days. Mean ± standard error values are shown (n=3).

Leaching Step	Days	Amendments	L/S (cumulative)	EC (µS/cm)	pH
1	7	None	10.05 ± 0.05	3290 ± 20.00	11.99 ± 0.02
		Açaí	10.02 ± 0.03	2403 ± 35.12	11.76 ± 0.01
		Soil	10.02 ± 0.01	2923 ± 98.66	11.94 ± 0.02
		Gypsum	10.02 ± 0.01	4430 ± 43.59	10.92 ± 0.02
2	14	None	20.07 ± 0.05	1762 ± 111.65	11.82 ± 0.01
		Açaí	20.04 ± 0.07	1340 ± 32.62	11.55 ± 0.02
		Soil	20.11 ± 0.04	1638 ± 31.22	11.76 ± 0.01
		Gypsum	20.03 ± 0.02	3010 ± 85.44	10.94 ± 0.01
3	21	None	30.10 ± 0.03	1241 ± 73.08	11.69 ± 0.03
		Açaí	30.08 ± 0.15	896 ± 6.56	11.33 ± 0.02
		Soil	30.12 ± 0.03	1125 ± 11.27	11.60 ± 0.02
		Gypsum	30.08 ± 0.05	1130 ± 28.59	11.41 ± 0.02
4	28	None	40.13 ± 0.03	953 ± 38.94	11.61 ± 0.02
		Açaí	40.11 ± 0.24	688 ± 8.54	11.28 ± 0.03
		Soil	40.14 ± 0.04	835 ± 4.36	11.32 ± 0.10
		Gypsum	40.13 ± 0.09	919 ± 11.37	11.54 ± 0.01
5	35	None	50.15 ± 0.05	777 ± 12.53	11.52 ± 0.02
		Açaí	50.14 ± 0.27	580 ± 3.51	11.21 ± 0.03
		Soil	50.21 ± 0.04	705 ± 10.69	11.32 ± 0.01
		Gypsum	50.14 ± 0.10	829 ± 11.53	11.44 ± 0.08

5.3 Electrical conductivity and pH

The results for pH are shown in the Figure 13. The samples show slightly different mean values and pH ranges from 10.9 to12 during the five leaching steps. The pH of bauxite residue without any amendments is the highest and bauxite residue mixed with gypsum is the lowest in the first step.

Bauxite residue with açaí and soil present a decreasing pattern. Bauxite with gypsum presents an increasing one. After the third leaching step, the pH of all samples are more stable with a final average of 11.4. Nonetheless, bauxite residue without amendments has the highest pH value out of all the steps.

Of all samples, the bauxite residue with açaí shows the largest pH decrease. The bauxite residue with gypsum shows the greatest variation of pH. Regardless of the addition of different types of amendments with bauxite residue, the small error of standard deviation display an acceptable replicability of each sample.

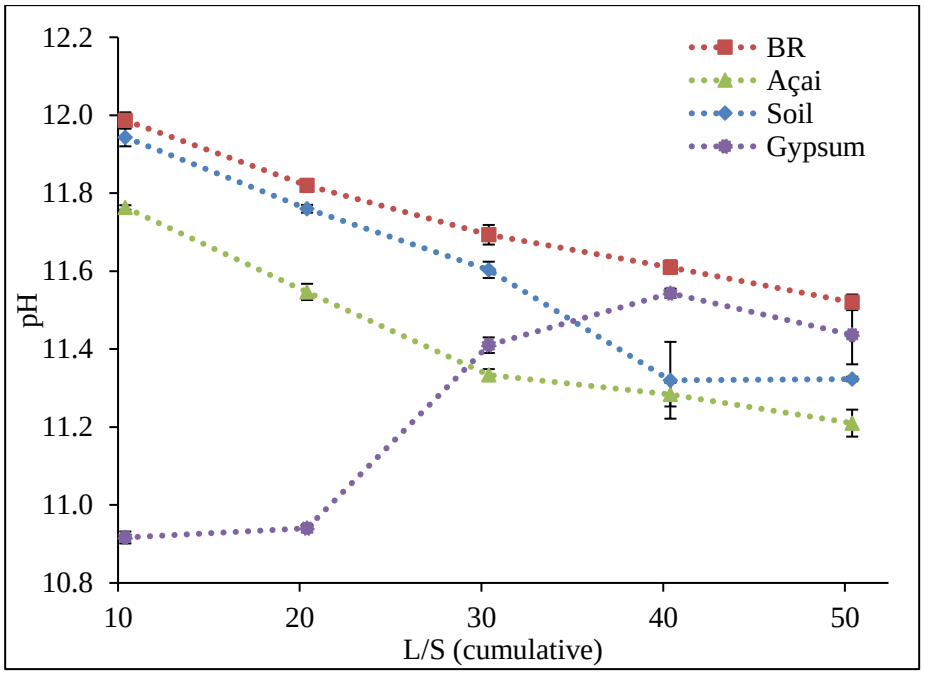

Figure 13. pH per liquid solid ratio (L/S) steps of Bauxite residue without amendments (BR), bauxite residue with açaí (Açaí), bauxite residue with soil (Soil), and bauxite residue with gypsum (Gypsum) within the Alunorte, Brazil samples. Mean ± standard error values are shown (n=3).

In the first L/S 10 ratio step, the electrical conductivity (EC) of bauxite residue without amendments displays an average of 3.261 µS/cm and decreases during the sequential batch leaching test (L/S 10) from 4.430 to 2.403 µS/cm (Figure 14). The EC of the mixture of bauxite residue with açaí decreases from 2.403 to 580 µS/cm, with soil from 2.923 µS/cm to 705 µS/cm, and with gypsum showing the highest initial measurement of 4.430 µS/cm to 829 µS/cm. The açaí amendment tends to lower the EC values from the first to the last leaching step. The bauxite residue with and without amendments tends to have lower ECs from the first leaching step until the last step. The samples present a higher decrease in the first three leaching steps and then they stabilize with a steadier decrease in the last two steps presenting an average of 704.75 µS/cm.

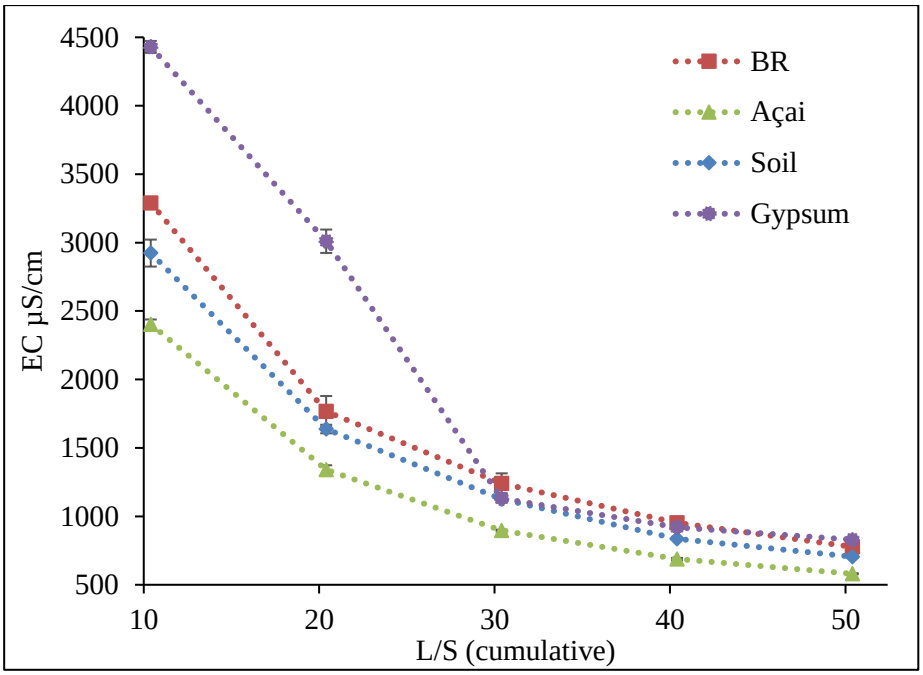

Figure 14. Electrical Conductivity in µS/cm per liquid solid ratio (L/S) steps of bauxite residue without amendments (BR), bauxite residue with açaí (Açaí), bauxite residue with soil (Soil), and bauxite residue with gypsum (Gypsum) within the Alunorte, Brazil samples. Mean ± standard error values are shown (n=3).

5.4 Elemental concentration in the eluates

The results in this chapter present the element concentration in mg/l in the five leaching steps made in the chemistry laboratory at the University of Oslo. Furthermore, the element concentrations are presented using the results of QICP-MS and IC selected in the master table (see Appendix 7) and additional graphs with the fraction of total leached element percentage.

The 60 leached samples were collected, filtered, and measured for main elements. The dilution factor of ten in IC was chosen for F, Cl, Br, and NO_3 concentrations. For the Ca, SO_4, and PO_4 concentrations, the dilution factor of one hundred was selected. The dilution factor of fifty in the ICP-MS was used for Na, K, Mg, Al, V, Cr, Mn, Fe, Cu, Zn, Ga, and As. Finally, the concentration of dissolved silica is calculated with the CFA results.

The general trend from these leaching steps was that F, Na, K, Al, V, Cr, Ga, and As decreased mainly in the first two steps and gradually stabilized in the last two leaching steps. For Ca, only the bauxite residue with gypsum presented this pattern. Ga and As in the bauxite residue without amendments increased in the last two leaching steps (Figure 15-18).

The second general pattern displays a moderately constant amount of Ca, Cl, Br, NO_3, Mn, Zn, and Cu leached per step. This pattern is only exhibited in açaí for Cl and Br. Additionally,

gypsum shows some variance in Br. The small amount of concentration below 1 mg/l increased the standard deviation of the samples close to the detection limit of the IC and QICP-MS.

The last trend pertains to Fe with an increased leached amount in the last three steps from 0-1.4 mg/l to 3-16 mg/l by açaí and soil. In addition, this pattern is also seen for Mn in the sample amended with açaí. The other types of samples do not present this pattern (Figure 16).

For the concentrations of SO_4 and PO_4, the amount (mg/l) is out of the detection limit for the first 4 leaching steps and only present in the last step of gypsum (see Appendix 7). The Mg element does not show any particular trend comparable with other elements. Additionally, more than half of the samples are below the detection limit.

The leached chemistry of the batch leaching test is generally dominated by the concentration of three elements: Na, Ca, and Al. Notice how the scale concentration in mg/l is different than the other elements mentioned before (Figure 15).

The highest concentration of aluminum in the first leaching step is 144.3 mg/l without amendments, followed by 122.4 mg/l for soil, 102 mg/l for açaí, and lastly 0.4 mg/l in with gypsum. The first, second, and third steps decrease faster in comparison to the last two steps. Gypsum is an exception with a slight increase of dissolved Al at the end of 10.7 mg/l and an average concentration of 23.5 mg/l leached for the other samples.

For Na, the relative leached amount was greater than Ca and Al combined. With gypsum, the first and last leaching steps (L/S 10, 50) show a decrease of Na from 741.5 mg/l to 57 mg/l. The other samples present a parallel pattern with an initial amount about 446.8 mg/l and an ending almost to 108.8 mg/l. This final result is more than double the final step with gypsum since the third leaching step starts to present lower concentrations of Na^+ in comparison to other samples.

The main difference between the leached amount of Ca with gypsum and the other samples is that in the chemical composition of gypsum is $CaSO_4H_2O$. The amount of Ca leached from initial step decreases significantly from 507 mg/l to 60.28 mg/l. The other samples keep a leached concentration below 50 mg/l from the first to the last leaching step.

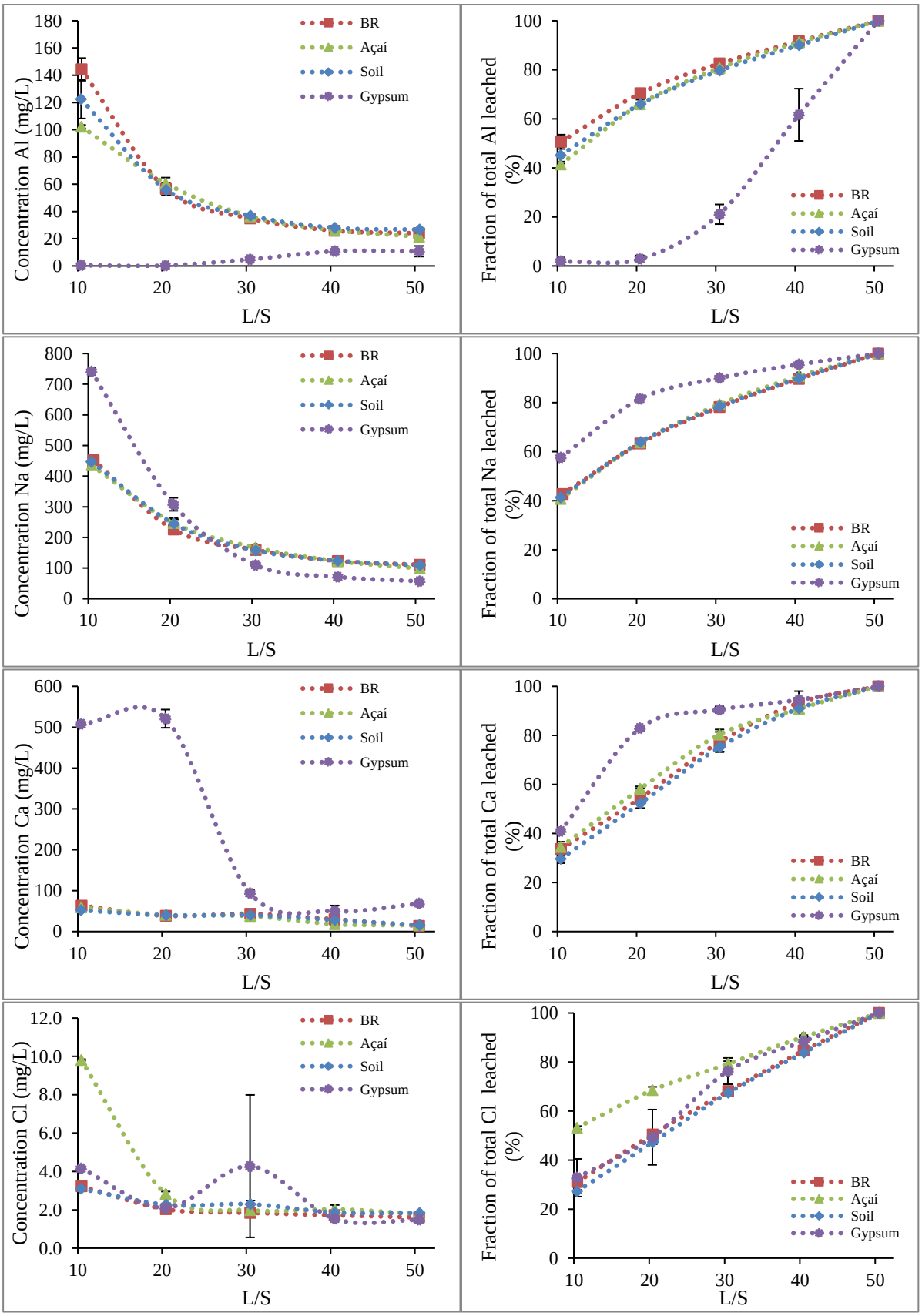

Figure 15. The total element concentration (mg/l) and fraction leached percentage (%) per liquid solid ratio (L/S) steps of Al, Na, Ca, and Cl for bauxite residue without amendments (BR), bauxite residue with açaí (Açaí), bauxite residue with soil (Soil), and bauxite residue with gypsum (Gypsum). Mean ± standard error values are shown (n=3).

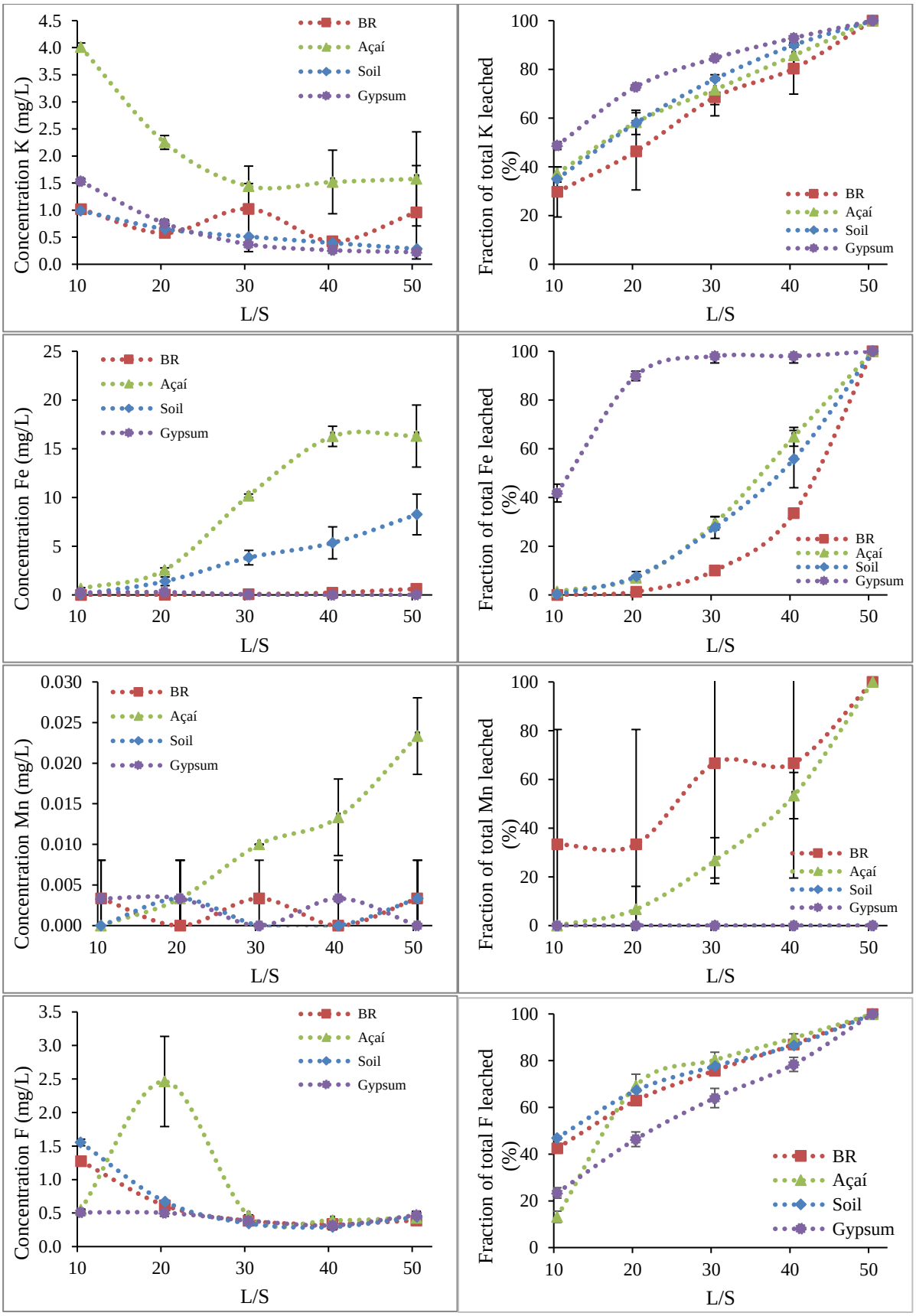

Figure 16. The total element concentration (mg/l) and fraction leached percentage (%) per liquid solid ratio (L/S) steps of K, Fe, Mn, and F for bauxite residue without amendments (BR), bauxite residue with açaí (Açaí), bauxite residue with soil (Soil), and bauxite residue with gypsum (Gypsum). Mean ± standard error values are shown (n=3).

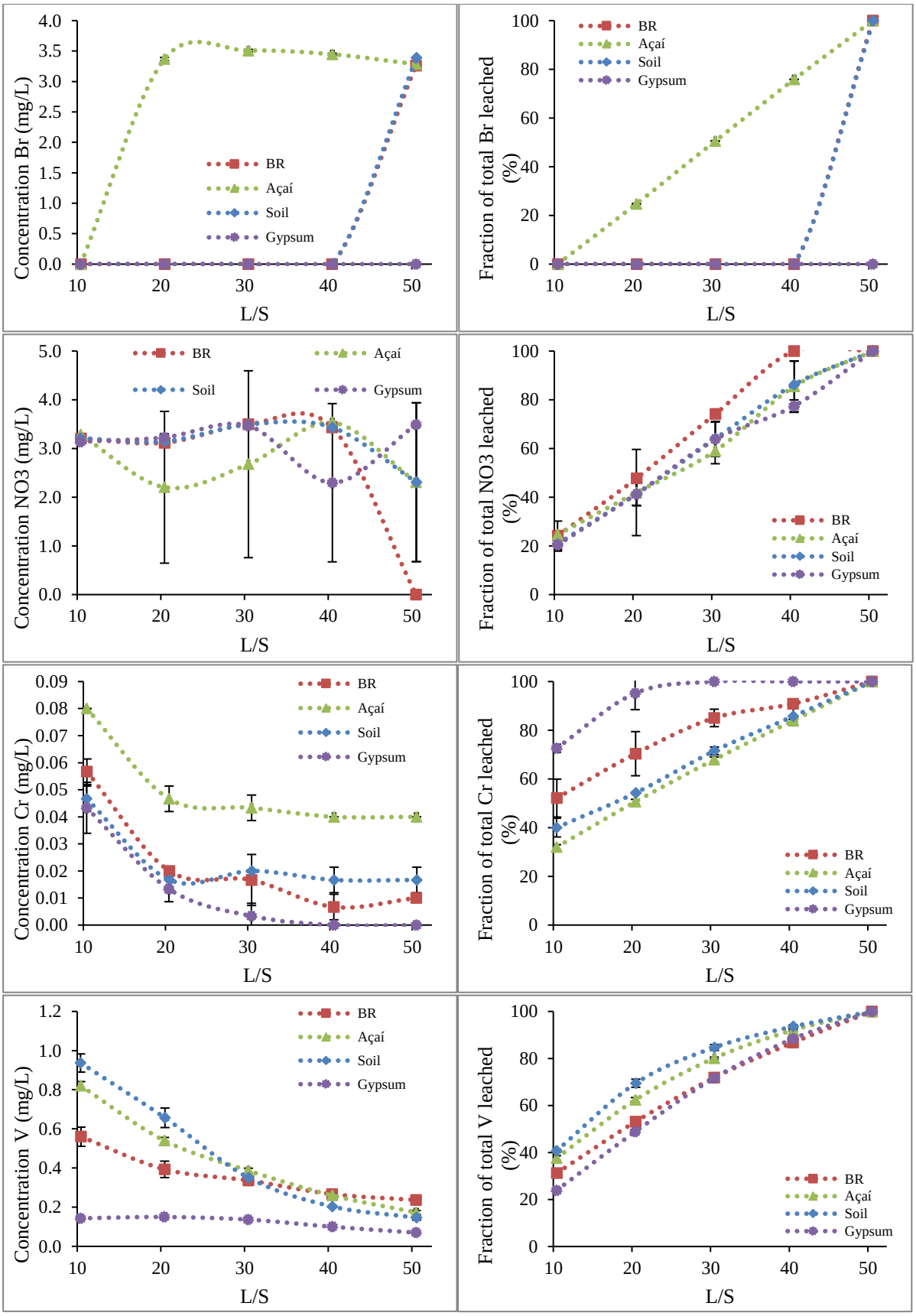

Figure 17.The total element concentration (mg/l) and fraction leached percentage (%) per liquid solid ratio (L/S) steps of Br, NO_3, Cr, and V for bauxite residue without amendments (BR), bauxite residue with açaí (Açaí), bauxite residue with soil (Soil), and bauxite residue with gypsum (Gypsum). Mean ± standard error values are shown (n=3).

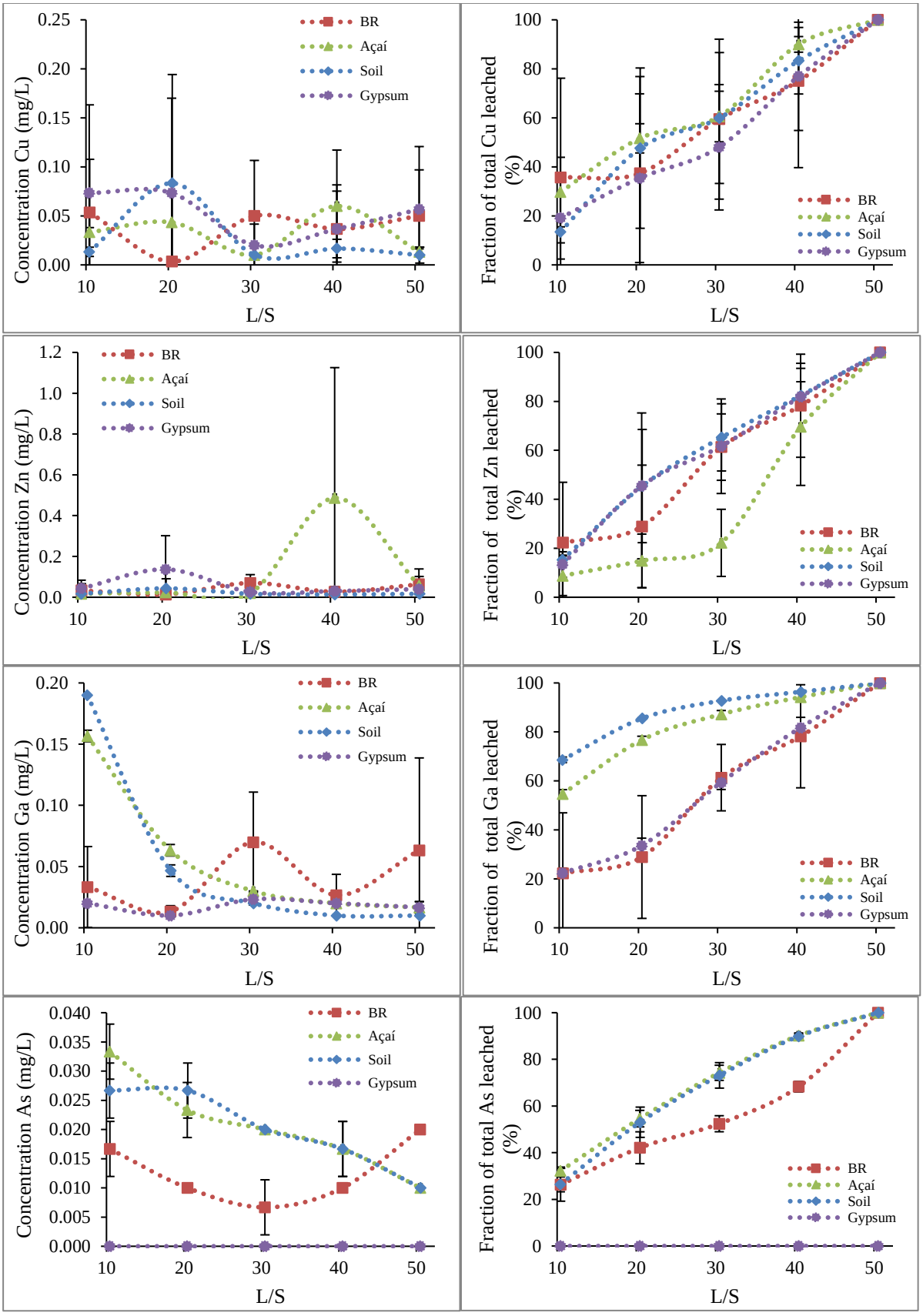

Figure 18. The total element concentration (mg/l) and fraction leached percentage (%) per liquid solid ratio (L/S) steps of Cu, Zn, Ga, and As for bauxite residue without amendments (BR), bauxite residue with açaí (Açaí), bauxite residue with soil (Soil), and bauxite residue with gypsum (Gypsum). Mean ± standard error values are shown (n=3).

5.5 Continuous flow analysis

The same filtered eluate used for IC and ICP-MS is used in the CFA analysis. The amount of silica dissolved varies significantly depending on the type of amendment. To verify that the pattern was correct, the samples were analyzed three times and the last two times, the samples were filtered again with a 0.45 µm pore filter. This decision was made after seeing precipitates in some of the sample tubes after the first filtration (Figure 19). The outcomes present a consistent trend regarding the dissolved silica per leaching step, meaning that the CFA provides good repeatability but with a significant standard deviation error for the triplicates of each amendment.

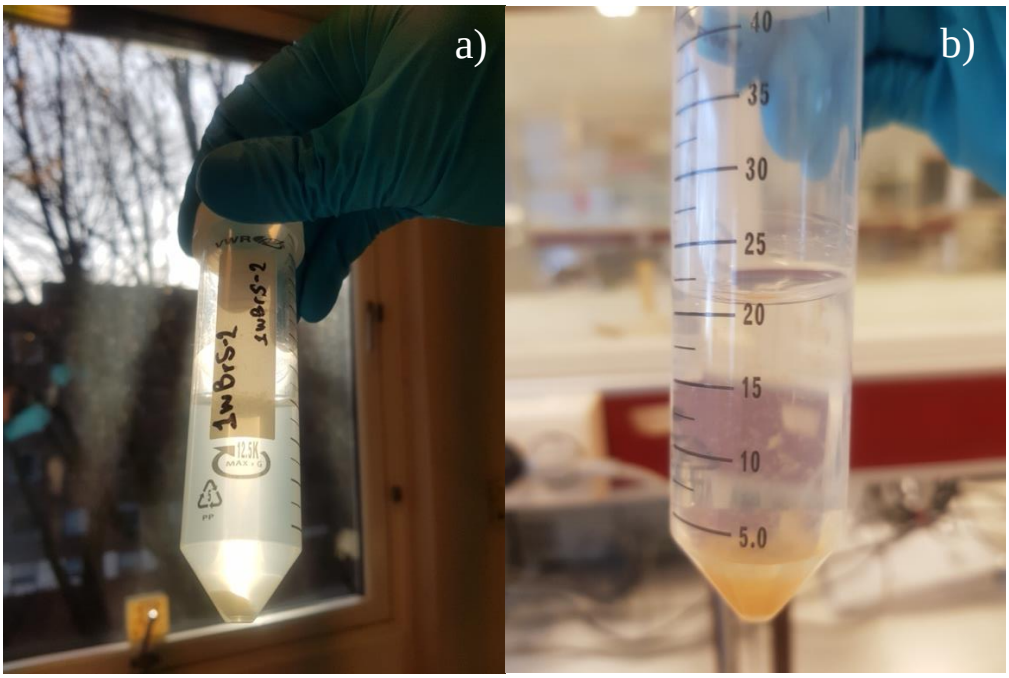

Figure 19. Samples for Continuous Flow Analysis (CFA) experiment, picture on the left a) is the filtered eluent in the first week for the bauxite residue with soil showing some white precipitates in the bottom of the polyethylene tube, picture on the right b) is the filtered eluent in the third week for the bauxite residue with açaí exposing some precipitates in suspension in the eluent fraction of the polyethylene tube after it was stored for 3 weeks.

Açaí is the single amendment with a more stable pattern of slightly increased leached concentration from 9.9 mg/l until the last step of 13.7 mg/l. On the contrary, soil presents a sinusoidal pattern that starts at 3.58 mg/l, 23.5 mg/l, 3.42 mg/l until 15.9 mg/l in the first, third, and final leaching steps (L/S 10, 30, and 50). The other two types—bauxite residue without amendments and gypsum—present a minor increase in concentration from the first to the second step, reaching their maximum value in the second step with values of 13.6 mg/l and 20.7 mg/l respectively. These samples reduce their concentration until they begin to decrease beneath 2.89 mg/l.

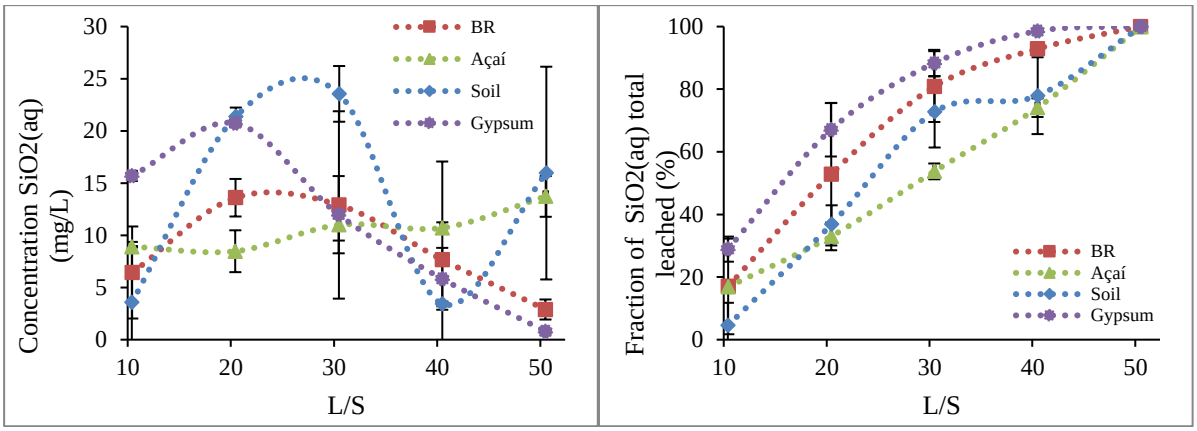

Figure 20. Continuous flow analysis (CFA) experiment: the total silica dissolved in mg/l per liquid solid ratio (L/S) steps of bauxite residue without amendments (BR), bauxite residue with açaí (Açaí), bauxite residue with soil (Soil), and bauxite residue with gypsum (Gypsum) within the Alunorte, Brazil samples and fraction of dissolved silica per leach step. Mean ± standard error values are shown (n=9)

The eluent pigment of the samples used in CFA varies with time and type of amendment (Figure 21). Samples without amendments display the same color during the first 35 days of the experiment and after being stored for three weeks once the test was completed.

Gypsum can promote flocculation of the suspended particles. This results in an aggregation of the suspended material and remains colorless throughout the experiment. Contrarily, açaí and soil samples present a yellowish color that increases over time. A more significant saturated color is observed through the leaching steps for the mixture of bauxite residue with açaí and soil samples.

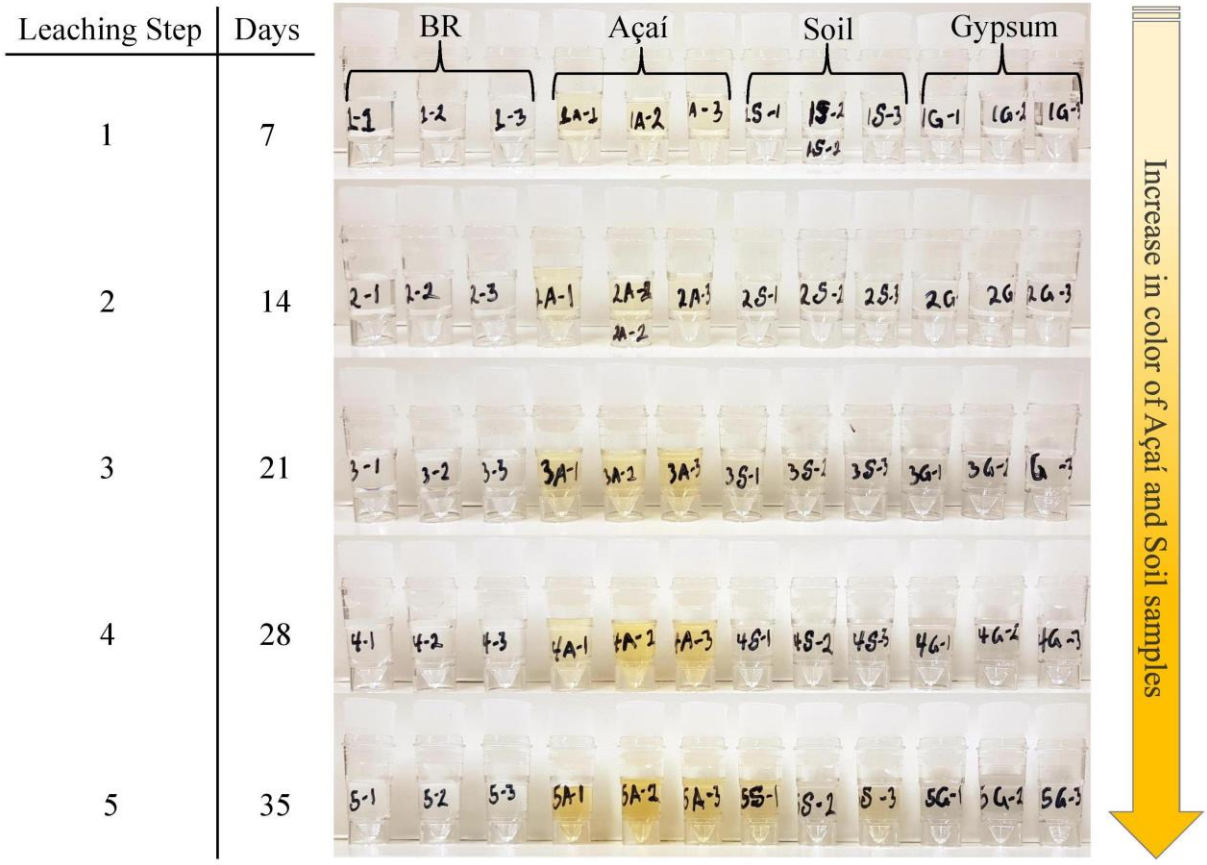

Figure 21. Samples before the Continuous Flow Analysis (CFA) was completed. Bauxite residue without amendments (BR), bauxite residue with açaí (Açaí), bauxite residue with soil (Soil), and bauxite residue with gypsum (Gypsum) within the Alunorte, Brazil samples.

5.6 Acid buffer capacity

The device Metrhohm 702 SM Titrino provides the volume of acid necessary to decrease the pH until it reaches a value of approximately 4.5 per sample. Additionally, it includes the concentration of the strength of weak acid (HCl) needed to reach the desired pH. With the initial sample volume, it is possible to produce the titration curve of the acid buffer capacity for the liquid solid ratio (L/S) of each leaching step.

Figure 22 provides information on the different patterns obtained by the titration curve. There is a continuous decrease for all samples especially in the two first leaching steps. An exception to this trend pertains with gypsum, showing minor concentrations of buffer capacity (mmol/l) during the entire experiment. A slight increase of 3.3 mmol/l occurs during the last step. Samples without amendments illustrate the highest concentration at the beginning of the experiment until its culmination with the lowest standard deviation error compared with the other samples with amendments. Overall, it is clear that the samples in the last leaching step

converge towards the same concentration amount of buffer capacity with an average of 3.8 mmol/l.

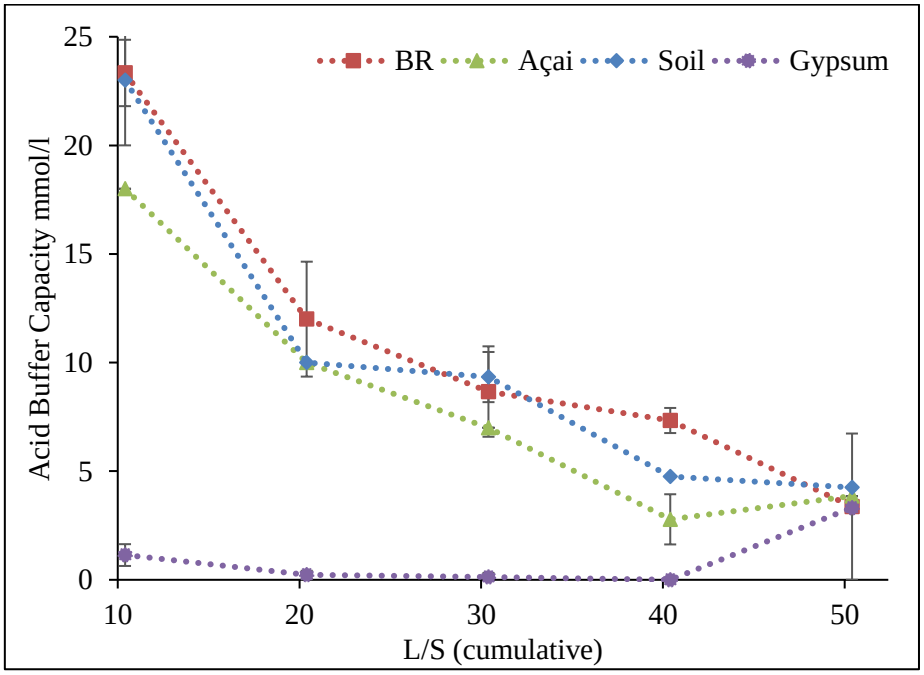

Figure 22. Acid buffer capacity in mmol/l per liquid solid ratio (L/S) steps of bauxite residue without amendments (BR), bauxite residue with açaí (Açaí), bauxite residue with soil (Soil), and bauxite residue with gypsum (Gypsum) within the Alunorte, Brazil samples. Mean ± standard error values are shown (n=3).

The alkalinity is often determined by titration with an HCl solution of known normality towards an endpoint pH of about 4.5. The principal goal of this method is to obtain the titration curve. It is achieved once all CO_3^{-2} and HCO_3^{-} has been transform to H_2CO_3 (pH closed to 4.3). The samples with gypsum could not reach the desired pH, limiting the accuracy of the buffer capacity measured.

5.7 Trace elements in the solid phase

The trace elements composition of the solid phase was obtained from the XRF analyses performed in the Activation Laboratories Ltd. (Actlabs). According to the QC of Actlabs, the only trace element below the lower detection limit is Cu. The values of Ba, Co, Cr, Ga, Nb, Ni, Pb, Rb, Sr, V, Y, Zn, and Zr are in the range above the detection limit.

The concentration of minor elements in the solid phase is parallel to the different types of samples, even if the bauxite residue was leached over five steps or without a batch leaching test. Their concentration is also similar with or without the amendments, except for the

concentration of Sr with gypsum, which shows twice as much concentration in mg/kg than the other types of samples (Figure 23).

The presence of Cr and V is significantly higher than the other trace elements with an average of 290 mg/kg and 536 mg/kg respectively. For the minor elements such as Ba, Co, Ga, Nb, Ni, Pb, Rb, Sr, Sn, and Zn, the concentration is lower than 100 mg/kg. For the transition metal yttrium, the amount is slightly higher with an average of 121.7 mg/kg.

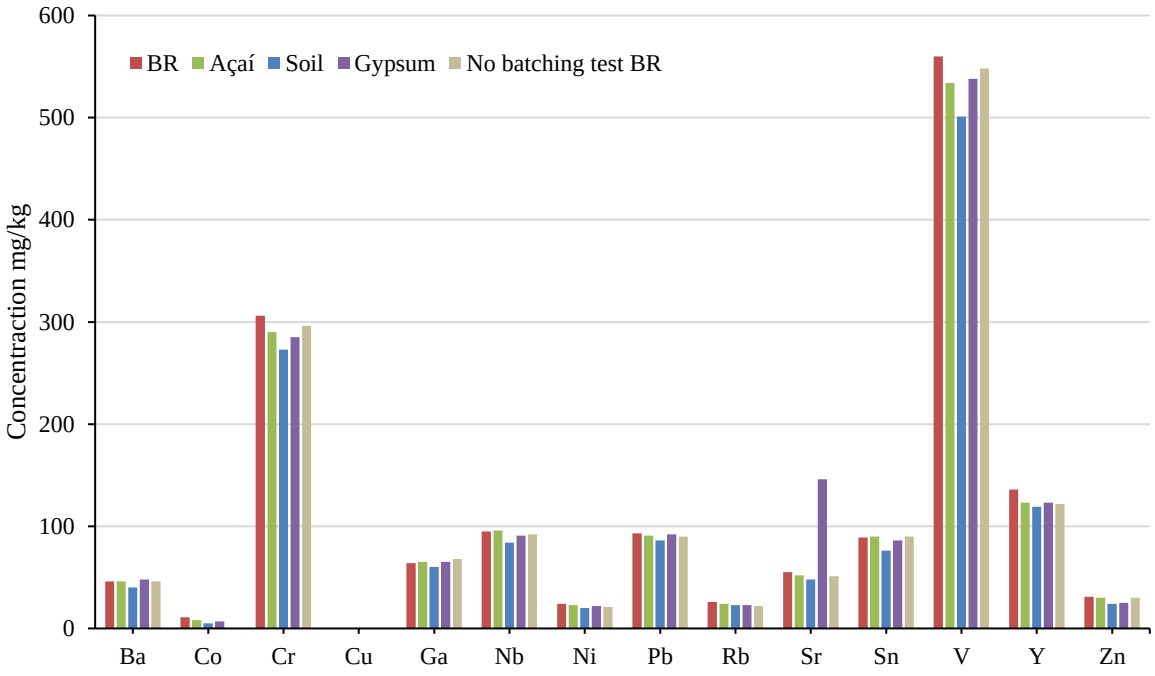

Figure 23. XRF minor elements concentration after five leaching steps of bauxite residue without amendments (BR), bauxite residue with açaí (Açaí), bauxite residue with soil (Soil), bauxite residue with gypsum (Gypsum), and No batch leaching test for bauxite residue (BR) within the Alunorte, Brazil samples.

5.8 Sodium adsorption ratio and exchangeable sodium percentage

The concentration of Na, Ca, and Mg in the eluent is determined by IC and ICP-MS. The SAR and ESP% calculation was performed for each sample. Details of the SAR and ESP% calculations can be found in Appendix 5.

The trends of SAR and ESP% are shown in Figure 24. For all samples, the SAR decreased mainly in the first two leaching steps and starts to stabilize after the third leaching step (L/S 30). Gypsum starts with 9.05 and ends with 1.9, the lowest ratio of SAR. The tendency of all other samples starts with an average of 16.12 and a final average of 6.26. The consistent

pattern established in the SAR ratio is noticeable in the ESP%. This is because ESP% has a direct relationship with the SAR ratio and, in most cases, tends to obtain a consistent pattern.

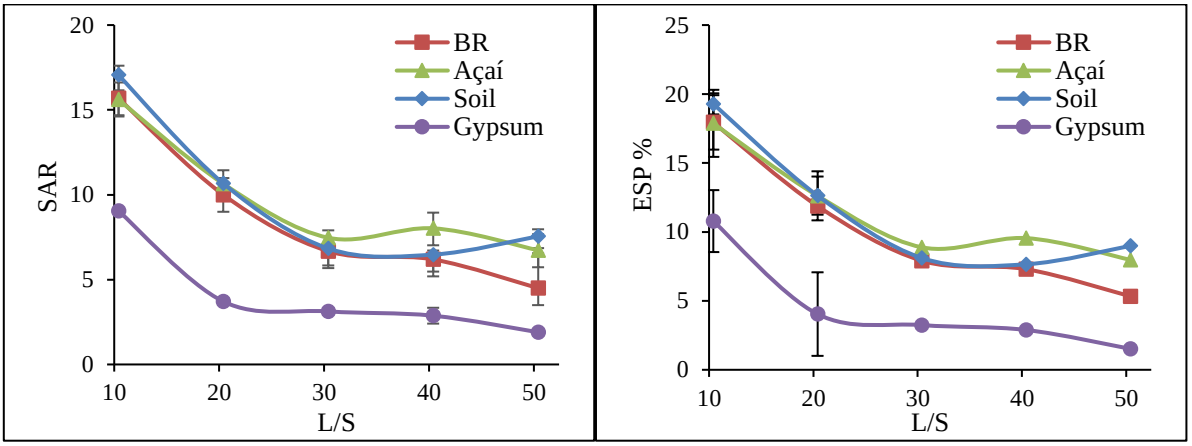

Figure 24. The Sodium Adsorption Ratio (SAR) and Exchangeable Sodium Percentage (ESP) for each liquid solid ratio L/S for bauxite residue without amendments (BR), bauxite residue with açaí (Açaí), bauxite residue with soil (Soil), and bauxite residue with gypsum (Gypsum). Mean ± standard error values are shown (n=3).

6 Geochemical modelling results

From the 60 samples, one replica of each case was selected. The selection was determined by one of the triplicates that had the intermediate pH values. These 20 selected samples contained bauxite residue samples with and without amendments for each of the five leaching steps.

The initial conditions for the PHREEQC code input file were the pH, temperature, and the concentrations of elements in mg/l that were quantified in the IC, ICP-MS, and CFA experiments. The alkalinity values measured in the titration curve are not included in the input file for all the simulations. This is because in all the samples the measured alkalinity is dominated by non-carbonate alkalinity, but PHREEQC only allows carbonate alkalinity in the input file. Nonetheless, in a system depleted in carbonates, such as the samples in this study, PHREEQC can calculate the non-carbonate alkalinity and write it in the output file, as it will be shown in this section.

The pH, charge balance, alkalinity, and electrical conductivity were compared with the values obtained in the laboratory and the differences between the model and laboratory measurements were studied.

The phreeqc.dat is used for a given dependence of thermodynamic reactions with molal voluminal of aqueous species of minerals, pressure, and temperature of gases used in the Peng-Robinson's equation of state (Parkhurst & Appelo, 1999). Additionally, phreeqc.dat determines the solution of master species and the alkalinity.

The EC is calculated in PHREEQC using the thermodynamic database phreeqc.dat instead of llnl.dat. This study uses the selected database with the knowledge that As, Cr, Ga, and V are not present in the EC measurement. Even though phreeqc.dat does not include these elements, it is still possible to calculate the EC while the same calculation in llnl.dat is not implicitly done in these simulations.

6.1 Aqueous speciation of the leachates with measured and calculated pH using phreeqc.dat (simulation 1 & 2)

Simulation 1 used the pH measured in the laboratory. In simulation 2, the pH was calculated using the model program. Obtaining both pH values makes it possible to compare the relative difference percentages of the pH modeled in phreeqc.dat with the pH values measured in the laboratory (Table 14). The same procedure is used for EC, however, simulation 1 for EC does not include of the laboratory EC measurements.

When comparing the pH difference in simulation 1 and 2, all the values of simulation 2 are slightly increased in the pH calculations. It is clear that the difference for all samples is less than 4.3%, with the exception of gypsum (Table 12). The percentage difference of simulation 2 for gypsum decreased with each leaching step. In the third leaching step (L/S 30), gypsum presented the same range as the other samples.

Regarding the EC percentage difference for the laboratory measurements in simulation 1 and 2, it is significantly higher compared with the pH difference. Simulation 1 used the pH measured in the laboratory for the EC calculation. This can explain why the percentage difference is lower compared with the laboratory measurements. When the pH is adjusted in the simulation 2 in PHREEQC, the EC percentage error is greater than simulation 1 (Table 12).

Samples of açaí and soil display the lowest percentage difference in both simulation 1 and 2. Gypsum shows the same persistent pattern of higher difference percentage in the pH calculations, followed by the samples without amendments.

Table 12. Values of pH, EC, and relative difference percentage of Simulation 1 (S-1, with the pH value measured in the laboratory), Simulation 2 (S-2, with the pH value calculated in PHREEQC to reach an electrically neutral aqueous solution), and the laboratory measured-EC (Lab.). Considering their liquid-solid ratio (L/S) and description of amendments.

L/S	Description	pH			E.C µS/cm				
		S-1	S-2	% difference	Lab.	S-1	% difference	S-2	% difference
10	BR	11.98	12.17	1.6	3290	3180	3.3	4386	33
	Açaí	11.76	12.17	3.5	2370	2293	3.2	4279	81
	Soil	11.93	12.15	1.8	2990	2928	2.1	4180	40
	Gypsum	10.92	12.62	15.6	4380	2743	37.4	12085	176
20	BR	11.82	11.93	0.9	1896	2019	6.5	2444	29
	Açaí	11.54	11.98	3.8	1378	1428	3.6	2744	99
	Soil	11.76	11.92	1.4	1648	1804	9.5	2357	43
	Gypsum	10.94	12.44	13.7	2920	1892	35.2	7837	168
30	BR	11.69	11.80	0.9	1206	1473	22.1	1775	47
	Açaí	11.33	11.81	4.2	903	913	1.1	1846	104
	Soil	11.61	11.81	1.7	1118	1308	17.0	1828	64
	Gypsum	11.41	11.89	4.2	1161	1045	10.0	2145	85
40	BR	11.60	11.67	0.6	939	1177	25.3	1318	40
	Açaí	11.29	11.60	2.7	679	707	4.1	1135	67
	Soil	11.35	11.67	2.8	832	805	3.3	1321	59
	Gypsum	11.55	11.67	1.0	932	1056	13.3	1306	40
50	BR	11.52	11.58	0.5	776	974	25.5	1079	39
	Açaí	11.23	11.53	2.7	577	618	7.2	970	68
	Soil	11.32	11.59	2.4	712	726	2.0	1118	57
	Gypsum	11.47	11.69	1.9	830	936	12.8	1354	63

In Table 13, the alkalinity values are represented for simulation 1 and 2 and compared with the laboratory measurements. Simulation 1 presents a lower percentage difference with the laboratory measurements. In the case of simulation 2, the percentage difference is more than double in comparison to simulation 1.

The charge balance error for simulation 1 and 2 is also present in Table 13. In simulation 2, the charge balance error is equal to 0 due to the fact that the program adjusted the pH in order to achieve a solution with electrical neutrality. Because the charge balance error is positive in simulation 1, this indicates that the cations are more abundant and the values are higher than the acceptable water analyses margin (<5%). The following simulations from 5 to 8 use the pH charge in PHREEQC. Therefore, the samples are electrically neutral.

Table 13. Values of acid buffer capacity, alkalinity, charge balance error, and relative difference percentage for Simulation 1 (S-1, with the pH value measured in the laboratory) and Simulation 2 (S-2, with the pH value calculated in PHREEQC to reach an electrically neutral aqueous solution). Considering their liquid-solid ratio (L/S) and description of amendments. The measured acid buffer capacity (Lab.) is used to compare with the PHREEQC-calculated alkalinity.

L/S	Description	Alkalinity mmol/L					Charge Balance error %	
		Lab.	S-1	% difference	S-2	% difference	S-1	S-2
10	BR	25	31.32	25	37.86	51	16.6	0
	Açaí	18	21.96	22	32.68	82	32.8	0
	Soil	23	29.69	29	36.46	59	18.0	0
	Gypsum	1.35	1.19	12	57.03	4109	95.4	0
20	BR	15	16.93	13	19.18	28	10.1	0
	Açaí	10	14.09	41	21.11	111	33.6	0
	Soil	-	14.21	-	17.15	-	14.5	0
	Gypsum	0.05	1.34	2336	37.10	67355	92.6	0
30	BR	7	10.78	54	12.38	77	10.2	0
	Açaí	7	8.35	19	13.31	90	36.5	0
	Soil	10	10.22	2	12.98	30	18.4	0
	Gypsum	-	3.97	-	9.95	-	44.3	0
40	BR	7	8.63	23	9.38	34	6.0	0
	Açaí	3.45	6.60	91	8.83	156	23.6	0
	Soil	4.75	6.81	43	9.53	101	25.6	0
	Gypsum	-	5.80	-	7.13	-	12.4	0
50	BR	-	7.34	-	7.89	-	5.3	0
	Açaí	3.85	5.86	52	7.70	100	21.9	0
	Soil	4.25	6.55	54	8.59	102	22.1	0
	Gypsum	3.35	5.29	58	7.53	125	22.4	0

6.2 Aqueous speciation of the leachates with measured and calculated pH using llnl.dat (simulation 3 & 4)

The thermodynamic database llnl.dat from Lawrence Livermore National Laboratory—converted to PHREEQC format by Greg Anderson and David Parkhurst—presents more geochemical reactions of interest for this study than the phreeqc.dat thermodynamic database. The llnl.dat is used to calculate the electrical charge balance, alkalinity, speciation of aqueous species, and saturation indices of selected minerals.

The initial conditions such as pH, temperature, and concentration of dissolved species are the same for simulations 1 and 3 (with the pH value measured in the laboratory) in addition to simulations 2 and 4 (with the pH value calculated in PHREEQC to reach an electrically neutral aqueous solution). The only difference is the thermodynamic database in use—phreeqc.dat for simulations 1 and 2, and llnl.dat for simulations 3 and 4.

The difference percentage of alkalinity in simulation 3 and 4 present the same pattern as simulation 1 and 4. An exception to this is simulation 3, which has a percentage value slightly greater than simulation 1. In specific samples of soil, gypsum, and bauxite residue without amendments, the alkalinity measured in both simulations presented unreasonably high values and are therefore not taken into consideration (Table 14).

In Table 14, the charge balance error obtained with database llnl.dat is lower in comparison to the database of phreeqc.dat for simulation 1. Some samples present values <5%, even reaching negative values, meaning that there is higher concentration of anions than cations. In the case of simulation 4, the charge balance error is still neutral.

Table 14. Values of acid buffer capacity, alkalinity, charge balance error, and relative difference percentage in Simulation 3 (S-3, with the pH value measured in the laboratory) and Simulation 4 (S-4, with the pH value calculated in PHREEQC to reach an electrically neutral aqueous solution). Considering their liquid-solid ratio (L/S) and description of amendments. The measured acid buffer capacity (Lab.) is used to compare with the PHREEQC-calculated alkalinity.

L/S	Description	Alkalinity mmol/L					Charge Balance error %	
		Lab.	S-3	% difference	S-4	% difference	S-3	S-4
10	BR	25	31.3	25	37.87	51	16.8	0
	Açaí	18	21.97	22	32.7	82	33.0	0
	Soil	23	32.85	43	36.48	59	9.0	0
	Gypsum	1.35	1.59	17	57.03	4109	94.1	0
20	BR	15	19.66	31	19.19	28	-1.9	0
	Açaí	10	15.65	57	21.13	111	24.5	0
	Soil	-	16.79	-	17.17	-	1.7	0
	Gypsum	0.05	1.69	2973	37.1	67355	91.1	0
30	BR	7	13	86	12.39	77	-3.4	0
	Açaí	7	9.18	31	13.32	90	29.0	0
	Soil	10	12.64	26	12.99	30	2.0	0
	Gypsum	-	5.13	-	9.96	-	33.5	0
40	BR	7	10.28	47	9.38	34	-6.4	0
	Açaí	3.45	7.27	111	8.84	156	15.5	0
	Soil	4.75	7.93	67	9.53	101	13.8	0
	Gypsum	0	6.84	-	7.14	-	2.6	0
50	BR	-	8.88	-	7.89	-	-8.3	0
	Açaí	3.85	6.6	71	7.7	100	12.1	0
	Soil	4.25	7.63	80	8.6	102	9.3	0
	Gypsum	3.35	6.99	109	7.53	125	4.8	0

Furthermore, in simulation 3 and 4, the saturation indices of the primary minerals in the solution were measured to visualize which minerals are undersaturated or supersaturated in a solution deprived of CO_2. For simulation 3, using the pH measured in the laboratory (Figure 25), the supersaturated minerals are goethite, boehmite, diaspore, gibbsite, pyrolusite, and

$Fe(OH)_3$. The undersaturated minerals are kaolinite and cuprite. However, magnetite, $Fe(OH)_3$, and goethite are also present in various samples in the undersaturated zone. Additionally, the pattern of saturation indices changes slightly over the liquid solid ratio (L/S), meaning that the ion activity product is nearly stable during the batching steps of the experiment. If the saturation indices is >0, the solution is in a supersaturated state. If it is <0, the solution is in the undersaturated state. SI = 0 indicates that the samples are in equilibrium solution. As well, the presence of amendments does not clearly change the saturation indices of the samples.

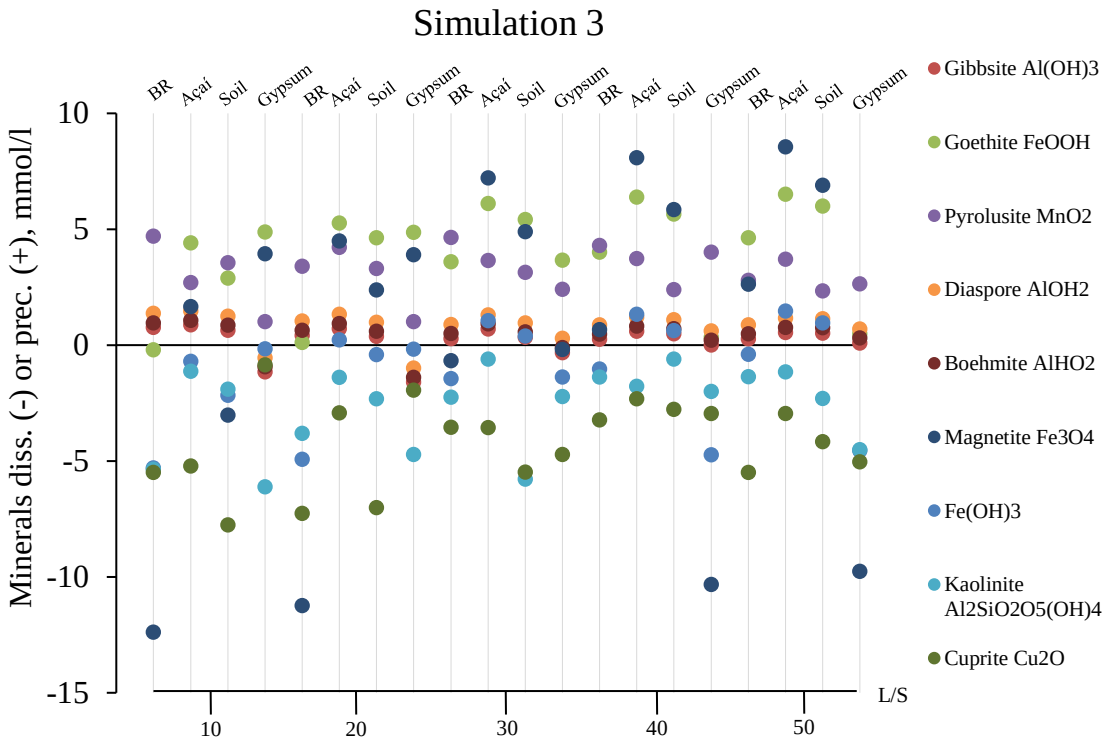

Figure 25. Simulation 3 with pH measured: Saturation indices (y-axis) over each liquid-solid ratio (L/S) (x-axis) for bauxite residue without amendments (BR), bauxite residue with açaí (Açaí), bauxite residue with soil (Soil), and bauxite residue with gypsum (Gypsum).

In contrast, simulation 4 (using the pH modified by PHREEQC) exposed a minor difference in the saturation indices pattern (Figure 26). A slight increase in the pH enables the saturation indices to decrease especially for kaolinite, $Fe(OH)_3$, cuprite, goethite, gibbsite, and boehmite. The pattern of saturation indices over liquid solid ratio (L/S) and presence of amendments are as consistent as described for simulation 3.

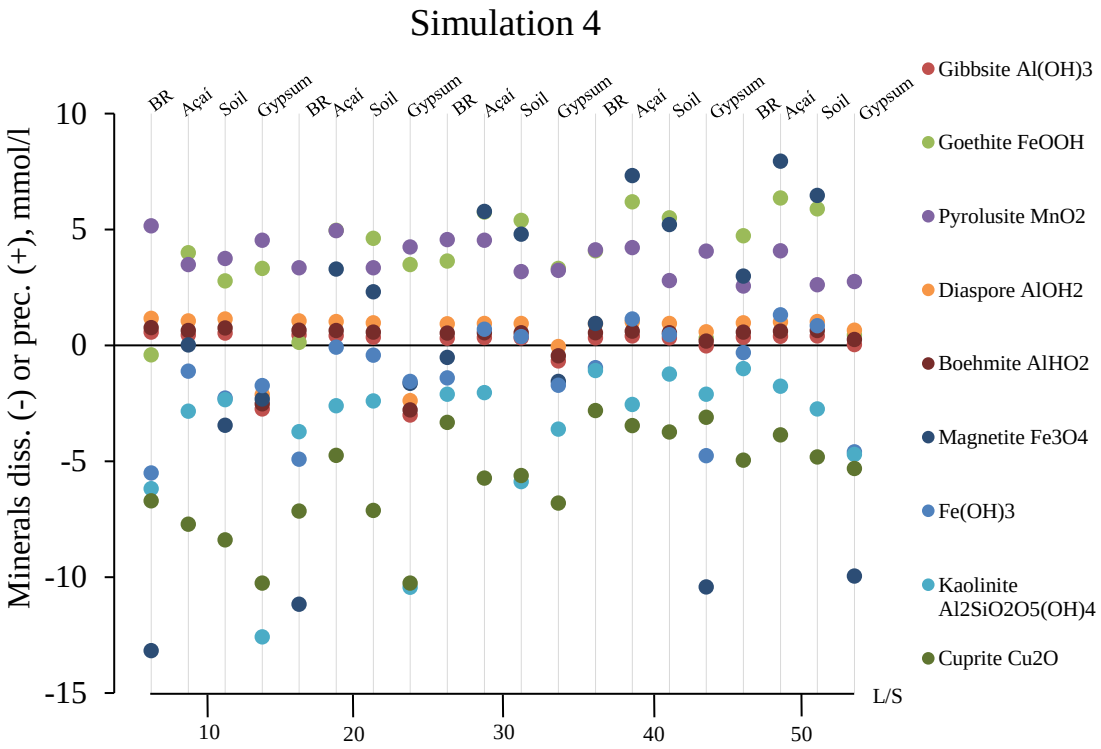

Figure 26. Simulation 4 with pH modeled: Saturation indices (y-axis) over each liquid-solid ratio (L/S) (x-axis) for bauxite residue without amendments (BR), bauxite residue with açaí (Açaí), bauxite residue with soil (Soil), and bauxite residue with gypsum (Gypsum).

6.3 Thermodynamic equilibrium between the aqueous leachates and the partial pressure of CO_2 in the atmosphere (simulation 5) and in the soil (simulation 6)

In PHREEQC, the simulation of the thermodynamic equilibrium between the selected leachates and CO_2 with the partial pressure typical in the atmosphere (simulation 5) allows to assess the geochemical reactions that may undergo in the field which can eventually decrease the pH and retain toxic elements. In addition, if a soil layer develops in the field, a higher partial pressure of CO_2 is expected in the soil water due to the degradation of organic matter. Therefore, simulation 6 simulates the thermodynamic equilibrium between the selected leachates and CO_2 with partial pressure typical in the region's soil.

The model used in each simulation runs the thermodynamics equations in equilibrium phases in a spontaneous reaction. This does not include the kinetic reactions that occur in nature. Omitting the kinetic process, the samples reach equilibrium by reacting with the presence of CO_2 in the atmosphere and soil. This alters the pH and saturations indices (SI) which limited the mobility of contaminants.

The activities of the CO_2 species are given for a constant gas pressure of CO_2 (0.01 atm). In literature, the CO_2 concentration in the atmosphere is fairly small—0.03 vol%—which is equivalent to $[PCO_2] = 3x10^{-4}$ of 1 atm = $10^{-3.5}$ (Appelo & Postma, 2004). The CO_2 pressure of groundwater is possible to be one or two orders of magnitude higher than in the atmosphere. This is due to the uptake of carbon dioxide during the infiltration of rainwater through the soil. The increase in the soil CO_2 is generated by root respiration and the decay of labile organic material (Hanson et al., 2000).

The same principal minerals considered in simulation 3 and 4 are studied in simulation 5 and 6 with the presence of CO_2. In Figure 27, simulation 5 presents additional minerals in the supersaturated solution (SI >0) (i.e., gibbsite, goethite, pyrolusite, diaspore, boehmite, magnetite, $Fe(OH)_3$, and kaolinite). With the presence of partial pressure of atmospheric CO_2, cuprite is in the undersaturated solution through the entire batch leaching test, along with a minor presence of magnetite, pyrolusite, and $Fe(OH)_3$. Samples with or without amendments do not display different behavior in the saturation indices.

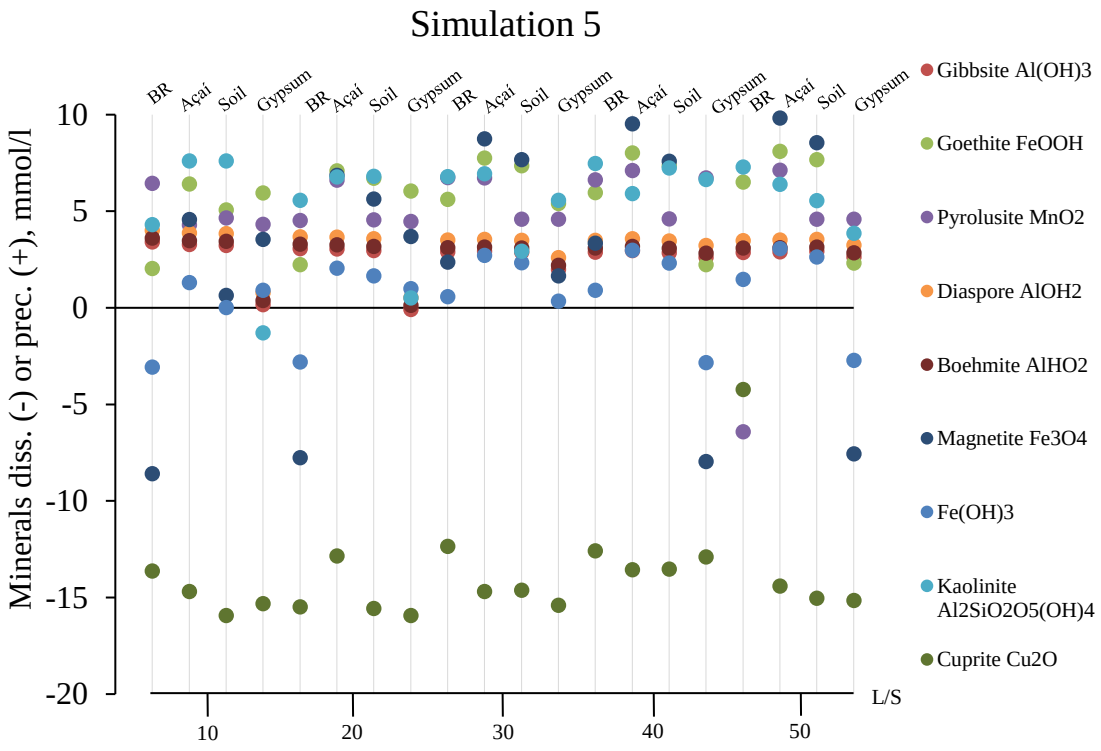

Figure 27. Simulation 5 with partial pressure of atmospheric CO_2 and pH modeled: Saturation indices (y-axis) over each liquid-solid ratio (L/S) (x-axis) for bauxite residue without amendments (BR), bauxite residue with açaí (Açaí), bauxite residue with soil (Soil), and bauxite residue with gypsum (Gypsum).

The main idea of introducing the partial pressure of atmospheric CO_2 in the geochemical model is to understand the behavior of the mineral's reaction that can precipitate toxic elements and form carbonates. In Figure 28, the main carbonate minerals that are in the supersaturated solution are displayed. The minerals that are present in the solution are constituted by dawsonite, hydrozincite, calcite, aragonite, monohydrocalcite, and dolomite. The minerals in the undersaturated solution are magnesite, rhodochrosite, and siderite. These results show that the excess of Na, Al, Ca, Zn, Mg, and OH can be precipitated and form carbonates with the available atmospheric CO_2 present in samples with or without amendments.

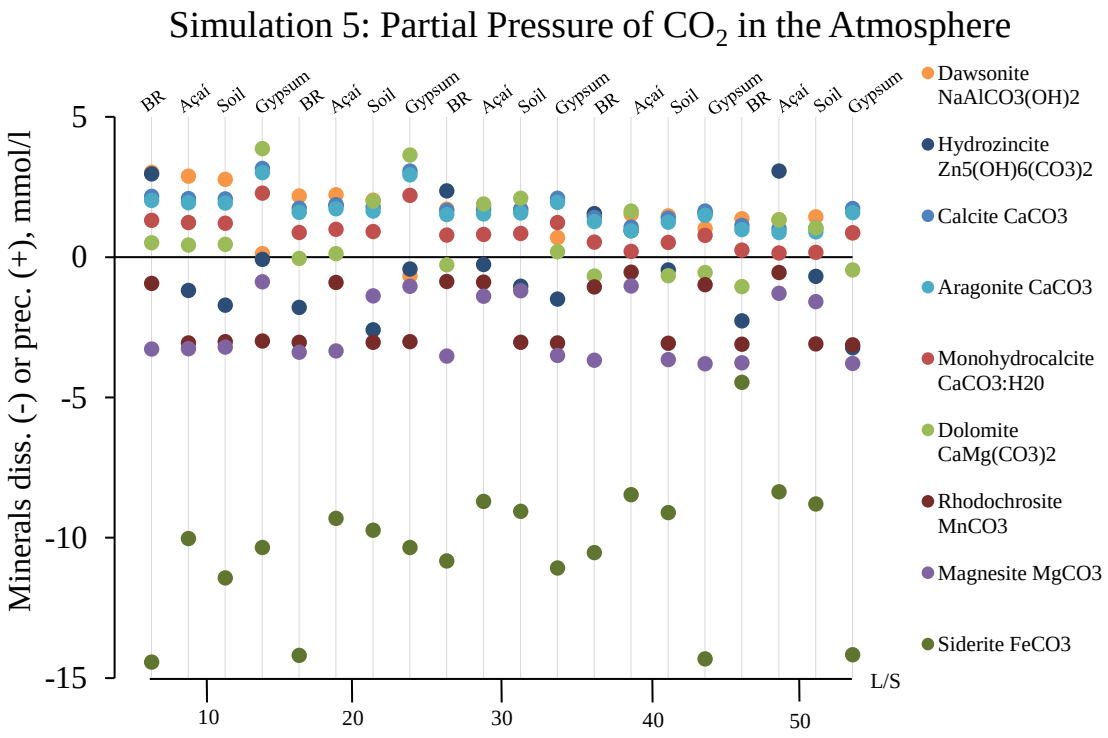

Figure 28. Simulation 5 with partial pressure of atmospheric CO_2 and minerals present with CO_3: Saturation indices (y-axis) over each liquid-solid ratio (L/S) (x-axis) for bauxite residue without amendments (BR), bauxite residue with açaí (Açaí), bauxite residue with soil (Soil), and bauxite residue with gypsum (Gypsum).

In Figure 29, displaying higher presence of CO_2 in the soil, simulation 6 presents the saturation indices of the principal minerals. The pattern is consistent with simulation 5, where the same supersaturated and undersaturated solutions are exposed. Simulation 6 obtained a greater undersaturated solution value for cuprite. Nonetheless, the general behavior is the same as explained in Figure 26.

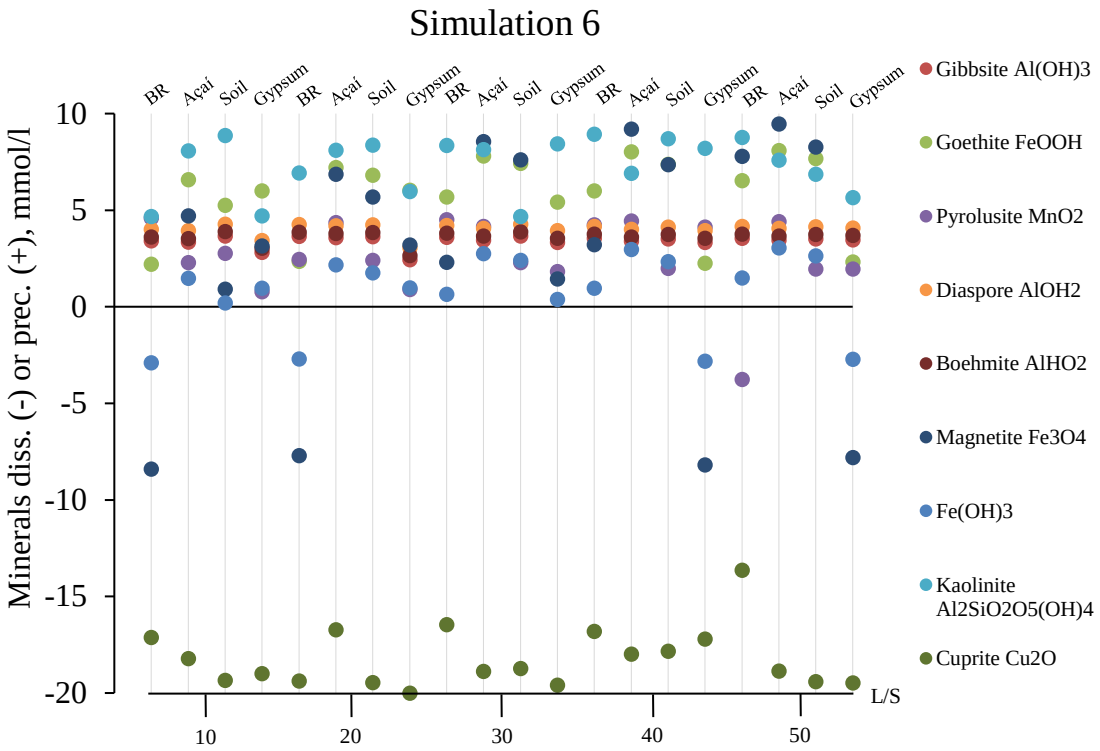

Figure 29. Simulation 6 with partial pressure of CO_2 in the soil and pH modeled: Saturation indices (y-axis) over each liquid-solid ratio (L/S) (x-axis) for bauxite residue without amendments (BR), bauxite residue with açaí (Açaí), bauxite residue with soil (Soil), and bauxite residue with gypsum (Gypsum).

The secondary carbonate minerals allowed to precipitate in simulation 6 are displayed in Figure 30. The higher presence of CO_2 in the soil changes the pattern seen in simulation 5. A distinctive configuration is present in the supersaturated solution where the main carbonates are dawsonite and aragonite. Additionally, some samples with calcite, dolomite, and monohydrocalcite are shown in the supersaturated solution. The other carbonates such as dolomite, hydrozincite, monohydrocalcite, rhodochrosite, magnesite, and siderite are in the undersaturated solution.

The saturation indices obtained by PHREEQC with the presence of CO_2 in the atmosphere is feasible to precipitate carbonate minerals. However, the presence of CO_2 in the soil reduces the pH significantly and the precipitation of carbonate mineral is reduced.

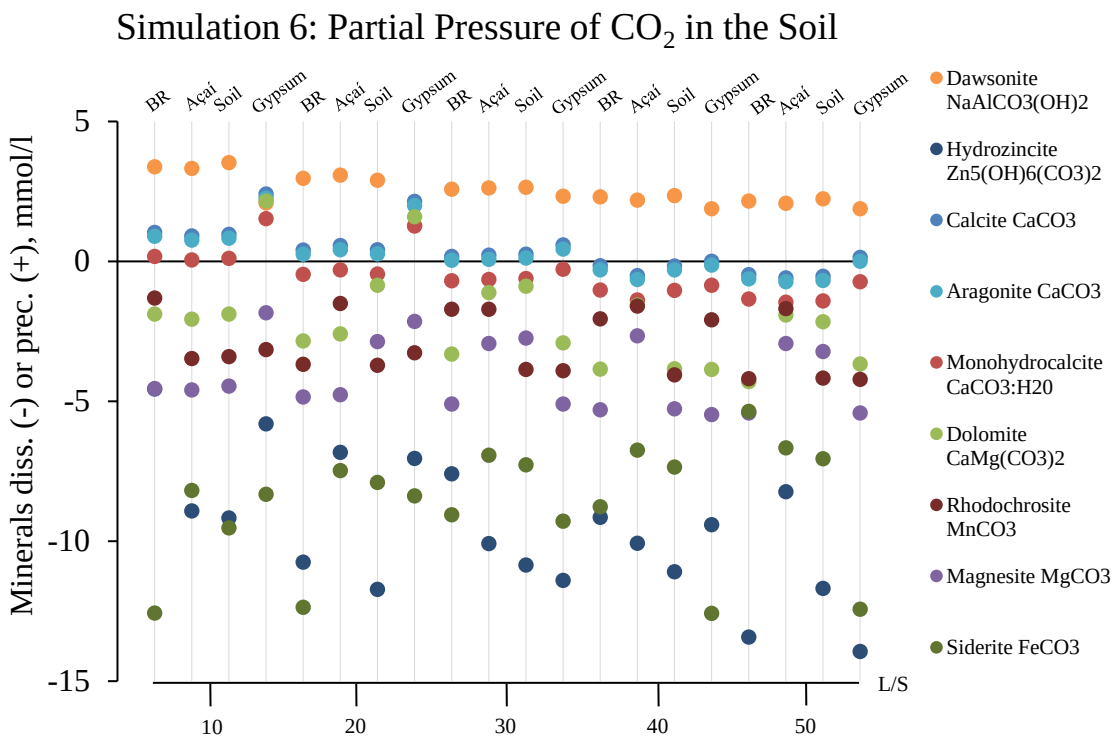

Figure 30. Simulation 6 with partial pressure of CO_2 in the soil and minerals present with CO_3: Saturation indices (y-axis) over each liquid-solid ratio (L/S) (x-axis) for bauxite residue without amendments (BR), bauxite residue with açaí (Açaí), bauxite residue with soil (Soil) and bauxite residue with gypsum (Gypsum).

6.4 Precipitation of secondary minerals from the aqueous leachates in equilibrium with CO_2 in the atmosphere (simulation 7) and in the soil (simulation 8).

Simulation 7 and 8 consider the equilibrium phases of the secondary minerals. When the specific minerals are determined (carbonates and Al-hydroxides) and brought into contact with the eluent solution, each phase will dissolve or precipitate to achieve equilibrium or they will dissolve completely (Parkhurst & Appelo, 1999). Therefore, simulations 7–8 allow the precipitation of secondary minerals to react with the partial pressure of CO_2 in the atmosphere and soil.

Table 15 summarizes the results for simulation 7 and 8, representing the pH achieved with the thermodynamic database llnl.dat. In addition, the computed EC for both simulations was accomplished using the thermodynamic database phreeqc.dat. This method is described in the PHREEQC flow diagram (Figure 12).

Comparing the pH obtained in the laboratory with simulation 7 and 8, the percentage difference increased with a higher presence of CO_2. For example, in simulation 7, the pH can

be reduced on average from 11.5 to 9.1. This implies a 20.8% difference. What is more, for simulation 8, there is an average of 11.5 to 7.2 and a 36.9% difference, almost reaching pH neutrality.

For the EC, the difference in simulation 7 and 8 is not as distinct as it is in the pH values. The EC in both simulations present similar percentage differences in regard to laboratory measurements. Although these percentage difference values are more than double compared with simulation 1 and 2, the presence of CO_2 in the geochemical model changes the EC calculation even if the same thermodynamic database phreeqc.dat is used.

Table 15. Values of pH and EC for the Simulation 7 S-7, Simulation 8 S-8. Considering their liquid-solid ratio (L/S) and description of amendments.

L/S	Description	pH					EC µS/cm				
		Lab.	S-7	% difference	S-8	% difference	Lab.	S-7	% difference	S-8	% difference
10	BR	11.98	9.41	21	7.56	37	3290	1746	47	1714	48
	Açaí	11.76	9.4	20	7.54	36	2370	1699	28	1672	29
	Soil	11.93	9.42	21	7.57	37	2990	1893	37	1858	38
	Gypsum	10.92	9.56	12	7.77	29	4380	3031	31	2961	32
20	BR	11.82	9.23	22	7.35	38	1900	1057	44	1100	42
	Açaí	11.54	9.26	20	7.39	36	1380	1192	14	1219	12
	Soil	11.76	9.2	22	7.33	38	1650	983	40	1039	37
	Gypsum	10.94	9.28	15	7.41	32	2920	1240	58	1260	57
30	BR	11.69	9.08	22	7.22	38	1210	698	42	818	32
	Açaí	11.33	9.1	20	7.24	36	903	745	18	854	5
	Soil	11.61	9.09	22	7.23	38	1120	721	36	836	25
	Gypsum	11.41	8.92	22	7.13	38	1160	507	56	702	39
40	BR	11.6	8.98	23	7.13	39	939	543	42	658	30
	Açaí	11.29	8.96	21	7.07	37	679	520	23	577	15
	Soil	11.35	8.99	21	7.14	37	832	563	32	670	19
	Gypsum	11.55	8.76	24	7.07	39	932	322	65	577	38
50	BR	11.52	8.94	22	7.05	39	776	482	38	552	29
	Açaí	11.23	8.91	21	7.02	38	577	455	21	517	10
	Soil	11.32	8.96	21	7.07	38	712	523	27	576	19
	Gypsum	11.47	8.67	24	7.04	39	830	275	67	563	32

Knowing which minerals are found in the supersaturated solution, the possible precipitation of secondary minerals in the presence of partial pressure of CO_2 in the atmosphere and the soil can be modeled. This is shown in Figure 31 for simulation 7, demonstrating the relative total staked percentage of the secondary minerals over each liquid solid ratio (L/S). The predominant formation of minerals include diaspore, calcite, and goethite with the same respective order. A small occurrence is feasible to precipitate kaolinite, dolomite,

hydrozincite, and pyrolusite. It is relevant to underline that calcite is the only type of carbonate that can significantly sequestrate calcium in proportion with the other Al-hydroxides (i.e., goethite, diaspore, and kaolinite). Moreover, the proportion of secondary minerals after the third liquid solid ratio (L/S) increases the formation of goethite and kaolinite. Then, calcite and diaspore precipitation is slightly reduced. At the same time, samples do not present a predominant pattern regarding bauxite residue with or without amendments.

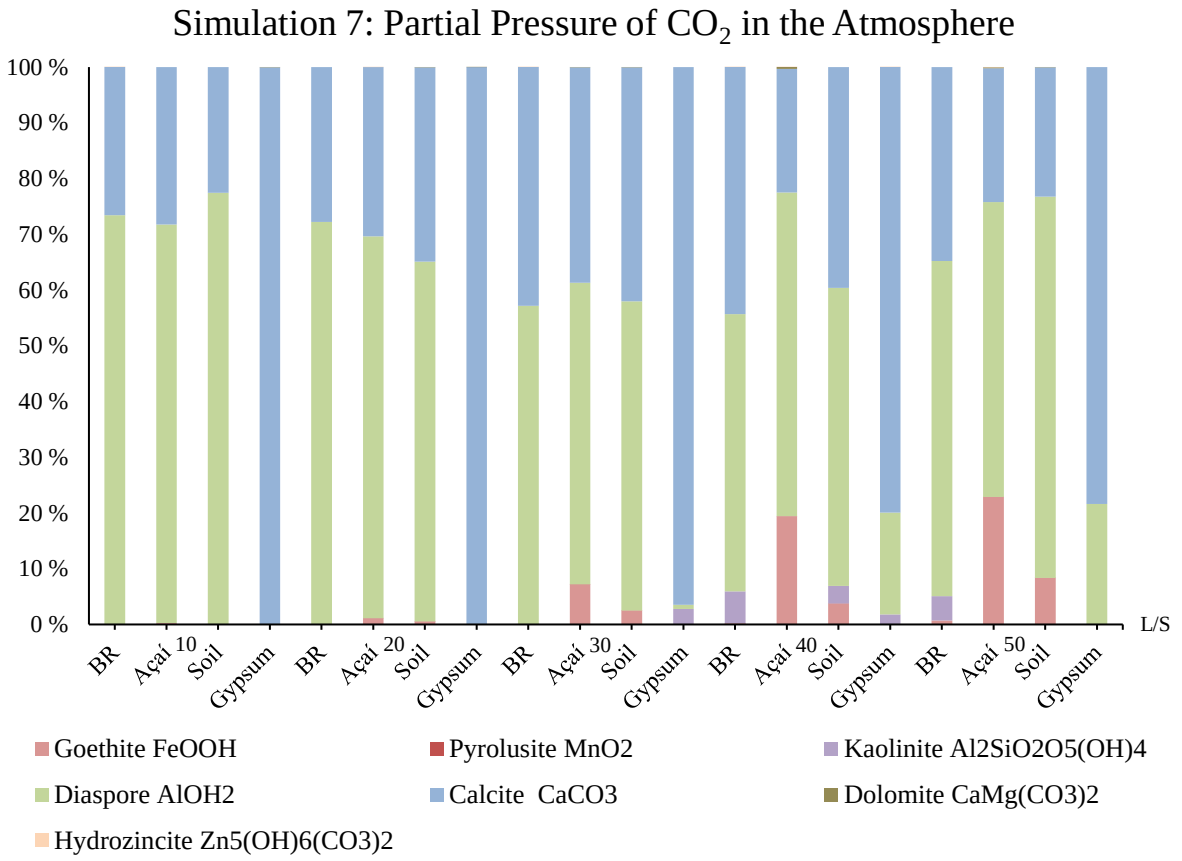

Figure 31. Simulation 7 with partial pressure of CO_2 in the atmosphere allowing precipitating minerals present with CO_3: Relative total stacked percentage (y-axis) over each liquid-solid ratio (L/S) (x-axis) for bauxite residue without amendments (BR), bauxite residue with açaí (Açaí), bauxite residue with soil (Soil), and bauxite residue with gypsum (Gypsum).

For simulation 8, with an average pH of 7.2 in the PHREEQC geochemical model, the precipitation of dolomite and hydrozincite is not possible. After the third liquid solid ratio (L/S), calcite is not precipitated and only present in the last leaching step with gypsum amendment (Figure 32). Overall, calcite precipitation is predominantly reduced by the increased formation of diaspore. In addition, goethite and kaolinite increase their precipitation

in the fourth and fifth leaching steps. Finally, there is no consistent pattern in respect to bauxite residue amendments.

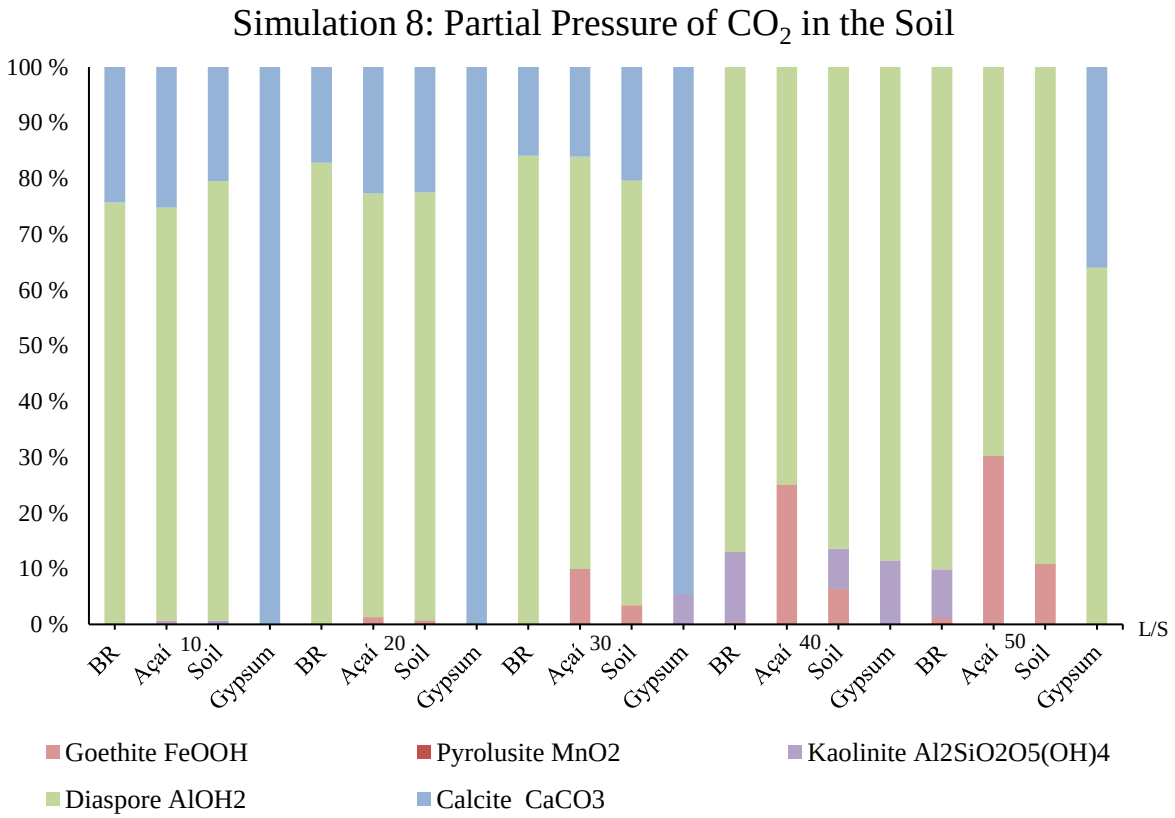

Figure 32. Simulation 8 with partial pressure of CO_2 in the soil allowing precipitating minerals present with CO_3: Relative total stacked percentage (y-axis) over each liquid-solid ratio (L/S) (x-axis) for bauxite residue without amendments (BR), bauxite residue with açaí (Açaí), bauxite residue with soil (Soil), and bauxite residue with gypsum (Gypsum).

6.4.1 SAR and ESP for simulation 7 and 8

Knowing the amount of Na, Ca, and Mg computed in the PHREEQC model with the presence of CO_2, it is possible to calculate the SAR and ESP%. In Figure 33, the trend shown in simulation 7 resembles the decreasing pattern for SAR and ESP% obtained in Figure 24. However, the different type of amendments expose different behaviors. For instance, gypsum constantly shows the lower values of SAR and ESP% throughout the entire experiment. This pattern is changed in simulation 7 and 8. The initial SAR ratio of gypsum is twice the initial ratio of the other amendments, and in the last leaching step, gypsum obtains lower values compared to the other samples.

The concentration of Ca calculated in simulation 7 is one order of magnitude lower than in simulation 8. This is displayed by the difference of the scale in the SAR and ESP% ratios. The

concentration of Na and Mg does not present a significant difference for both simulations. However, both simulations present the same pattern despite having different concentrations of CO_2.

For both simulation 7 and 8, the fifth liquid solid ratio step (L/S 50) of bauxite residue, açaí, and soil present the lowest overall values of SAR and ESP%. The concentration of Ca calculated in the simulation 8 is one order of magnitude higher than in simulation 7. This is because Ca concentration has been less present in the dissolved fraction. Instead, the amount of Ca is in the precipitated of carbonates, such as calcite and dolomite (Figure 31). This is shown in the change of magnitude in the SAR and ESP% ratios (Figure 33 and 34). The concentration of Na and Mg does not present a significant difference for both simulations. However, both simulations present the same pattern despite having different magnitude values and concentrations of CO_2. Gypsum is the least effective amendment to reduce the SAR and ESP% in the first leaching step, and the most effective in the last leaching step. According to the ratios of sodium, calcium, and magnesium with presence of CO_2 in the atmosphere and soil.

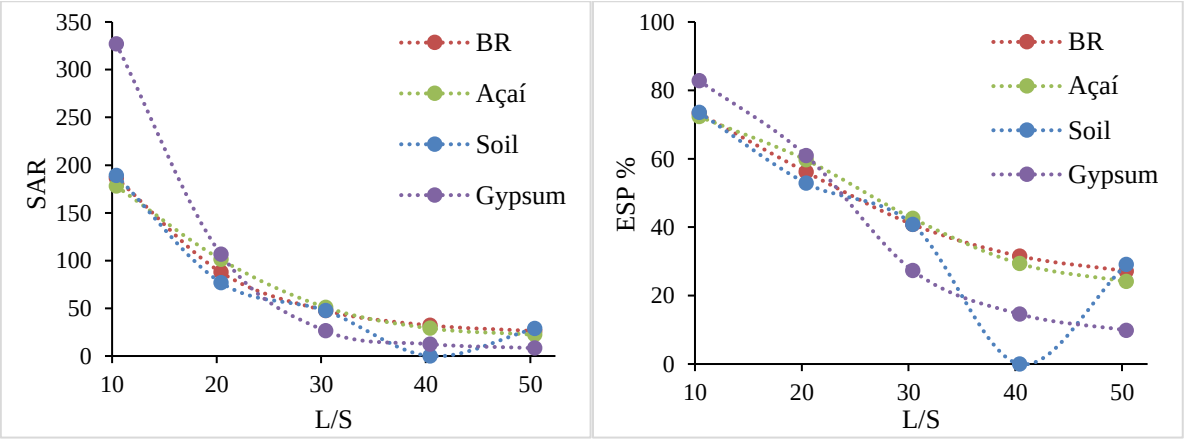

Figure 33. The Sodium Adsorption Ratio (SAR) and Exchangeable Sodium Percentage (ESP) for each liquid solid ratio L/S of simulation 7 allowing precipitation of secondary minerals with partial pressure of CO_2 in the atmosphere. For bauxite residue without amendments (BR), bauxite residue with açaí (Açaí), bauxite residue with soil (Soil), and bauxite residue with gypsum (Gypsum). Mean ± standard error values are shown (n=3).

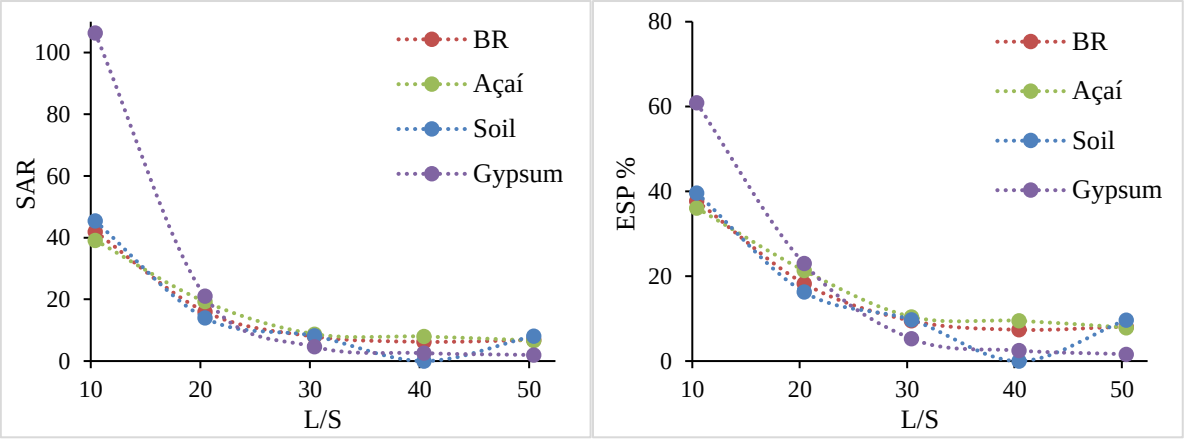

Figure 34. The Sodium Adsorption Ratio (SAR) and Exchangeable Sodium Percentage (ESP) for each liquid solid ratio L/S of simulation 8 allowing precipitation of secondary minerals with partial pressure of CO_2 in the soil. For bauxite residue without amendments (BR), bauxite residue with açaí (Açaí), bauxite residue with soil (Soil), and bauxite residue with gypsum (Gypsum). Mean ± standard error values are shown (n=3).

6.4.2 The pH and alkalinity in all simulations

The main idea of using the concentration of elements (acquired in the batching leaching steps) in PHREEQC was to assess the pH behavior and the acid buffer capacity with different concentrations of CO_2 and amendments.

Simulations 4 to 8 indicate that the dissolved elements do not differ greatly for Al, Fe, and Ca despite the fact that some react with CO_2 and were modeled with the same initial pH by the PHREEQC program. The Al and Ca are in the same order of magnitude and coincide with the leaching pattern shown in Figure 15. The alkalinity modeled by PHREEQC shows a small variance with the presence of CO_2 in the simulations 5 to 8, compared with simulation 4 which was deprived of CO_2. However, the same trend is maintained until the end of the liquid solid ratio (L/S) steps. The substantial change in the simulations is that the presence of CO_2 decreased the pH considerably. Simulation 4 presented the highest pH, followed by the resembling pH in simulation 5-7 and finally, the lowest values are shown in simulation 6-8. Simulations 5 and 6 exhibit the same amount of alkalinity even if the partial pressure of CO_2 is two orders of magnitude difference. In general, the variance of all simulations is negligible and the same tendency is acquired (Figure 35). For all simulations, the pH decreases slightly in the first three liquid solid ratio (L/S 30) steps and stabilizes towards the end of the experiment, following the same pattern with amendments described for the concentration of elements in Figure 15.

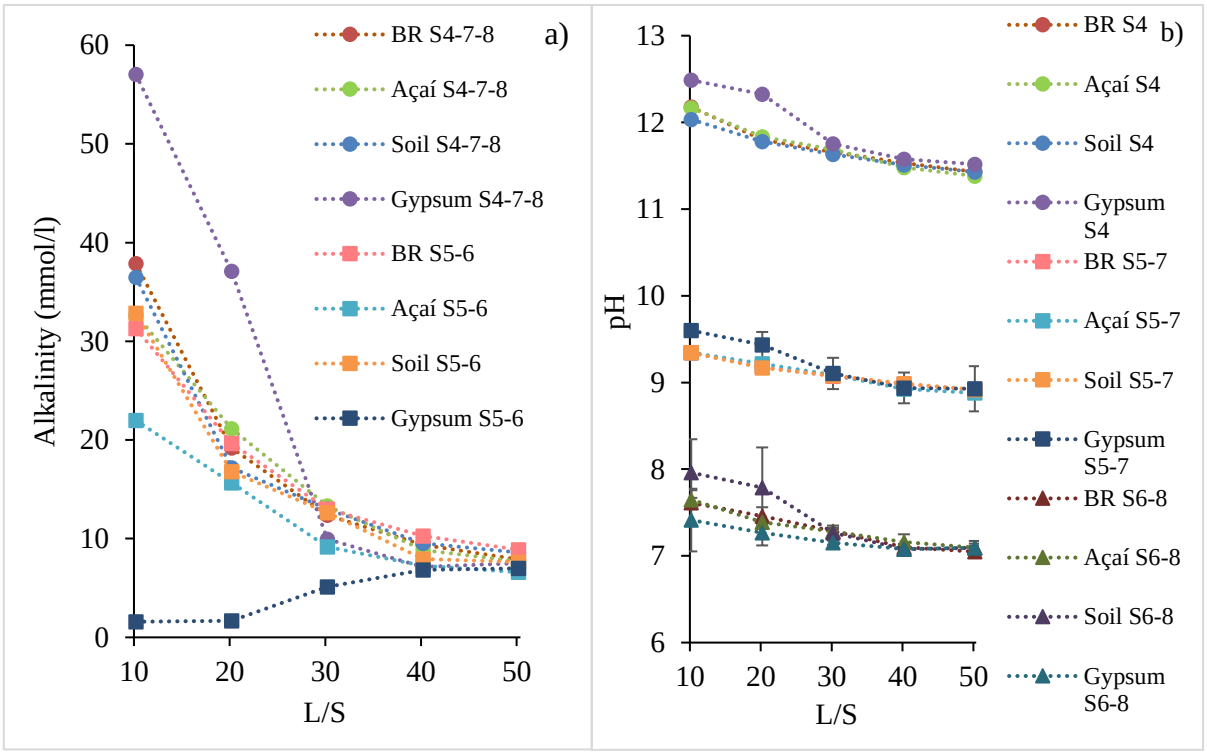

Figure 35. a) Alkalinity concentration for different simulations: S4 -Simulation 4, S5 -Simulation 5, S6 -Simulation, S7 -Simulation 7, and S8-Simulation 8, b) The correlation of pH of different simulations: S4-5-6-7-8 with each liquid-solid ratio (L/S) steps. The initial conditions are explained in the methodology PHREEQC diagram (Figure 12)

7 Discussion

Having thoroughly explained the constructs of this project and its results, this section addresses the implication of my findings. The discussion is organized following the three objectives defined in the introduction. The first section considers the bauxite residue and amendments through the sequential batch leaching test.

7.1 Batch leaching test behavior of bauxite residue and potential amendments

In general, the sequential batch test showed a significant decrease of EC, pH, and concentration of dissolved elements in the third leaching step (L/S 30) independent of the amendment. In addition, the concentration of Na, Al, and Ca is at least one order of magnitude higher compared to other elements (Fe, F, Cl, Br, Mn, K, Cu, Ga, As, Zn, Cr, and V, and NO_3)(Figure 15-18). The concentrations of dissolved elements show clear variation when compared to the different amendments used. The leaching behavior in this study is similar with results by Bray et al., (2018) for the dissolved concentrations of Na, Al, and Ca. In the first two leaching steps (L/S 10-20), most of the Na is leached out, similar to what was seen in the studies of Bray et al. (2018) and Wik (2020). The initial high dissolved content of Na (741 mg/l) is possibly due to the remaining sodium hydroxide applied in the Bayer process.

The dissolution of Fe, Mn, and Br increases for each leaching step, similar to the pattern described for Rare Earth Elements (REE) by Borra et al., (2015) using hydrochloric acid (HCl), for extraction instead of deionized ultrapure Mili-Q water. Furthermore, the dissolution of Na in the first two leaching steps (L/S 10-20) found in this study present a similar result using a liquid solid (L/S) ratio of 5 and 10 used by Borra et al., (2015), meaning that the leaching behavior is similar to other types of bauxite residue (e.g., in Agios Nikolaos, Greece).

Several studies show that the formation of Fe-hydroxides is possible under the extreme conditions in bauxite residue (Courtney et al., (2003); Santini, et al., (2015)). Therefore, it would be expected to find these types of minerals in the batch experiment. However, the concentration of dissolved Fe is consistently low (Figure 16) and the average saturation index (SI) of goethite (FeO(OH)) is 3.73, and ferryhydrite ($Fe(OH)_3$) -1.31, meaning that the

formation of goethite (SI >0) is possible and the formation of ferryhydrite (SI<0) is not possible (Figure 26). The saturation index can assess if the formation of Fe-hydroxides is restricted. These findings indicate that, over time, the leachate fraction is able to form a dominant mineral iron hydroxide—namely, goethite. These findings indicate that the final mineral composition of bauxite residue could differ from the studies mentioned previously.

In the batch tests performed, dissolved Al values were found of 144mg/l in the first leaching step (L/S 10) and 10 mg/l in the last step (L/S 50). Açaí contributes to the reduction of the dissolved amount of Al in the first batch step (100 mg/l) compared with bauxite residue without amendments (144 mg/l). The high concentration of Al can present health risks, such as renal osteodystrophy, microcytic anemia, and dialysis encephalopathy (Crisponi et al., 2011). The World Health Organization (WHO, 2003) set a maximum limit of 0.2 mg/l in drinking water. Even though there is a decrease of leached Al, these results still surpass the limits of WHO and should be studied in more detail.

The results found in this study indicate that the solution pH of the bauxite residue was buffered by alkaline ions in the solution and the pH did not change drastically until the buffer capacity of the alkaline anions was leached out. These findings are supported by Thornber and Binet (1999) who conducted an experiment with a sequential batch leaching test and determined that the amount of the dissolved solids decreased with each step. Despite the fact that the concentration of dissolved elements decreased, neither the pH, $Al(OH)_4^-$, CO_3^{2-}, nor OH^- concentrations changed considerably in the solution (Gräfe et al., 2011).

The results of the sequential batch leaching test procedure demonstrate that a high concentration of dissolved Al (140 mg/l) is leached in the first step (L/S 10) and, at a pH greater than 9, Al-hydroxide species are highly mobile and present in solution (Table 16). These conditions create a toxic environment for plant growth and humans. With such deteriorated conditions, the distribution of these species needs to be studied further (Vardar and Ünal, 2007; Woodburn et al., 2011).

Table 16. Values of pH measured in the laboratory with the presence of the main Al-hydroxides mineral phases saturation index (SI), considering their last liquid solid ratio step (L/S 50) and description of amendments.

L/S	Description	pH	Al-hydroxides mineral phases Saturation Index (SI)		
		Lab.	Gibbsite	Boehmite	Diaspore
50	BR	11.52	0.36	0.58	0.98
	Açaí	11.21	0.40	0.62	1.02
	Soil	11.32	0.42	0.64	1.04
	Gypsum	11.47	0.04	0.26	0.66

The sequential batch leaching test shows a low dissolved concentration of Fe (<20 mg/l) and Mn (0.025 mg/l) compared with Al (<140 mg/l) and Na (<741 mg/l). The low concentrations of Fe and Mn indicate a possible presence in the solid phase. This behavior is explained by Jones and Haynes (2011), who described that the electrical charge of the mineral surface absorbs the Fe, Mn, and (OH) in clay. These results, comparable with literature, argue that these elements are not easily leached in the liquid phase.

For Ca, the dissolved concentration is higher for the sample with gypsum ($CaSO_4 \cdot 2H_2O$) (520 mg/l) compared with other amendments (40 mg/l). With this concentration, the formation of calcite is possible in the presence of CO_2 (as shown in section 6.4). In addition, the existence of calcite in bauxite residue without contact with carbon dioxide is possible due to the remaining CaO and Ca(OH) lime added in the Bayer process.

In the dissolved silica analysis, a high discrepancy between replicate tubes of some of the samples and their aspects (either translucent or reddish) are displayed. This could indicate that, in this high pH environment, Si is very sensitive and partitions between solid, colloid, and liquid phases in different ways. In each triplicate tube, the amount of Si shows a high discrepancy in the CFA results for each type of amendment (Figure 20). Similar results were described by Marin et al., (2017). The dissolution of silica during a leaching test (L/S 5) using sulfuric acid (H_2SO_4) is a complex process controlled by different chemical reactions (e.g., the partial adsorption of the silica on the surface particles, diffusion process, and aggregation). The distinctive color of the açaí and soil eluent samples could be attributed to the presence of dissolved organic matter (DOM) with a C/N ratio in the eluate of 44.5% and 11.7% respectively (Table 6). The presence of DOM can explain the varying color intensity over time and the absence of color in bauxite residue without amendments and bauxite residue with gypsum. The next section will examine the different findings for each type of sample.

7.2 Chemical changes of the amended and non-amended bauxite residue

7.2.1 Difference in EC and pH

The EC with açaí exhibits the lowest values throughout the whole batch leaching test, meaning that açaí has the potential to reduce most of the concentration of dissolved salts in red mud. Soil can also be used for this purpose as it is the second best amendment for reducing the EC concentration. Gypsum is the only amendment that shows EC values higher than bauxite residue without any amendments (Table 17). According to Horneck et al., (2007), EC >2000 µS/cm is considered excessively high for plants and can affect the root system, increasing the mortality rate. Thereby, the EC in the first leaching step (L/S 10) is still unsuitable for plant growth in BRDA. These measurements confirm that the non-amended bauxite residue found in Brazil is within the range described for other bauxite refineries around the world. This is confirmed in the first liquid solid ratio step (L/S 10) with an EC value of 3.290 µS/cm. Data from Fuller et al., (1982) shows values of EC ranging between 1.400-16.900 µS/cm from World Alumina Australia's alumina refinery at Pinjarra, Western Australia. In summary, even with the addition of amendments, the EC in the first step is not reduced enough to fall below the non-amended bauxite residue conditions.

Table 17. Values of pH and EC measured in the laboratory, considering their first and last liquid solid ratio step (L/S 10, 50) and description of amendments.

L/S	Description	pH	EC (µS/cm)
		Lab.	
10	BR	11.99	3.290
	Açaí	11.76	2.403
	Soil	11.94	2.923
	Gypsum	10.92	4.430
50	BR	11.52	777
	Açaí	11.23	580
	Soil	11.32	705
	Gypsum	11.47	829

The difference in temperature at the moment of measuring the EC ranges between 25-30 C°. This range of temperatures is obtained because the samples are centrifuged at a high speed of 4.000 rpm for one hour. These conditions cause the samples to obtain a certain amount of heat. In addition, the measurement of EC was taken between 5-10 minutes after the finalization of the centrifuged step affecting the temperature change of the samples measured.

Coincidentally, similar temperatures are found the field conditions of Belém, Brazil (Medeiros et al., 2017).

In order to overcome the effect of temperature change, the EC was also calculated using the geochemical model PHREEQC. The difference between the measured and calculated EC using the measured pH ranges between 2 – 35.2 % (Table 12). The greater difference is found in samples with gypsum and non-amended bauxite residue (≥ 10%) and the lowest with açaí and soil (≤ 10%). This means that if the pH increases less than 3% (values obtain using PHREEQC), the measurement of EC presents an average difference of >70%. These results present a difference between the calculated and modeled pH relation with EC. Even if the samples have the same temperature, the EC calculation can alter considerably.

In this study, pH has been considered as the main characteristic of changing geochemical conditions. According to the results from the batch leaching experiment, the pH is above 10.3 in all five steps for all amendments in the pH region where Al is soluble. Açaí obtains the lowest pH values, followed by soil and gypsum (Table 17). This high pH leads to negatively charged aluminate ions in the aqueous phase, which are negatively correlated with nutrient elements such as Ca, K, Mg, P, and N. These nutrient elements are vital for sustaining life (Xue et al., 2016). In simulation 4, where the pH was calculated using phreeqc.dat to study the aqueous speciation of the leachates, high saturation indexes indicate the possible formation of gibbsite, boehmite, and diaspore in supersaturated states in the solutions throughout all the liquid solid (L/S) ratio steps (Table 16). If it is not possible for the pH to reach values below 9.0, it can have negative implications in root respiration and inhibition of plant growth (Jones and Haynes, 2011). Nevertheless, pH cannot be the only controlling variable for natural remediation. The sodicity, salinity, and general soil conditions also play a significant role in the improvement of the BRDA.

7.2.2 Acid buffer capacity

Based on the results of the titration curve and the computational modelling, alkalinity is the most uncertain parameter. This can be explained by the presence of the sodium hydroxide used in the Bayer process that alters the amount of OH^- compared to its natural amount.

Different strengths of hydrochloric acid (HCl) change the behavior of the titration curve. As a result, different buffer capacity values are estimated. For example, bauxite residue with gypsum shows that some of the data points were not possible to measure due to the large

volume of acid needed to achieve a successful titration curve (Figure 22). This type of error can explain the differences between the alkalinity measured in the laboratory (0.05 – 25 mmol/l) and the one obtained in PHREEQC modelling (7.14 – 57.03 mmol/l) without any additional reactions with CO_2. It is possible that the titration curve made in the laboratory for this study is out of range due to the initial high pH of the samples and the amount of acid needed, reducing the applicability of this method.

The samples obtained from the sequential batch leaching test present high alkalinity and neither the titration curve nor the numerical modelling used in this case can quantify the actual alkalinity without being highly uncertain. Some possible solutions include making a better titration curve with different acid strengths (HCl) and using different initial amounts of volume of the sample. Moreover, the alkalinity obtained with the titration curve could be verified using a different database in PHREEQC where the alkalinity measured in the laboratory can be included in the input file expressed in terms of non-carbonate alkalinity, and with the solubility constants for cancrinte, sodalite, and other DSP products.

The pH obtained in the batch leaching test has significant relevance as it is always above 10.91. In order to reduce the pH below 10.3, it is necessary that the alkaline solids dissolve and the reaction products are removed (Thornber and Binet, 1999). The high pH can be attributed to varying alkaline solids such as sodalite and cancrinite among others. These DSPs can be made with the addition of sodium hydroxide and lime in the extraction of alumina when the Bayer process is performed. The principal alkaline buffering capacity in the solution of bauxite residue at high pH conditions are OH^-, CO_3^{2-}/HCO_3^-, and $Al(OH)_4^-/Al(OH)_{3(aq)}$ (Gräfe et al., 2011).

7.2.3 Trace elements

According to the results of the minor elements found in XRF, the presence of vanadium (≈536.2 mg/kg) and chromium (≈290 mg/kg) in the solid phase is relatively constant with or without amendments. These high concentrations present in bauxite residue can produce genotoxic effects for plant growth (Gomes et al., 2016). Due to the high alkalinity and pH, the solubility of Cr and V is generally low (Figure 17). This is supported by the study made by Van der Sloot and Kosson (2010). They illustrate that high concentrations of vanadium and chromium at a pH above 10 indicate that the presence of these elements do not leach to the aqueous phase.

The batch leaching test with or without amendments does not considerably affect the concentration of vanadium and chromium in the solid phase. Additionally, the dissolved amount of vanadium and chromium in the sequential batch leaching test is lower than 1 mg/l for both elements (Figure 17). It is possible that due to the high alkalinity and pH, the mobility of these elements is low and they remain present in the solid phase for a considerable amount of time (Evans, 2016). It is challenging to reduce the presence of these elements in the soil. Nevertheless, these elements may present an environmental hazard despite the low dissolved concentration.

The distribution of species in simulation 4 for Cr is mainly present in chromate CrO_4^{-2} and CrO_4^{-3} ($5.13e^{-9}$ and $4.93e^{-7}$ mol/kg). In respect to V, the three major species are ortho-vanadate VO_4^{-3}, hydrogen vanadate HVO_4^{-2} and hydroxidotrioxidovanadate VO_3OH^{-2} ($1.56e^{-7}$, $9.23e^{7}$, and $8.88\ e^{-6}$ mol/kg). If the pH conditions change through the amelioration of the BRDA, the mobility of these contaminants in the aqueous phase could increase and potentially be of environmental concern. Although the concentrations are low, speciation analyses are needed to estimate the environmental hazard of Cr and V (Milačič et al., 2012)

7.2.4 SAR and ESP%

The results of this study show values of SAR and ESP% < 20% (Figure 24). Gräfe et al., (2011) found ESP% above 30%. This means that the conditions obtained in this specific bauxite residue are lower in comparison with other bauxite residue deposited in Alabama, USA (Fuller et al., 1982).

Based on the salinity classification system (Table 3), the conditions of bauxite residue of Brazil without amendments at the first liquid-solid ratio (L/S 10) is categorized as sodic soil. With an EC <4000µS/cm, SAR and ESP% >15, and pH >8.5, poor physical soil conditions are the result.

As noted, several studies such as Fuller et al., (1982), Courtney and Timpson, (2003) and Liu et al., (2007) present ESP% values of bauxite residue without amendments above 30. With these high ESP%, an impermeable material and with poor conditions for plant growth is produced by the sodic soil with poor structure due to clay dispersion and high bulk density. However, after the first leaching step (L/S 10), the SAR and ESP% was reduced in bauxite residue with or without amendments (<15). These circumstances are representative for normal soil conditions. Although the resultant bauxite residue with or without amendments after the

first leaching step (L/S 10) conserved a pH >8.5, it still cannot be characterized in the standard U.S. salinity classification system.

The gypsum amendment has shown that it can reduce the SAR and ESP% ratios (<10) better than the other amendments through the batch leaching test, followed by açaí and soil (15-20 ESP %) (Figure 24). This indicates that the sodium, calcium, and magnesium ratio is more beneficial for plant growth with the addition of gypsum in bauxite residue. However, this is only true if the influence of CO_2 entrapment and carbonate formation is excluded. Before proceeding to examine the best possible amendment, it is important to first review the main findings of the geochemical model in PHREEQC.

7.3 Geochemical modelling

7.3.1 Geochemical characteristics

The element distribution given by the batch leaching test is used in PHREEQC geochemical modelling. This is used to calculate the element speciation in the eluent fraction for each liquid solid ratio (L/S). According to the calculated saturation indices, the solutions with or without amendments are supersaturated in several type of minerals, for example, Al-hydroxides such as gibbsite, boehmite, and diaspore. This also includes iron hydroxide goethite, iron oxide hematite, pyrolusite, and magnetite through the entire batch leaching test. These mineral were also identified in the XRD studies of Borra et al., (2015) and Wik (2020). The positive saturation indices in the leachates and their presence in the solid phase, confirmed by XRD data, suggests that these minerals might form during the batch leaching test, despite the decreasing concentration of Al, Fe, and OH^- throughout the test. In addition, these minerals are present in the bauxite ore, and therefore, a fraction of them may remain after the Bayer process.

According to the saturation indices in the output file of simulation 4, the primary mineral phases of Al-hydroxides are diaspore ($Al(OH)_2$) and gibbsite ($Al(OH)_3$). Under these high pH conditions (>11), the presence of $Al(OH)_4^-$ it is not identified. These results can be compared with Milačič et al., (2012), which describes that the $Al(OH)_3$ is the dominant mineral phase with a pH above 9.2. This could explain why the Al-hydroxide complexes' solubility increases with the pH which is supported by the results of this study that shows that the dissolved concentration of Al in bauxite residue is significantly high (144 mg/l), previously explained in the discussion section 7.1.

Additionally, if the concentration of Al, Mn, and Fe decreases over the five leaching steps, the saturation indices of the main minerals do not present a clear variation with or without the açaí, soil, and gypsum amendments. The alkalinity values are the same in the cases where samples are deprived of CO_2 (simulation 4) and when secondary minerals are allowed to form in the presence of CO_2 in the atmosphere (simulation 7) and soil (simulation 8). The difference in simulation 4 and 7-8 is that allowing the precipitation of secondary minerals does not affect the final alkalinity achieved. In addition, the same alkalinity is obtained in the case where CO_2 in the atmosphere (simulation 5) and soil (simulation 6) is equilibrated with the leachate, meaning that the equilibrium phases and the CO_3^{2-} activity with different fixed partial pressures does not affect the resultant alkalinity.

7.3.2 Modelling the presence of CO_2

According to the results in this study, the solutions are more supersaturated in carbonate minerals (calcite and dolomite) in the presence of atmospheric CO_2 than with a higher CO_2 concentration typical of the soil. This can be explained by the substantial decrease in pH from the atmospheric CO_2 concentration (pH 8.67-9.41) to a typical soil CO_2 concentration (pH 7.02-7.77) (Figure 30).

The average partial pressure of CO_2 in the atmosphere is $10^{-3.5}$, but in the soil, the CO_2 partial pressure can be up to $10^{-1.5}$. The difference of two orders of magnitude is because of the organic matter degradation that increases CO_2 in the soil gas phase. If a sufficient amount of time is given, the formation of carbonate minerals is possible with the presence of CO_2 in the atmosphere and this could play an important role in reducing the pH and subsequently enhance the retention of contaminants.

Additionally, sodium bicarbonate ($NaHCO_3$) will not reach equilibrium with atmospheric pressure of CO_2 that can potentially precipitate the excess of Na. This is not possible because the initial conditions to precipitate this type of mineral are not optimal (temperature, diffusion, rate constants, surface charge density, pH, and other distribution of species).

Moreover, when secondary minerals are allowed to form in the presence of CO_2 in the atmosphere (simulation 7), gypsum can diminish favorable sodicity and salinity conditions (Figure 33). The values of SAR >160, ESP% >70, EC <4000µS/cm, and pH >9.4 are obtained in the first leaching step (L/S 10). These characteristics resemble the poor physical soil

conditions described for bauxite residue without amendments. This suggests that gypsum is not an ideal method of amelioration of this study site.

7.3.3 Precipitation of secondary minerals in the presence of CO_2

In accordance with the case where CO_2 in the atmosphere is equilibrated with the leachate (simulation 5), dawsonite ($NaAlCO_3(OH)_2$) is supersaturated. Nonetheless, when secondary minerals are allowed to form in the presence of CO_2 in the atmosphere (simulation 7) with a pH between 8.88-9.41 indicates that it is not possible to precipitate this mineral—it is only stable in pH ranges 4.1-7.8 (Su and Suarez, 1997). Different arrangements of simulations in PHREEQC shows that hydroxides such as diaspore and goethite, alongside the clay mineral kaolinite are the dominant secondary minerals. Other minerals such as carbonates like hydrozincite, aragonite, monohydrocalcite, calcite, and dolomite may also precipitate. Still, it is only achievable for most minerals to precipitate such as calcite, dolomite, and hydrozincite.

When secondary minerals are allowed to form in the presence of CO_2 in the soil (simulation 8), the occurrence of carbonate minerals is only present in calcite form. This might be explained by the relation shown in the case where CO_2 in the soil is equilibrated with the leachate (simulation 6) with an increase of minerals in the undersaturated zone compared with the case where CO_2 in the atmosphere is equilibrated with the leachate (simulation 5). A possible explanation for this result might be the difference of pH. In simulation 5 and when secondary minerals are allowed to form in the presence of CO_2 in the atmosphere (simulation 7), the pH is in the range of 8.88-9.41, for simulation 6 and 8 it is between 7-8. As a consequence, if the concentration of CO_2 is higher in the system, the pH will decrease more. This is the outcome of the CO_2 concentration in the soil that is two orders of magnitude higher than in the atmosphere.

The aqueous carbonate distribution of species varies depending on the pH in the environment. In this specific case of study, the initial pH is higher than 11.32. At a pH >10.3, the $[CO_3^{-2}]$ becomes the predominant carbonate species, meaning that the initial activity of CO_3^{-2} is higher than the HCO_3^- (Appelo & Postma, 2004).

In addition to these considerations, the amount of dissolved Ca is 10 times higher in the first leaching steps (L/S 10) for gypsum (520 mg/l) compared with açaí and soil (<40 mg/l). Furthermore, the amount of dissolved Mg in the majority of the samples is below the detection limit ($5.85e^{-4}$ mg/l). It is important to realize that the possibility of carbon

sequestration can be limited by the Ca and Mg concentration to transform into carbonates (Doucet, 2010).

The carbonate minerals may play a significant role in amelioration strategies for BRDA (Ducet, 2010). It involves the reaction between Ca and Mg with CO_2 in gas phase to from stable mineral carbonates (Gomes et al., 2016). Still, the understanding of the carbonization in these sites presenting high alkalinity need to be studied further (Kunzler et al., 2011; Zingaretti et al., 2014). More complex processes such as transport mechanisms of CO_2 diffusion, dissolution of $Ca(OH)_2$, particle surface reaction, and precipitate coating need to be studied (Pan et al., 2012). This section has analyzed the geochemical model characteristics, the different mineral configurations, carbonates precipitation in the presences of CO_2, and the final pH changes. The next part of this chapter will address the general features of amendments as potential remediation methods.

7.4 Possible remediation of BRDA at Hydro Alunorte

Any method implemented to ameliorate the "soil" conditions at a BRDA should not only consider the pH, but include alkalinity, toxic level of elements, sodicity and salinity of the bauxite residue as well. For a successful improvement of BRDAs, the pH needs to be reduced below 9 and the dissolved concentration of Na, Al, and Ca should be leached out and decreased at least one order of magnitude to create potential suitable conditions for plant growth.

Given the challenging location of the Hydro aluminum plant and the need to increase organic carbon to support plant growth in the bauxite residue, açaí seed is one of the best natural amendment alternatives available for rehabilitation areas in Pará, Brazil. The decomposition of organic matter enhances the available plant nutrients and the degradation of organic matter can produce CO_2 that can catalyze the formation of carbonate minerals. The sequential batch leaching test shows the effectiveness of the açaí seed amendment to decrease the pH (11.76 to 11.23), compared with soil (11.93 to 11.32) and gypsum (showing an increase in pH, 10.92 to 11.47) amendments from the first to the last step (L/S 10-50), in the absence of CO_2.

Other amendments such as soil can improve microbial and plant root respiration producing acidifying agents that can reduce the alkalinity of red mud and improve conditions for the rehabilitation of a BRDA. According to the batch test results, soil has a similar effect as açaí seed and can be considered as a good alternative to ameliorate bauxite residue. However, the

amount of soil used in this study necessary to obtain these positive effects (proportion of 10%) is higher than using açaí seed (with the same initial proportion of amendment used).

It is complicated to understand how gypsum amendment can ameliorate the chemical characteristics of bauxite residue. On the one hand, the laboratory experiments in this study showed that the pH can increase initially from 10.92 to 11.47 and reduced the sodic conditions (10 to 1 ESP%). On the other hand, the geochemical modelling indicated that in the presence of CO_2 (simulation 7) the sodic conditions can deteriorate (82 to 10 ESP%). Particularly, the pH and ESP% decrease the most in the first leaching step (L/S 10). On the contrary, it is the least effective method to neutralize bauxite residue sodicity and EC in the first leaching step, compared with açaí and soil in the presence of atmospheric CO_2.

Several studies have evaluated the efficacy of a gypsum ($CaSO_4 \cdot 2H_2O$) amendment for plant growth. The additional Ca promotes calcium carbonate precipitation, thus causing a decrease in pH (Barrow, 1982). In addition, Ca displaces Na^+ ions from cation exchange sites, implying an increase in Na^+ leaching (seen in L/S 10 for gypsum of 741mg/l and ≈ 440 mg/l for açaí and soil). In several BRDAs, gypsum has been implemented to stabilize the residue surface, decreasing wind and aerial erosion and improving aesthetics (Sun et al., 2004). Gypsum will precipitate the alkalinity of the solution reducing pH, EC, exchangeable and soluble Na, and Al solution concentration (Courtney, & Kirwan, 2012). However, due to the low leaching rate, it can take more than a decade before the conditions for plant growth are acceptable (Wong and Ho, 1991; Wik, 2020).

The mixture of different amendments can produce better results to improve the BRDA conditions. A study by Bray et al., (2018) presents how mixing different amounts of gypsum, organic matter (mushroom compost), and sand reduce the pH and sodium presence. However, only the first meter shows a substantial improvement over 20 years.

Extrapolating the results of the sequential batch leaching test to the residence time under field conditions in the upper 0.25 meters of the BRDA will remain an unfavorable environment for plants growth for more than 25 years (Wik, 2020). This creates a major challenge to remediate these extremely deteriorated areas.

Finally, one of the main limitations of this study has been that the behavior of the amendments in the bauxite residue could not be followed over time. Several studies show significant changes in pH, alkalinity, and sodicity decades after amendments have been

applied (Bray et al., 2018). This study is restricted to the immediate changes after application of amendments and the first steps of amelioration of the bauxite residue. The high pH and alkalinity are not the only factors that limit the rehabilitation of the BRDA. The presence of toxic elements for plant growth such as vanadium and chromium is a crucial topic to consider. These elements were still present in the solid phase after five leaching steps, and the availability for plants is a topic of concern that should be studied in more detail for the full recovery of the BRDA.

7.5 Sources of error

Several sources of error could have influenced the results in this study. The instrument used to measure pH must be calibrated before being used with a neutral pH. The same procedure should be performed for the EC instrument previously calibrated to 0.01 M KCL. In addition, the electrodes were cleaned with distilled water before and after use. If the calibration is incorrect and there is possible contamination, the incorrect pH could have given an inaccurate determination of the buffer capacity and distribution of species. These can subsequently influence the results of the computational modelling by an incorrect activity of alkalinity and equilibrium phases (Appelo & Postma, 2004).

The sequential batch leaching test shows a loss of solid fraction due to liquid extraction in each iteration. This loss was quantified to be 2.6% per leaching step. This small solid loss could occur when the solid is collected on the 0.45 µm filter and on the electrode when the EC is measured. However, the behavior of the sequential batch leaching test is possible to be analyzed and, in further studies, this loss of solid should be taken in consideration.

Analytical uncertainties like the detection limit can influence the results. Detection limits are considered satisfactory for F, Cl, Br, and NO_3 with IC and Na, K, Mg, Al, V, Cr, Mn, Fe, Cu, Zn, Ga, and As with ICP-MS. What is more, the standard deviation of the samples increases when approaching the detection limit especially for Mn, NO_3, Cu, and Zn. Furthermore, the concentrations of SO_4 and PO_4 are outside of the detection limit and only present until the third leaching step in gypsum for PO_4.

In the case of CFA, the measurements of dissolved silica showed a consistently leached trend in the replicates of the experiment even though it shows a significant deviation error in the replicates of the samples with or without amendments. This could be attributed to the sensitivity of total silica dissolved at this high pH, which could have been influenced by

storage of the samples and the experiment should be performed immediately after the completion of the batch leaching test to reduce the precipitation of dissolved silica in the samples and avoid possible changes with time.

One of the limitations of using PHREEQC numerical code is that the available databases of thermodynamic data (phreeqc.dat or llnl.dat) do not include the thermodynamic equations for critical minerals in bauxite residue such as sodalite, cancrinite, or other minerals that can be categorized as desilication products (DSP). This factor limits the applicability of the calculation of saturation indices and the possible minerals that can precipitate in the presence or absence of CO_2. In addition, the CO_2 concentration used in the simulations may differ from what can be expected at the study site, especially the varying partial pressure in the local soil.

8 Conclusions

Large amounts of bauxite residue are produced worldwide and rehabilitation of these disposal sites is a major challenge. In this thesis, several amendments were studied to improve rehabilitation. The results found in this thesis help to develop bauxite residue rehabilitation plans to stimulate soil formation and has generated basic knowledge for future closure plans of BRDAs. Bauxite residue amendments with açaí seed, soil, and gypsum in a proportion of 10% improved the environmental conditions in the residue improving the conditions for plant growth and rehabilitation of the affected area. However, these amendments are not enough to guarantee the basic conditions for plant growth.

The location of Hydro's bauxite refinery presents its own challenge for the possible ameliorated solutions. In this specific case, gypsum amendment might give the best results for reduction of pH, SAR, and ESP% initially. However, in the long term, it is not the most beneficial amendment. If the local availability makes açaí a sustainable alternative and the need to increase the organic carbon in the red mud is considered, açaí seed is one of the best natural amendment alternatives based on nutritional analysis and its ability to reduce the sodicity, EC, and pH. For the initial dissolved concentrations of Na, Al, Ca, Fe, Cr and V, soil is the amendment which leached out the most, followed by açaí and gypsum. Nevertheless, considering all the experimental results, açaí is the best amendment sustained until the conclusion of the experiment, improving the chemical stability of bauxite residue.

Despite the fact that these amendments can ameliorate some of the conditions for plant growth on the bauxite residue, the master variable pH is not possible to clearly reduce without neutralization of bauxite residue with carbon dioxide. This reaction is feasible to occur at the study site if a certain amount of time is given. Carbon dioxide can promote the precipitation of different carbonate minerals leading to the reduction of pH. The reaction with carbon dioxide can also reduce leaching of the Na, Al, and Ca. Additionally, the geochemical model created with PHREEQC shows potential mineral formations. The secondary minerals which might form under the specified conditions are diaspore ($AlOH_2$), calcite ($CaCO_3$), goethite (FeOOH), kaolinite ($Al_2SiO_2O_5(OH)_4$) and pyrolusite (MnO_2) with all amendments and atmospheric CO_2.

The pH is not the only parameter to address, it is also relevant to consider other parameters. It is also important to reduce the high alkalinity of the bauxite residue with amendments and

carbon dioxide. Moreover, the vanadium and chromium are consistently present in the BRDA in the solid phases after the completion of the batch test. This can have toxic effects for plant growth and should be studied further. In general, for the successful rehabilitation of the bauxite residue in the northeastern state of Pará, Brazil, it is required to take all of the following into account: the pH, EC, SAR, ESP%, acid buffer capacity, major chemical composition change, and reaction with carbon dioxide in the atmosphere and soil.

9 Further work

For a successful remediation of the BRDA in Pará, some of the physical chemical characteristics need to be addressed in addition to the chemical processes studied here. The physical properties of the bauxite residue will change with the amendments such as porosity, permeability, hydraulic conductivity, and waterlogging. These processes need to be considered in further studies. The understanding of these parameters can decide which of the amendments gives the optimal outcome for rehabilitation of the BRDA.

The reduction of alkalinity can be studied while the pH declines with the presence of CO_2 in the gas phase. Further studies can analyze the changes of mineral reactions related to sodium hydroxide trapping CO_2 and the diffusion rates and kinetics of these processes not considered in this study. Some carbonization trials can be performed at the field site that focus on the chemical behavior of the bauxite residue, including the effect of different amendments. It is crucial to perform these experiments over a significant amount of time to see the changes in the composition of the mixture of bauxite residue and amendments in the presence of CO_2. Additionally, the experiment should quantify the potential of long term CO_2 sequestration in BRDAs. This will allow for the assessment of the changes in leaching behavior and aid in an understanding of how these sites can be treated with local available and affordable waste materials like açaí seed.

In the process of improving the environmental conditions at a BRDA, the inclusion of amendments could generate the most beneficial long-lasting conditions suitable for native plant growth. This can be done using each amendment or a mixture of amendments to study plant response and design successful rehabilitation of industrial aluminum waste.

10 References

Appelo, C. A. J. & Postma, D. 2004. Geochemistry, groundwater and pollution. 2nd Edition, Balkema, Rotterdam. http://dx.doi.org/10.1201/9781439833544

Berner, R.A., 1971. Principles of chemical sedimentology. McGraw-Hill New York, 240 pp.

Barrow, N. J. (1982). Possibility of using caustic residue from bauxite for improving the chemical and physical properties of sandy soils. Australian Journal of Agricultural Research 33, 275–285.

Borra, C. R., Pontikes, Y., Binnemans, K. & Van Gerven, T. (2015). Leaching of rare earths from bauxite residue (red mud). *Minerals engineering*, *76*, s. 20–27. doi:10.1016/j.mineng.2015.01.005.

Bray, A. W., et al. (2018). "Sustained Bauxite Residue Rehabilitation with Gypsum and Organic Matter 16 years after Initial Treatment." Environ Sci Technol 52(1): 152-161. doi:10.1021/acs.est.7b03568

Cooling, D. J. (2007). Improving the sustainability of residue management practices—Alcoa World Alumina. In A. B. Fourie and R. J. Jewell (Eds.), Paste 2007—Proceedings of the Tenth International Seminar on Paste and Thickened Tailings (pp. 3–15). Australian Center for Geomechanics, Perth, Australia.

Costa, M. L. (1991). "Aspectos Geológicos Dos Lateritos Da Amazônia " Revista Brasileira de Geociências 21(2): 146-160, junho de 1991

Courtney, R. & Kirwan, L. (2012). Gypsum amendment of alkaline bauxite residue – Plant available aluminium and implications for grassland restoration. Ecological engineering, 42, s. 279–282. doi:10.1016/j.ecoleng.2012.02.025

Courtney, R., Timpson, J. P. & Grennan, E. (2003). Growth of Trifolium pratense in Red Mud Amended With Process Sand, Gypsum and Thermally Dried Sewage Sludge. *International journal of surface mining, reclamation and environment*, *17* (4), s. 227–233. doi:10.1076/ijsm.17.4.227.17481

Crisponi, G., Nurchi, V. M., Faa, G., & Remelli, M. (2011). Human diseases related to aluminium overload. *Monatshefte für Chemie-Chemical Monthly*, *142*(4), 331.

Doucet, F.J., 2010. Effective CO2-specific sequestration capacity of steel slags and variability in their leaching behavior in view of industrial mineral carbonation. Miner. Eng. 23, 262e269.

Evans, K. (2016). The History, Challenges, and New Developments in the Management and Use of Bauxite Residue. *Journal of sustainable metallurgy*, *2* (4), s. 316–331. doi:10.1007/s40831-016-0060-x

Evans, K. (2015). Successes and challenges in the management and use of bauxite residue. Bauxite residue valorisation and best practices, Leuven, Belgium, 53-60.

Franzen D. and Wick, A., 2021. Saline and Sodic Soils. Available: https://www.ag.ndsu.edu/langdonrec/soil-health/saline-sodic-soils [Accessed 12.01.2021]

Freire, T. S. S. et al. (2012). Electroacoustic Isoelectric Point Determinations of Bauxite Refinery Residues: Different Neutralization Techniques and Minor Mineral Effects. *Langmuir*, *28* (32), s. 11802–11811. doi:10.1021/la301790v

Fuller, R.D., Nelson, E.D.P., Richardson, C.J., 1982. Reclamation of red mud (bauxite residues) using alkaline-tolerant grasses with organic amendments. J. Environ. Qual. 11 (3), 533–539.

Gill, R. (2014). Modern Analytical Geochemistry: an introduction to quantitative chemical analysis techniques for Earth, environmental and materials scientists. Routledge.

Gomes, H. I., Mayes, W. M., Rogerson, M., Stewart, D. I. & Burke, I. T. (2016). Alkaline

residues and the environment: a review of impacts, management practices and opportunities. *Journal of cleaner production, 112*, s. 3571–3582. doi:10.1016/j.jclepro.2015.09.111
Gräfe, M., Power, G., & Klauer, C. (2011). Bauxite residue issues: III. Alkalinity and associated chemistry. Hydrometallurgy, 108(1), 60-79. doi:10.1016/j.hydromet.2011.02.004
Hanson, P.J., Edwards, N.T., Garten, C.T. and Andrews, J.A., 2000. Separating root and soil microbial contributions to soil respiration: A review of methods and observations. Biogeochem. 48, 115–146.
Harris, D. C. (2010). Quantitative chemical analysis. Macmillan.
Horneck, D.S., Ellsworth, J.W., Hopkins, B.G., Sullivan, D.M., Stevens, R.G., 2007. Managing Salt-Affected Soils for Crop Production. PNW 601-E. Oregon State University, University of Idaho, Washington State University
Hue, N. V. (1995). Sewage sludge. In J. E. Rechcigl (Ed.), Soil amendments and environmental quality (pp. 199–247). Lewis, Boca Raton, FL.
INMET, (2020). NORMAIS CLIMATOLÓGICAS DO BRASIL. Retrieved from http://www.inmet.gov.br/portal/index.php?r=clima/normaisClimatologicas [Accessed 02.01.2021]
Jones, B. E. H. and R. J. Haynes (2011). "Bauxite Processing Residue: A Critical Review of Its Formation, Properties, Storage, and Revegetation." Critical Reviews in Environmental Science and Technology 41(3): 271-315.
King, H. M. 2021 Almost all of the aluminum that has ever been produced has been made from bauxite. Available: https://geology.com/minerals/bauxite.shtml [Accessed 15.04.2021]
Kong, X., et al. (2018). "Development of alkaline electrochemical characteristics demonstrates soil formation in bauxite residue undergoing natural rehabilitation." Land Degradation & Development 29(1): 58-67.
Kotschoubey, Basile & Calaf, José & Lobato, Augusto & Leite, Alessandro & Azevedo, Carlos. (2005). Caracterização e gênese dos depositos de bauxita da Provincia Bauxitifera de Paragominas, noroeste da Bacia do Grajau, nordeste do Para/oeste do Maranhão; 687-782.
Kumar, S., Kumar, R., and Bandopadhyay, A. (2006). Innovative methodologies for the utilization of wastes from metallurgical and allied industries. Resources, Conservation and Recycling 48, 301–314.
Kunzler, C., Alves, N., Pereira, E., Nienczewski, J., Ligabue, R., Einloft, S., Dullius, J.,2011. CO2 storage with indirect carbonation using industrial waste. Energy Procedia 4, 1010e1017.
Liu, C., et al., 2007. Adsorption removal of phosphate from aqueous solution by active red mud. J. Environ. Sci. 19 (10), 1166–1170 China
Marin Rivera, R., Ulenaers, B., Ounoughene, G., Binnemans, K., & Van Gerven, T. (2017). Behaviour of silica during metal recovery from bauxite residue by acidic leaching. In *Travaux 46, Proceedings of 35th International ICSOBA Conference, Hamburg, Germany, 2–5 October, 2017.* (pp. 547-556).
Medeiros, A. C., et al. (2017). "Quality index of the surface water of Amazonian rivers in industrial areas in Para, Brazil." Mar Pollut Bull 123(1-2): 156-164.
Melo, P. S. et al. (2021). Açaí seeds: An unexplored agro-industrial residue as a potential source of lipids, fibers, and antioxidant phenolic compounds. Industrial crops and products, 161, s. 113204. doi:10.1016/j.indcrop.2020.113204.
Meyer, F. M. (2004). Availability of bauxite reserves. Natural Resources Research 13,

161–172.
Milačič, R., Zuliani, T. & Ščančar, J. (2012). Environmental impact of toxic elements in red mud studied by fractionation and speciation procedures. *Science of the total environment*, *426*, s. 359–365. doi:10.1016/j.scitotenv.2012.03.080
Ministério Público do Estado do Pará (MP-PA)/Ministério Público Federal (MPF-PA), 2015. Inquérito civil público n° 1.23.000.000661/2015-70: Ação civil pública com pedido de liminar. http://www.mpf.mp.br/pa/sala-de-imprensa/documentos/2016/ acp-agua-potavel-barcarena.
Moors, E. H. M. (2006). Technology strategies for sustainable metals production systems: A case study of primary aluminum production in The Netherlands and Norway. Journal of Cleaner Production 14, 1121–1138.
Nguyen, Q. D., and Boger, D. V. (1998). Application of rheology to solving tailings disposal problems. International Journal of Mineral Processing 54, 217–233.
Pan, S.-Y., Chang, E., Chiang, P.-C., 2012. CO2 capture by accelerated carbonation of alkaline wastes: a review on its principles and applications. Aerosol Air Qual. Res. 12, 770e791.
Pan, X., Yu, H. & Tu, G. (2015). Reduction of alkalinity in bauxite residue during Bayer digestion in high-ferrite diasporic bauxite. *Hydrometallurgy*, *151*, s. 98–106. doi:10.1016/j.hydromet.2014.11.015
Paramguru, R. K., Rath, P. C., and Misra, V. N. (2005). Trends in red mud utilization—a review. Mineral Processing and Extractive Metallurgy Review 26, 1–29.
Parkhurst, D. L., & Appelo, C. A. J. (1999). User's guide to PHREEQC (Version 2): A computer program for speciation, batch-reaction, one-dimensional transport, and inverse geochemical calculations. Water-resources investigations report, 99(4259), 312.
Santini, T., Fey, M. & Gilkes, R. (2015). Experimental Simulation of Long Term Weathering in Alkaline Bauxite Residue Tailings. *Metals*, *5* (3), s. 1241–1261. doi:10.3390/met5031241
Schneider, Jan. (2020) Mineralogical and Geotechnical Characterization of Bauxite Residue A case study from NE Brazil. Master thesis, University of Oslo.URN:NBN:no-84857
Seelig, B. (2000). Salinity and sodicity in North Dakota soils. Available: https://library.ndsu.edu/ir/bitstream/handle/10365/5412/eb57.pdf?sequence=1 [Accessed 03.04.2021]
Seilsepour, M., Rashidi, M., & Khabbaz, B. G. (2009). Prediction of soil exchangeable sodium percentage based on soil sodium adsorption ratio. *American-Eurasian Journal of Agricultural and Environmental Sciences*, *5*(1), 1-4.
Su, C., Suarez, D.L., 1997. In situ infrared speciation of adsorbed carbonate of aluminum and iron oxides. Clays Clay Miner. 45 (6), 814–825.
Sun, Q., An,S.,Yang,L.,Wang,Z.,2004. Chemical properties of the upper tailings beneath biotic crusts. Ecol. Eng. 23,47–53.
Thornber, M.R., Binet, D., 1999. Caustic soda adsorption on Bayer residues. In: Alumina, Worsley (Ed.), 5th International Alumina Quality Workshop. Bunbury, AQW Inc., pp. 498–507.
Towett, E. K., Shepherd, K. D. & Lee Drake, B. (2016). Plant elemental composition and portable X-ray fluorescence (pXRF) spectroscopy: quantification under different analytical parameters. *X-ray spectrometry*, *45* (2), s. 117–124. doi:10.1002/xrs.2678
US Salinity Laboratory Staff (1954) Diagnosis and improvement of saline and alkali soils. US Department of Agriculture Handbook 60, Washington, DC.
Van der Sloot, H. A., & Kosson, D. S. (2010). Leaching Assessment Methodologies For Disposal And Use of Bauxite Residues. Hans van der Sloot Consultancy

Vardar F, Ünal M. Aluminum toxicity and resistance in higher plants: review. Adv Mol Biol 2007;1:1-12.
Wehr, J. B., Fulton, I., and Menzies, N. W. (2006). Revegetation strategies for bauxite refinery residue: A case study of Alcan Gove in Northern Territory, Australia. Environmental Management 37, 297–306.
Wehr, J. B., So, H. B., Menzies, N. W., and Fulton, I. (2005). Hydraulic properties of layered soils influence survival of Rhodes grass (Chloris gayana Kunth.) during water stress. Plant and Soil 270, 287–297.
Wentworth, C. K. (1922). A Scale of Grade and Class Terms for Clastic Sediments. *The Journal of Geology*, *30*(5), 377-392. Retrieved from www.jstor.org/stable/30063207
Whittington, B. I. (1996). The chemistry of CaO and Ca(OH)2 relating to the Bayer process. Hydrometallurgy 43, 13–35.
WHO (2003). Aluminium in drinking-water: background document for development of WHO guidelines for drinking-water quality. Addendum to Vol. 2Health criteria and other supporting information. Geneva: World Health Organization; 2003. Access online February 27, 2012. http://www.who.int/water_sanitation_health/dwq/chemicals/en/aluminium.pdf
Wik, Sebastian Aas. (2020) Mobility of Chemical Elements in Bauxite Residue: A case study from NE Brazil. Master thesis, University of Oslo. URN:NBN:no-83792
Witt, K. J., and Schönhardt, M. (2004). Tailings management facilities–-risks and reliability. Report of the European RTD project TAILSAFE.
Wong, J. W. C., and Ho, G. E. (1991). Effects of gypsum and sewage-sludge amendment on physical properties of fine bauxite refining residue. Soil Science 152, 326–332.
Wong, J. W. C., and Ho, G. (1994). Sewage-sludge as organic ameliorant for revegetation of fine bauxite refining residue. Resources Conservation and Recycling 11, 297–309.
Woodburn, K., Walton, R., Mccrohan, C. & White, K. (2011). Accumulation and toxicity of aluminium-contaminated food in the freshwater crayfish, Pacifastacus leniusculus. *Aquatic toxicology*, *105* (3-4), s. 535–542. doi:10.1016/j.aquatox.2011.08.008
World aluminum 2015 Bauxite Residue Management: Best practice Available: https://bauxite.world-aluminium.org/fileadmin/user_upload/Bauxite_Residue_Management_-_Best_Practice__English__Compressed.pdf [Accessed 04.02.2021]
Xue, S. et al. (2016). A review of the characterization and revegetation of bauxite residues (Red mud). *Environmental science and pollution research*, *23* (2), s. 1120–1132. doi:10.1007/s11356-015-4558-8
Zingaretti, D., Costa, G. & Baciocchi, R. (2014). Assessment of Accelerated Carbonation Processes for CO2Storage Using Alkaline Industrial Residues. *Industrial & engineering chemistry research*, *53* (22), s. 9311–9324. doi:10.1021/ie403692h

11 Appendix

Appendix 1. Initial amount used in each sequential batch leaching test.

Sample	BR (g)	ANM (g)	TOTAL (g)	Water (g)	l/S
BR1	3.90		3.90	38.96	10
BR2	3.90		3.90	38.96	10
BR3	3.90		3.90	38.96	10
BRA1	3.90	0.42	4.32	43.18	10
BRA2	3.90	0.42	4.32	43.18	10
BRA3	3.90	0.42	4.32	43.18	10
BRG1	3.90	0.41	4.31	43.06	10
BRG2	3.90	0.41	4.31	43.06	10
BRG3	3.90	0.41	4.31	43.06	10
BRS1	3.90	0.43	4.33	43.26	10
BRS2	3.90	0.43	4.33	43.26	10
BRS3	3.90	0.43	4.33	43.26	10

Appendix 2. Sequential batch leaching test: loss of solid material after 32 days of the experiment.

Sample	Tube with cap	Tube with cap + Total Solid (g) BEFORE DRY	Tube with cap + Total Solid (g) AFTER DRY	Solid lost after 5 weeks (g) with cap	Remain of solid (g) with cap	loss of solid (%) with cap	Per week loss %
BR1	13.36	16.96	16.51	22.13	3.15	12.54	2.51
BR2	13.46	17.06	16.60	21.95	3.13	12.98	2.60
BR3	13.70	17.30	16.80	22.11	3.10	13.76	2.75
BRA1	13.49	17.49	16.88	25.68	3.39	15.15	3.03
BRA2	13.39	17.39	16.79	26.04	3.40	15.13	3.03
BRA3	13.41	17.41	16.80	25.81	3.39	15.21	3.04
BRS1	13.50	17.50	17.12	25.80	3.62	9.50	1.90
BRS2	13.52	17.52	17.14	25.84	3.62	9.53	1.91
BRS3	13.50	17.50	17.15	25.81	3.65	8.77	1.75
BRG1	13.35	17.35	16.71	25.81	3.36	15.99	3.20
BRG2	13.44	17.44	16.76	25.69	3.32	16.98	3.40
BRG3	13.48	17.48	16.84	25.62	3.36	16.01	3.20
						Total average	2.69

Appendix 3. Acid buffer capacity values for the initial 10 ml of each sample.

		pH	volume ml	Conc. HCl mol/l	mols Acid mmol	Buffer capacity mol/l
1	1WBR1	4.6	2.5	0.1	2.50E-01	2.50E-02
2	1WBR2	4.6	2.3	0.1	2.30E-01	2.30E-02
3	1WBR3	4.6	2.2	0.1	2.20E-01	2.20E-02
4	1WBRA1	4.5	1.8	0.1	1.80E-01	1.80E-02
5	1WBRA2	4.4	1.8	0.1	1.80E-01	1.80E-02
6	1WBRA3	4.4	1.8	0.1	1.80E-01	1.80E-02
7	1WBRS1	4.8	2.3	0.1	2.30E-01	2.30E-02
8	1WBRS2	3.1	2.6	0.1	2.60E-01	2.60E-02
9	1WBRS3	4.4	2	0.1	2.00E-01	2.00E-02
10	1WBRG1	4.5	5.7	0.001	5.65E-03	5.65E-04
11	1WBRG2	4.5	13.6	0.001	1.36E-02	1.36E-03
12	1WBRG3	4.5	15.0	0.001	1.50E-02	1.50E-03
13	2WBR1	4.7	1.5	0.1	1.50E-01	1.50E-02
14	2WBR2	4.8	1.1	0.1	1.10E-01	1.10E-02
15	2WBR3	5.1	1	0.1	1.00E-01	1.00E-02
16	2WBRA1	4.8	1	0.1	1.00E-01	1.00E-02
17	2WBRA2	4.8	1	0.1	1.00E-01	1.00E-02
18	2WBRA3	4.3	1	0.1	1.00E-01	1.00E-02
19	2WBRS1	3.9	1	0.1	1.00E-01	1.00E-02
20	2WBRS2	4.7	1	0.1	1.00E-01	1.00E-02
21	2WBRS3	4.4	1	0.1	1.00E-01	1.00E-02
22	2WBRG1	4.1	0.55	0.001	5..50E-04	5.50E-05
23	2WBRG2	4.6	2.35	0.001	2.35E-03	2.35E-04
24	2WBRG3	4.6	4.15	0.001	4.15E-03	4.15E-04
25	3WBR1	3.9	1.1	0.1	1.10E-01	1.10E-02
26	3WBR2	4.1	0.7	0.1	7.00E-02	7.00E-03
27	3WBR3	3.7	0.8	0.1	8.00E-02	8.00E-03
28	3WBRA1	3.7	0.7	0.1	7.00E-02	7.00E-03
29	3WBRA2	4.0	0.7	0.1	7.00E-02	7.00E-03
30	3WBRA3	3.7	0.7	0.1	7.00E-02	7.00E-03
31	3WBRS1	3.7	1	0.1	1.00E-01	1.00E-02
32	3WBRS2	3.6	1	0.1	1.00E-01	1.00E-02
33	3WBRS3	4.0	0.8	0.1	8.00E-02	8.00E-03
34	3WBRG1	4.3	1.25	0.0005	6.25E-04	6.25E-05
35	3WBRG2	4.6	6.8	0.0005	3.40E-03	3.40E-04
36	3WBRG3	n.a	n.a	n.a	n.a	n.a
37	4WBR1	5.0	0.8	0.1	8.00E-02	8.00E-03
38	4WBR2	4.7	0.7	0.1	7.00E-02	7.00E-03
39	4WBR3	3.7	0.7	0,1	7.00E-02	7.00E-03
40	4WBRA1	4.8	1.45	0.01	1.45E-02	1.45E-03
41	4WBRA2	4.3	3.45	0.01	3.45E-02	3.45E-03
42	4WBRA3	4.6	3.45	0.01	3.45E-02	3.45E-03
43	4WBRS1	4.4	4.75	0.01	4.75E-02	4.75E-03

44	4WBRS2	4.3	4.75	0.01	4.75E-02	4.75E-03
45	4WBRS3	4.3	4.75	0.01	4.75E-02	4.75E-03
46	4WBRG1	8.7	20	0.0005	n.a	n.a
47	4WBRG2	10.3	20	0.0005	n.a	n.a
48	4WBRG3	10.5	20	0.0005	n.a	n.a
49	5WBR1	4.6	5.65	0.01	5.65E-02	5.65E-03
50	5WBR2	n.a	n.a	0.01	n.a	n.a
51	5WBR3	4.5	4.45	0.01	4.45E-02	4.45E-03
52	5WBRA1	4.5	3.85	0.01	3.85E-02	3.85E-03
53	5WBRA2	4.6	3.85	0.01	3.85E-02	3.85E-03
54	5WBRA3	4.6	3.85	0.01	3.85E-02	3.85E-03
55	5WBRS1	4.5	4.25	0.01	4.25E-02	4.25E-03
56	5WBRS2	4.5	4.25	0.01	4.25E-02	4.25E-03
57	5WBRS3	4.5	4.25	0.01	4.25E-02	4.25E-03
58	5WBRG1	4.6	3.35	0.01	3.35E-02	3.35E-03
59	5WBRG2	4.8	3.35	0.01	3.35E-02	3.35E-03
60	5WBRG3	4.8	3.25	0.01	3.25E-02	3.25E-03

Appendix 4. Values of pH and EC for the Simulation 5 S-5 and Simulation 6 S-6. Considering their liquid-solid ratio (L/S) and description of amendments.

L/S	Description	pH					E.C µS/cm				
		Lab.	S-5	% difference	S-6	% difference	Lab.	S-5	% difference	S-6	% difference
10	BR	11.98	9.34	22	7.64	36	3290	1680	49	1755	47
	Açaí	11.76	9.34	21	7.61	35	2370	1656	30	1711	28
	Soil	11.93	9.34	22	7.65	36	2990	1784	40	1848	38
	Gypsum	10.92	9.6	12	7.96	27	4380	3628	17	4538	4
20	BR	11.82	9.18	22	7.41	37	1900	1050	45	1079	43
	Açaí	11.54	9.21	20	7.46	35	1380	1192	14	1236	10
	Soil	11.76	9.17	22	7.39	37	1650	1013	39	1049	36
	Gypsum	10.94	9.43	14	7.79	29	2920	2129	27	3001	3
30	BR	11.69	9.07	22	7.27	38	1210	769	36	799	34
	Açaí	11.33	9.09	20	7.29	36	903	806	11	843	7
	Soil	11.61	9.08	22	7.28	37	1120	798	29	835	25
	Gypsum	11.41	9.1	20	7.27	36	1160	829	28	935	19
40	BR	11.6	8.98	23	7.15	38	939	601	36	618	34
	Açaí	11.29	8.93	21	7.1	37	679	527	22	544	20
	Soil	11.35	8.99	21	7.16	37	832	611	27	630	24
	Gypsum	11.55	8.94	23	7.08	39	932	526	44	562	40
50	BR	11.52	8.92	23	7.08	39	776	509	34	517	33
	Açaí	11.23	8.88	21	7.05	37	577	470	18	490	15
	Soil	11.32	8.92	21	7.1	37	712	526	26	536	25
	Gypsum	11.47	8.93	22	7.09	38	830	542	35	592	29

Appendix 5. Sodium adsorption ratio and exchangeable sodium percentage per leaching step with their respective days. Mean ± standard error values are shown (n=3).

Leaching Step	Days	Amendments	SAR	ESP %
1	7	None	15.69 ± 0.93	17.94 ± 0.93
		Açaí	15.61 ± 0.54	17.87 ± 0.54
		Soil	17.06 ± 0.55	19.29 ± 0.53
		Gypsum	9.05 ± 0.13	10.78 ± 0.16
2	14	None	10.00 ± 0.72	11.88 ± 0.83
		Açaí	10.65 ± 0.34	10.65 ± 0.38
		Soil	10.66 ± 0.78	12.63 ± 0.89
		Gypsum	3.71 ± 0.17	4.04 ± 0.02
3	21	None	6.68 ± 0.24	7.91± 0.30
		Açaí	7.47 ± 0.44	8.88 ± 0.53
		Soil	6.83 ± 0.17	8.11 ± 0.21
		Gypsum	3.13 ± 0.19	3.24 ± 0.26
4	28	None	6.19 ± 0.17	7.30 ± 0.22
		Açaí	8.02 ± 0.92	9.55 ± 1.11
		Soil	6.47 ± 0.24	7.65 ± 0.31
		Gypsum	2.87 ± 0.47	2.89 ± 0.65
5	35	None	4.50 ± 3.18	5.33 ± 3.77
		Açaí	6.73 ± 0.13	7.97 ± 0.16
		Soil	7.55 ± 0.41	8.99 ± 0.50
		Gypsum	1.90 ± 0.07	1.52 ± 0.10

Appendix 6. Dilution factor used for IC-PMS for all samples.

#	Sample	Weight Sample (g)	Total Weight (sample + HNO3 1%) (g)	Dilution Factor
1	1WBR1	0.1	5.04	50.40
2	1WBR2	0.1	5.14	51.40
3	1WBR3	0.1	5.2	52.00
4	1WBRA1	0.1	5.04	50.40
5	1WBRA2	0.1	5.06	50.60
6	1WBRA3	0.1	5.1	51.00
7	1WBRS1	0.1	5.04	50.40
8	1WBRS2	0.1	5.16	51.60
9	1WBRS3	0.1	5.04	50.40
10	1WBRG1	0.1	5.04	50.40
11	1WBRG2	0.1	5.04	50.40

12	1WBRG3	0.1	5	50.00
13	2WBR1	0.1	5.02	50.20
14	2WBR2	0.1	5.01	50.10
15	2WBR3	0.1	5	50.00
16	2WBRA1	0.09	4.91	54.56
17	2WBRA2	0.1	5.03	50.30
18	2WBRA3	0.1	5.05	50.50
19	2WBRS1	0.1	5.05	50.50
20	2WBRS2	0.09	4.57	50.78
21	2WBRS3	0.09	4.69	52.11
22	2WBRG1	0.1	5.02	50.20
23	2WBRG2	0.1	4.99	49.90
24	2WBRG3	0.09	4.52	50.22
25	3WBR1	0.1	5.04	50.40
26	3WBR2	0.1	5.11	51.10
27	3WBR3	0.1	5.11	51.10
28	3WBRA1	0.09	4.56	50.67
29	3WBRA2	0.1	5.07	50.70
30	3WBRA3	0.1	5	50.00
31	3WBRS1	0.1	5.05	50.50
32	3WBRS2	0.1	5.07	50.70
33	3WBRS3	0.1	5.06	50.60
34	3WBRG1	0.1	4.91	49.10
35	3WBRG2	0.1	5.07	50.70
36	3WBRG3	0.1	5.01	50.10
37	4WBR1	0.1	5.07	50.70
38	4WBR2	0.1	5.04	50.40
39	4WBR3	0.1	5.04	50.40
40	4WBRA1	0.1	5.1	51.00
41	4WBRA2	0.1	5.06	50.60
42	4WBRA3	0.1	5.06	50.60
43	4WBRS1	0.1	5.06	50.60
44	4WBRS2	0.1	5.01	50.10
45	4WBRS3	0.1	5.34	53.40
46	4WBRG1	0.1	5.05	50.50
47	4WBRG2	0.1	5.07	50.70
48	4WBRG3	0.1	5.02	50.20
49	5WBR1	0.1	5.03	50.30
50	5WBR2	0.1	5.06	50.60
51	5WBR3	0.1	5.26	52.60
52	5WBRA1	0.1	5.07	50.70
53	5WBRA2	0.1	5.18	51.80
54	5WBRA3	0.1	5.08	50.80

55	5WBRS1	0.1	5.08	50.80
56	5WBRS2	0.1	5.18	51.80
57	5WBRS3	0.1	5.08	50.80
58	5WBRG1	0.1	5.01	50.10
59	5WBRG2	0.1	5	50.00
60	5WBRG3	0.1	5.13	51.30

Appendix 7. Master table: values selected from IC with a dilution factor of 10 and 100, ICP-MS dilution factor of 50, and CFA.

No.	Units (mg/L)	Methods																		
		IC x10				IC x100			ICP-MS x50											CFA
		F	Cl	Br	NO3	Ca	SO4	PO4	Na	K	Mg	Al	V	Cr	Mn	Fe	Cu	Zn	Ga	As	Dissolved Silica
1	1WBR1	1.18E+00	3.26E+00	n.a.	3.16E+00	7.26E+01	n.a.	n.a.	4.47E+02	1.02E+00	n.a.	1.35E+02	5.00E-01	6.00E-02	1.00E-02	n.a.	1.30E-01	8.00E-02	1.90E-01	1.00E-02	2.13E-01
2	1WBR2	1.29E+00	3.26E+00	n.a.	3.25E+00	5.88E+01	n.a.	n.a.	4.48E+02	1.08E+00	n.a.	1.44E+02	5.60E-01	5.00E-02	n.a.	n.a.	1.00E-02	1.00E-02	1.90E-01	2.00E-02	9.88E+00
3	1WBR3	1.35E+00	3.17E+00	n.a.	3.20E+00	5.85E+01	n.a.	n.a.	4.61E+02	9.50E-01	n.a.	1.55E+02	6.20E-01	6.00E-02	n.a.	n.a.	2.00E-02	1.00E-02	2.00E-01	2.00E-02	9.22E+00
4	2WBR1	6.40E-01	2.06E+00	n.a.	3.11E+00	3.65E+01	n.a.	n.a.	2.41E+02	5.50E-01	n.a.	6.29E+01	3.50E-01	2.00E-02	n.a.	n.a.	0.00E+00	1.00E-02	6.00E-02	1.00E-02	1.21E+01
5	2WBR2	5.90E-01	2.00E+00	n.a.	3.12E+00	3.79E+01	n.a.	n.a.	2.19E+02	6.20E-01	n.a.	5.46E+01	3.80E-01	2.00E-02	n.a.	2.00E-02	0.00E+00	1.00E-02	4.00E-02	1.00E-02	1.26E+01
6	2WBR3	6.10E-01	2.03E+00	n.a.	3.12E+00	4.14E+01	n.a.	n.a.	2.16E+02	5.60E-01	n.a.	5.22E+01	4.50E-01	2.00E-02	n.a.	2.00E-02	1.00E-02	2.00E-02	4.00E-02	1.00E-02	1.61E+01
7	3WBR1	4.00E-01	1.82E+00	n.a.	3.55E+00	5.25E+01	n.a.	n.a.	1.67E+02	4.90E-01	n.a.	3.81E+01	3.10E-01	1.00E-02	n.a.	3.00E-02	1.00E-02	2.00E-02	2.00E-02	1.00E-02	1.69E+01
8	3WBR2	3.70E-01	1.77E+00	n.a.	3.40E+00	3.87E+01	n.a.	n.a.	1.56E+02	4.40E-01	n.a.	3.40E+01	3.30E-01	3.00E-02	1.00E-02	7.00E-02	1.30E-01	7.00E-02	2.00E-02	n.a.	4.66E-01
9	3WBR3	3.80E-01	1.94E+00	n.a.	3.54E+00	3.90E+01	n.a.	n.a.	1.54E+02	2.14E+00	4.00E-02	3.24E+01	3.70E-01	1.00E-02	n.a.	1.30E-01	1.00E-02	1.20E-01	2.00E-02	1.00E-02	2.13E+01
10	4WBR1	3.40E-01	1.66E+00	n.a.	3.42E+00	3.36E+01	n.a.	n.a.	1.26E+02	4.00E-01	n.a.	2.70E+01	2.60E-01	1.00E-02	n.a.	8.00E-02	0.00E+00	2.00E-02	1.00E-02	1.00E-02	9.91E-01
11	4WBR2	3.40E-01	1.81E+00	n.a.	3.40E+00	2.83E+01	n.a.	n.a.	1.21E+02	3.80E-01	n.a.	2.53E+01	2.70E-01	1.00E-02	0.00E+00	1.50E-01	1.00E-01	5.00E-02	1.00E-02	1.00E-02	1.05E+00
12	4WBR3	3.30E-01	1.69E+00	n.a.	3.47E+00	2.84E+01	n.a.	n.a.	1.23E+02	4.90E-01	n.a.	2.53E+01	2.70E-01	n.a.	n.a.	4.50E-01	1.00E-02	1.00E-02	1.00E-02	1.00E-02	2.10E+01
13	5WBR1	4.00E-01	1.60E+00	3.26E+00	n.a.	2.24E+01	n.a.	n.a.	1.15E+02	3.50E-01	n.a.	2.50E+01	2.50E-01	1.00E-02	n.a.	2.20E-01	0.00E+00	1.00E-02	1.00E-02	2.00E-02	2.00E+00
14	5WBR2	3.90E-01	1.60E+00	3.26E+00	n.a.	1.80E+01	n.a.	n.a.	1.06E+02	3.50E-01	n.a.	2.24E+01	2.30E-01	1.00E-02	n.a.	4.90E-01	0.00E+00	1.00E-02	1.00E-02	2.00E-02	2.44E+00
15	5WBR3	3.80E-01	1.61E+00	3.26E+00	n.a.	n.a.	n.a.	n.a.	1.13E+02	2.18E+00	7.00E-02	2.44E+01	2.30E-01	1.00E-02	1.00E-02	1.15E+00	1.50E-01	1.70E-01	1.00E-02	2.00E-02	4.23E+00
16	1WBRA1	5.50E-01	9.76E+00	n.a.	3.31E+00	5.47E+01	n.a.	n.a.	4.40E+02	4.07E+00	n.a.	1.02E+02	8.10E-01	8.00E-02	n.a.	5.20E-01	3.00E-02	2.00E-02	1.60E-01	3.00E-02	8.96E+00
17	1WBRA2	5.40E-01	9.86E+00	n.a.	3.28E+00	5.96E+01	n.a.	n.a.	4.31E+02	3.91E+00	n.a.	1.01E+02	8.00E-01	8.00E-02	n.a.	7.70E-01	4.00E-02	1.00E-02	1.50E-01	3.00E-02	8.81E+00
18	1WBRA3	5.60E-01	9.82E+00	n.a.	3.26E+00	6.26E+01	n.a.	n.a.	4.35E+02	4.06E+00	n.a.	1.04E+02	8.50E-01	8.00E-02	n.a.	6.60E-01	3.00E-02	2.00E-02	1.60E-01	4.00E-02	8.94E+00
19	2WBRA1	3.15E+00	2.97E+00	3.37E+00	3.29E+00	4.44E+01	n.a.	n.a.	2.70E+02	2.43E+00	n.a.	6.66E+01	5.60E-01	5.00E-02	1.00E-02	2.29E+00	1.00E-01	5.00E-02	7.00E-02	2.00E-02	1.08E+01
20	2WBRA2	2.69E+00	2.66E+00	3.34E+00	n.a.	3.87E+01	n.a.	n.a.	2.36E+02	2.17E+00	n.a.	5.80E+01	5.20E-01	4.00E-02	n.a.	2.81E+00	2.00E-02	1.00E-02	6.00E-02	2.00E-02	8.80E+00
21	2WBRA3	1.55E+00	2.85E+00	3.40E+00	3.32E+00	3.89E+01	n.a.	n.a.	2.36E+02	2.15E+00	n.a.	5.70E+01	5.40E-01	5.00E-02	n.a.	2.57E+00	1.00E-02	1.00E-02	6.00E-02	3.00E-02	5.87E+00
22	3WBRA1	4.70E-01	1.84E+00	3.48E+00	3.63E+00	3.53E+01	n.a.	n.a.	1.74E+02	1.51E+00	6.00E-02	3.89E+01	4.00E-01	5.00E-02	1.00E-02	1.04E+01	1.00E-02	3.00E-02	3.00E-02	2.00E-02	1.03E+01
23	3WBRA2	4.70E-01	2.15E+00	3.51E+00	4.40E+00	3.94E+01	n.a.	n.a.	1.67E+02	1.42E+00	4.00E-02	3.63E+01	3.90E-01	4.00E-02	1.00E-02	1.00E+01	1.00E-02	2.00E-02	3.00E-02	2.00E-02	9.64E+00
24	3WBRA3	4.50E-01	1.94E+00	3.53E+00	n.a.	3.89E+01	n.a.	n.a.	1.59E+02	1.40E+00	6.00E-02	3.40E+01	3.70E-01	4.00E-02	1.00E-02	1.01E+01	1.00E-02	1.00E-02	3.00E-02	2.00E-02	1.31E+01
25	4WBRA1	4.00E-01	1.74E+00	3.43E+00	3.55E+00	2.32E+01	n.a.	n.a.	1.22E+02	1.12E+00	8.00E-02	2.67E+01	2.70E-01	4.00E-02	1.00E-02	1.63E+01	1.40E-01	1.39E+00	2.00E-02	1.00E-02	1.02E+01
26	4WBRA2	3.90E-01	2.05E+00	3.44E+00	3.53E+00	1.58E+01	n.a.	n.a.	1.16E+02	1.09E+00	1.60E-01	2.54E+01	2.50E-01	4.00E-02	2.00E-02	1.76E+01	3.00E-02	4.00E-02	2.00E-02	2.00E-02	1.15E+01
27	4WBRA3	3.90E-01	2.29E+00	3.47E+00	3.52E+00	1.50E+01	n.a.	n.a.	1.30E+02	2.35E+00	1.10E-01	2.67E+01	2.60E-01	4.00E-02	1.00E-02	1.50E+01	1.00E-02	3.00E-02	2.00E-02	2.00E-02	1.05E+01
28	5WBRA1	4.30E-01	1.77E+00	3.28E+00	3.47E+00	1.59E+01	n.a.	n.a.	9.63E+01	8.70E-01	1.00E-01	2.15E+01	1.80E-01	4.00E-02	2.00E-02	1.77E+01	2.00E-02	2.00E-02	2.00E-02	1.00E-02	1.24E+01
29	5WBRA2	4.30E-01	1.78E+00	3.28E+00	3.45E+00	1.60E+01	n.a.	n.a.	9.75E+01	2.80E+00	1.10E-01	2.16E+01	1.80E-01	4.00E-02	2.00E-02	1.93E+01	1.00E-02	1.20E-01	2.00E-02	1.00E-02	1.23E+01
30	5WBRA3	4.30E-01	1.84E+00	3.29E+00	n.a.	1.51E+01	n.a.	n.a.	1.03E+02	1.06E+00	1.04E+00	2.14E+01	1.60E-01	4.00E-02	3.00E-02	1.19E+01	1.00E-02	3.00E-02	1.00E-02	1.00E-02	1.65E+01

31	1WBRS1	1.49E+00	3.11E+00	n.a.	3.20E+00	5.68E+01	n.a.	n.a.	4.48E+02	9.80E-01	n.a.	1.30E+02	8.90E-01	5.00E-02	n.a.	3.00E-02	1.00E-02	1.00E-02	1.90E-01	3.00E-02	3.16E-01
32	1WBRS2	1.56E+00	3.12E+00	n.a.	3.20E+00	4.97E+01	n.a.	n.a.	4.53E+02	1.02E+00	n.a.	1.03E+02	9.20E-01	4.00E-02	n.a.	4.00E-02	2.00E-02	3.00E-02	1.90E-01	2.00E-02	1.51E-01
33	1WBRS3	1.61E+00	3.06E+00	n.a.	3.23E+00	4.96E+01	n.a.	n.a.	4.39E+02	9.70E-01	n.a.	1.35E+02	1.00E+00	5.00E-02	n.a.	7.00E-02	1.00E-02	1.00E-02	1.90E-01	3.00E-02	1.03E+01
34	2WBRS1	6.60E-01	2.20E+00	n.a.	3.13E+00	4.07E+01	n.a.	n.a.	2.22E+02	6.00E-01	3.00E-02	5.00E+01	5.90E-01	1.00E-02	n.a.	8.90E-01	0.00E+00	1.00E-02	4.00E-02	3.00E-02	2.08E+01
35	2WBRS2	6.90E-01	2.23E+00	n.a.	3.15E+00	3.83E+01	n.a.	n.a.	2.55E+02	6.10E-01	3.00E-02	5.87E+01	6.70E-01	2.00E-02	1.00E-02	1.33E+00	2.40E-01	1.10E-01	5.00E-02	2.00E-02	2.10E+01
36	2WBRS3	6.60E-01	2.37E+00	n.a.	3.16E+00	3.97E+01	n.a.	n.a.	2.55E+02	7.40E-01	4.00E-02	5.90E+01	7.10E-01	2.00E-02	n.a.	1.97E+00	1.00E-02	1.00E-02	5.00E-02	3.00E-02	2.24E+01
37	3WBRS1	3.50E-01	2.11E+00	n.a.	3.38E+00	3.71E+01	n.a.	n.a.	1.54E+02	5.20E-01	4.00E-02	3.63E+01	3.50E-01	2.00E-02	n.a.	3.18E+00	1.00E-02	1.00E-02	2.00E-02	2.00E-02	2.52E+01
38	3WBRS2	3.50E-01	2.56E+00	n.a.	3.51E+00	4.25E+01	n.a.	n.a.	1.57E+02	4.90E-01	6.00E-02	3.71E+01	3.50E-01	2.00E-02	n.a.	3.43E+00	1.00E-02	1.00E-02	2.00E-02	2.00E-02	2.50E+01
39	3WBRS3	3.30E-01	2.21E+00	n.a.	3.59E+00	4.05E+01	n.a.	n.a.	1.61E+02	5.20E-01	4.00E-02	3.73E+01	3.50E-01	2.00E-02	n.a.	4.87E+00	1.00E-02	3.00E-02	2.00E-02	2.00E-02	2.05E+01
40	4WBRS1	3.00E-01	1.81E+00	n.a.	3.41E+00	2.66E+01	n.a.	n.a.	1.23E+02	3.80E-01	n.a.	2.60E+01	2.10E-01	1.00E-02	n.a.	3.39E+00	3.00E-02	2.00E-02	1.00E-02	1.00E-02	3.31E+00
41	4WBRS2	3.00E-01	1.84E+00	n.a.	3.45E+00	2.48E+01	n.a.	n.a.	1.22E+02	3.90E-01	4.00E-02	2.85E+01	2.00E-01	2.00E-02	n.a.	5.23E+00	1.00E-02	1.00E-02	1.00E-02	2.00E-02	3.29E+00
42	4WBRS3	2.80E-01	1.92E+00	n.a.	3.43E+00	3.23E+01	n.a.	n.a.	1.27E+02	4.10E-01	n.a.	2.94E+01	2.00E-01	2.00E-02	n.a.	7.41E+00	1.00E-02	1.00E-02	1.00E-02	2.00E-02	3.69E+00
43	5WBRS1	3.60E-01	1.78E+00	3.39E+00	n.a.	1.59E+01	n.a.	n.a.	1.05E+02	3.00E-01	6.00E-02	2.80E+01	1.60E-01	2.00E-02	1.00E-02	1.12E+01	1.00E-02	1.00E-02	1.00E-02	1.00E-02	2.11E+01
44	5WBRS2	4.90E-01	1.82E+00	3.39E+00	3.44E+00	1.46E+01	n.a.	n.a.	1.13E+02	2.90E-01	4.00E-02	2.68E+01	1.50E-01	1.00E-02	n.a.	6.75E+00	0.00E+00	2.00E-02	1.00E-02	1.00E-02	4.23E+00
45	5WBRS3	4.80E-01	1.90E+00	3.39E+00	3.48E+00	1.65E+01	n.a.	n.a.	1.09E+02	2.60E-01	4.00E-02	2.52E+01	1.30E-01	2.00E-02	0.00E+00	6.81E+00	2.00E-02	2.00E-02	1.00E-02	1.00E-02	2.26E+01
46	1WBRG1	5.70E-01	4.14E+00	n.a.	3.14E+00	5.10E+02	2.35E+01	n.a.	7.58E+02	1.60E+00	n.a.	9.80E-01	1.50E-01	5.00E-02	n.a.	2.30E-01	0.00E+00	1.00E-02	2.00E-02	n.a.	1.50E+01
47	1WBRG2	4.70E-01	4.19E+00	n.a.	3.16E+00	5.09E+02	2.27E+01	n.a.	7.32E+02	1.53E+00	4.00E-02	2.30E-01	1.40E-01	5.00E-02	n.a.	2.50E-01	2.00E-02	2.00E-02	2.00E-02	n.a.	1.61E+01
48	1WBRG3	4.90E-01	4.14E+00	n.a.	3.11E+00	5.03E+02	2.33E+01	n.a.	7.35E+02	1.46E+00	3.00E-02	1.20E-01	1.40E-01	3.00E-02	1.00E-02	2.50E-01	2.00E-01	1.00E-01	2.00E-02	n.a.	1.60E+01
49	2WBRG1	5.40E-01	2.06E+00	n.a.	3.12E+00	4.98E+02	1.54E+01	n.a.	2.86E+02	6.90E-01	4.00E-02	8.00E-02	1.40E-01	1.00E-02	n.a.	2.60E-01	1.00E-02	2.00E-02	1.00E-02	n.a.	2.03E+01
50	2WBRG2	4.30E-01	2.09E+00	n.a.	3.29E+00	5.13E+02	1.61E+01	n.a.	3.02E+02	7.40E-01	n.a.	1.20E-01	1.50E-01	2.00E-02	n.a.	2.50E-01	0.00E+00	2.00E-02	1.00E-02	n.a.	2.07E+01
51	2WBRG3	5.40E-01	2.16E+00	n.a.	3.27E+00	5.51E+02	1.65E+01	n.a.	3.36E+02	8.40E-01	4.00E-02	6.80E-01	1.60E-01	1.00E-02	1.00E-02	3.40E-01	2.10E-01	3.70E-01	1.00E-02	n.a.	2.12E+01
52	3WBRG1	4.20E-01	1.66E+00	n.a.	3.41E+00	9.88E+01	9.80E-01	4.97E+00	1.06E+02	4.00E-01	n.a.	4.95E+00	1.40E-01	1.00E-02	n.a.	6.00E-02	5.00E-02	5.00E-02	2.00E-02	n.a.	1.47E+01
53	3WBRG2	3.10E-01	1.64E+00	n.a.	3.44E+00	8.29E+01	1.08E+00	5.30E+00	1.12E+02	3.60E-01	n.a.	5.30E+00	1.40E-01	n.a.	n.a.	4.00E-02	1.00E-02	2.00E-02	3.00E-02	n.a.	6.74E+00
54	3WBRG3	4.30E-01	9.53E+00	n.a.	3.55E+00	9.96E+01	1.52E+00	5.24E+00	1.11E+02	3.50E-01	n.a.	4.30E+00	1.30E-01	0.00E+00	n.a.	4.00E-02	0.00E+00	1.00E-02	2.00E-02	n.a.	1.45E+01
55	4WBRG1	2.70E-01	1.52E+00	n.a.	n.a.	6.02E+01	n.a.	2.16E+00	7.09E+01	2.90E-01	n.a.	1.13E+01	1.00E-01	n.a.	n.a.	n.a.	2.00E-02	2.00E-02	2.00E-02	n.a.	9.72E+00
56	4WBRG2	2.70E-01	1.52E+00	n.a.	3.39E+00	5.91E+01	n.a.	8.14E+00	7.20E+01	2.50E-01	n.a.	1.04E+01	1.00E-01	n.a.	1.00E-02	n.a.	9.00E-02	6.00E-02	2.00E-02	n.a.	2.53E+00
57	4WBRG3	4.10E-01	1.54E+00	n.a.	3.50E+00	3.04E+01	n.a.	3.88E+00	7.08E+01	2.40E-01	n.a.	1.07E+01	1.00E-01	n.a.	n.a.	n.a.	0.00E+00	1.00E-02	2.00E-02	n.a.	5.24E+00
58	5WBRG1	3.90E-01	1.46E+00	n.a.	3.44E+00	6.49E+01	n.a.	1.22E+01	5.56E+01	2.00E-01	n.a.	5.29E+00	6.00E-02	n.a.	0.00E+00	n.a.	9.00E-02	6.00E-02	1.00E-02	n.a.	6.45E-01
59	5WBRG2	5.00E-01	1.47E+00	n.a.	3.52E+00	7.43E+01	n.a.	1.21E+01	5.70E+01	2.20E-01	n.a.	1.31E+01	7.00E-02	n.a.	n.a.	n.a.	0.00E+00	1.00E-02	2.00E-02	n.a.	6.90E-01
60	5WBRG3	5.20E-01	1.50E+00	n.a.	3.50E+00	6.57E+01	n.a.	1.33E+01	5.84E+01	2.50E-01	n.a.	1.39E+01	8.00E-02	n.a.	0.00E+00	4.00E-02	8.00E-02	5.00E-02	2.00E-02	n.a.	1.07E+00

Appendix 8. PHREEQC selected values for simulation 1 to 8.

No.	Description	pH	pe	Temp	Na	K	Mg	Ca	F	Cl	S(+6)	Br	N(+5)	P(5)	Al	V	Cr	Mn	Fe	Cu	Zn	Ga	As	Si
1	1WBR1	11.98	4	25.6	4.5E+02	1.0E+00	3.0E-04	7.3E+01	1.2E+00	3.3E+00	0.0E+00	0.0E+00	7.1E-01	0.0E+00	1.3E+02	5.0E-01	5.8E-02	6.2E-03	3.2E-05	1.3E-01	7.5E-02	1.9E-01	1.2E-02	2.1E-01
2	1WBRA2	11.76	4	25.6	4.3E+02	3.9E+00	3.0E-04	6.0E+01	5.4E-01	9.9E+00	0.0E+00	0.0E+00	7.4E-01	0.0E+00	1.0E+02	8.0E-01	8.4E-02	4.6E-05	7.7E-01	3.7E-02	1.1E-02	1.5E-01	3.1E-02	1.3E+01
3	1WBRS1	11.93	4	29.3	4.5E+02	9.8E-01	3.0E-04	5.7E+01	1.5E+00	3.1E+00	0.0E+00	0.0E+00	3.2E+00	0.0E+00	1.3E+02	8.9E-01	5.0E-02	4.6E-05	2.6E-02	6.3E-03	9.1E-03	1.9E-01	3.1E-02	1.7E+01
4	1WBRG2	10.92	4	30.2	7.3E+02	1.5E+00	3.8E-02	5.1E+02	4.7E-01	4.2E+00	7.6E+00	0.0E+00	7.1E-01	0.0E+00	2.3E-01	1.4E-01	4.5E-02	4.6E-05	2.5E-01	2.2E-02	1.8E-02	2.1E-02	3.1E-05	1.0E+00
5	2WBR1	11.82	4	29.8	2.4E+02	5.5E-01	3.0E-04	3.7E+01	6.4E-01	2.1E+00	0.0E+00	0.0E+00	7.0E-01	0.0E+00	6.3E+01	3.5E-01	2.4E-02	4.6E-05	3.2E-05	4.6E-03	9.6E-03	5.9E-02	9.3E-03	2.0E+00
6	2WBRA1	11.54	4	30.1	2.7E+02	2.4E+00	3.0E-04	4.4E+01	3.2E+00	3.0E+00	0.0E+00	3.4E+00	7.4E-01	0.0E+00	6.7E+01	5.6E-01	4.9E-02	6.0E-03	2.3E+00	9.7E-02	5.0E-02	7.0E-02	2.4E-02	9.0E+00
7	2WBRS1	11.76	4	30.1	2.2E+02	6.0E-01	3.1E-02	4.1E+01	6.6E-01	2.2E+00	0.0E+00	0.0E+00	7.1E-01	0.0E+00	5.0E+01	5.9E-01	1.4E-02	4.6E-05	8.9E-01	4.0E-03	6.7E-03	4.2E-02	2.8E-02	1.1E+01
8	2WBRG1	10.94	4	29.6	2.9E+02	6.9E-01	3.6E-02	5.0E+02	5.4E-01	2.1E+00	5.2E+00	0.0E+00	7.0E-01	0.0E+00	8.1E-02	1.4E-01	1.2E-02	4.6E-05	2.6E-01	6.8E-03	1.6E-02	1.3E-02	3.1E-05	1.0E+01
9	3WBR2	11.69	4	30.2	1.6E+02	4.4E-01	3.0E-04	3.9E+01	3.7E-01	1.8E+00	0.0E+00	0.0E+00	7.7E-01	0.0E+00	3.4E+01	3.3E-01	2.5E-02	7.0E-03	6.8E-02	1.3E-01	7.0E-02	1.8E-02	3.1E-05	1.1E+01
10	3WBRA2	11.33	4	29.6	1.7E+02	1.4E+00	4.1E-02	3.9E+01	4.7E-01	2.2E+00	0.0E+00	3.5E+00	9.9E-01	0.0E+00	3.6E+01	3.9E-01	4.0E-02	6.6E-03	1.0E+01	1.0E-02	2.1E-02	3.0E-02	1.8E-02	1.2E+01
11	3WBRS2	11.61	4	31.4	1.6E+02	4.9E-01	6.0E-02	4.2E+01	3.5E-01	2.6E+00	0.0E+00	0.0E+00	7.9E-01	0.0E+00	3.7E+01	3.5E-01	2.2E-02	4.6E-05	3.4E+00	7.8E-03	1.5E-02	1.9E-02	1.7E-02	1.5E-01
12	3WBRG3	11.41	4	29.7	1.1E+02	3.5E-01	3.0E-04	1.0E+02	4.3E-01	9.5E+00	5.1E-01	0.0E+00	8.0E-01	1.7E+00	4.3E+00	1.3E-01	5.0E-03	4.6E-05	4.4E-02	4.8E-03	1.2E-02	2.3E-02	3.1E-05	2.2E+01
13	4WBR2	11.6	4	29.9	1.2E+02	3.8E-01	3.0E-04	2.8E+01	3.4E-01	1.8E+00	0.0E+00	0.0E+00	7.7E-01	0.0E+00	2.5E+01	2.7E-01	6.6E-03	4.8E-03	1.5E-01	9.5E-02	5.3E-02	1.0E-02	9.2E-03	2.5E+01
14	4WBRA2	11.29	4	29.3	1.2E+02	1.1E+00	1.6E-01	1.6E+01	3.9E-01	2.1E+00	0.0E+00	3.4E+00	8.0E-01	0.0E+00	2.5E+01	2.5E-01	4.3E-02	1.7E-02	1.8E+01	3.1E-02	4.2E-02	2.2E-02	1.7E-02	3.3E+00
15	4WBRS1	11.35	4	30.7	1.2E+02	3.8E-01	3.0E-04	2.7E+01	3.0E-01	1.8E+00	0.0E+00	0.0E+00	7.7E-01	0.0E+00	2.6E+01	2.1E-01	1.2E-02	4.6E-05	3.4E+00	2.8E-02	2.1E-02	9.9E-03	9.7E-03	2.1E+01
16	4WBRG2	11.55	4	28.1	7.2E+01	2.5E-01	3.0E-04	5.9E+01	2.7E-01	1.5E+00	0.0E+00	0.0E+00	7.6E-01	2.7E+00	1.0E+01	1.0E-01	3.7E-05	6.6E-03	3.2E-05	9.5E-02	6.5E-02	2.0E-02	3.1E-05	1.6E+01
17	5WBR2	11.52	4	30.4	1.1E+02	3.5E-01	3.0E-04	1.8E+01	3.9E-01	1.6E+00	0.0E+00	3.3E+00	0.0E+00	0.0E+00	2.2E+01	2.3E-01	5.4E-03	4.6E-05	4.9E-01	3.9E-03	9.9E-03	7.9E-03	1.6E-02	2.1E+01
18	5WBRA2	11.23	4	30.2	9.7E+01	2.8E+00	1.1E-01	1.6E+01	4.3E-01	1.8E+00	0.0E+00	3.3E+00	7.8E-01	0.0E+00	2.2E+01	1.8E-01	4.2E-02	1.7E-02	1.9E+01	9.7E-03	1.2E-01	2.0E-02	1.2E-02	6.7E+00
19	5WBRS2	11.32	4	30.9	1.1E+02	2.9E-01	4.4E-02	1.5E+01	4.9E-01	1.8E+00	0.0E+00	3.4E+00	7.8E-01	0.0E+00	2.7E+01	1.5E-01	1.5E-02	4.6E-05	6.7E+00	4.5E-03	2.1E-02	1.1E-02	8.9E-03	2.5E+00
20	5WBRG2	11.47	4	30.3	5.7E+01	2.2E-01	3.0E-04	7.4E+01	5.0E-01	1.5E+00	0.0E+00	0.0E+00	7.9E-01	3.9E+00	1.3E+01	7.4E-02	3.7E-05	4.6E-05	3.2E-05	4.8E-03	7.9E-03	1.5E-02	3.1E-05	6.9E-01

Appendix 9. Values for the ESP% and SAR for Simulation 5 to 8.

No.	Description	Simulation 5			Simluation 6			Simluation 7			Simulation 8		
		Na (mol/l)	Mg (mol/l)	Ca (mol/l)	Na (mol/l)	Mg (mol/l)	Ca (mol/l)	Na (mol/l)	Mg (mol/l)	Ca (mol/l)	Na (mol/l)	Mg (mol/l)	Ca (mol/l)
1	1WBR1	1.94E-02	1.23E-08	1.81E-03	1.94E-02	1.23E-08	1.81E-03	1.94E-02	1.23E-08	1.08E-05	1.94E-02	1.23E-08	2.15E-04
2	1WBRA2	1.87E-02	1.23E-08	1.49E-03	1.87E-02	1.23E-08	1.49E-03	1.87E-02	1.23E-08	1.11E-05	1.87E-02	1.23E-08	2.29E-04
3	1WBRS1	1.95E-02	1.23E-08	1.42E-03	1.95E-02	1.23E-08	1.42E-03	1.95E-02	1.23E-08	1.06E-05	1.95E-02	1.23E-08	1.84E-04
4	1WBRG2	3.19E-02	1.56E-06	1.27E-02	3.19E-02	1.56E-06	1.27E-02	3.19E-02	3.19E-07	9.17E-06	3.19E-02	1.56E-06	8.82E-05
5	2WBR1	1.05E-02	1.23E-08	9.12E-04	1.05E-02	1.23E-08	9.12E-04	1.05E-02	1.23E-08	1.43E-05	1.05E-02	1.23E-08	4.28E-04
6	2WBRA1	1.17E-02	1.23E-08	1.11E-03	1.17E-02	1.23E-08	1.11E-03	1.17E-02	1.23E-08	1.34E-05	1.17E-02	1.23E-08	3.70E-04
7	2WBRS1	9.67E-03	1.27E-06	1.02E-03	9.67E-03	1.27E-06	1.02E-03	9.67E-03	6.89E-07	1.51E-05	9.67E-03	1.27E-06	4.72E-04
8	2WBRG1	1.24E-02	1.48E-06	1.24E-02	1.24E-02	1.48E-06	1.24E-02	1.24E-02	5.64E-07	1.30E-05	1.24E-02	1.48E-06	3.46E-04
9	3WBR2	6.78E-03	1.23E-08	9.65E-04	6.78E-03	1.23E-08	9.65E-04	6.78E-03	1.23E-08	2.03E-05	6.78E-03	1.23E-08	7.25E-04
10	3WBRA2	7.28E-03	1.67E-06	9.83E-04	7.28E-03	1.67E-06	9.83E-04	7.28E-03	9.63E-07	1.94E-05	7.28E-03	1.67E-06	6.91E-04
11	3WBRS2	6.81E-03	2.45E-06	1.06E-03	6.81E-03	2.45E-06	1.06E-03	6.81E-03	9.52E-07	1.96E-05	6.81E-03	2.45E-06	6.92E-04
12	3WBRG3	4.85E-03	1.23E-08	2.49E-03	4.85E-03	1.23E-08	2.49E-03	4.85E-03	1.23E-08	3.40E-05	4.85E-03	1.23E-08	1.09E-03
13	4WBR2	5.26E-03	1.23E-08	7.06E-04	5.26E-03	1.23E-08	7.06E-04	5.26E-03	1.23E-08	2.68E-05	5.26E-03	1.23E-08	7.06E-04
14	4WBRA2	5.04E-03	6.77E-06	3.94E-04	5.04E-03	6.77E-06	3.94E-04	5.04E-03	1.55E-06	2.87E-05	5.04E-03	6.77E-06	3.94E-04
15	4WBRS1	5.36E-03	1.23E-08	6.64E-04	5.36E-03	1.23E-08	6.64E-04	5.36E-03	1.23E-08	2.56E-05	5.36E-03	1.23E-08	6.64E-04
16	4WBRG2	3.13E-03	1.23E-08	1.47E-03	3.13E-03	1.23E-08	1.47E-03	3.13E-03	1.23E-08	6.35E-05	3.13E-03	1.23E-08	1.47E-03
17	5WBR2	4.59E-03	1.23E-08	4.50E-04	4.59E-03	1.23E-08	4.50E-04	4.59E-03	1.23E-08	3.08E-05	4.59E-03	1.23E-08	4.50E-04
18	5WBRA2	4.24E-03	4.33E-06	4.00E-04	4.24E-03	4.33E-06	4.00E-04	4.24E-03	1.87E-06	3.41E-05	4.24E-03	4.33E-06	4.00E-04
19	5WBRS2	4.93E-03	1.79E-06	3.65E-04	4.93E-03	1.79E-06	3.65E-04	4.93E-03	1.49E-06	2.82E-05	4.93E-03	1.79E-06	3.65E-04
20	5WBRG2	2.48E-03	1.23E-08	1.85E-03	2.48E-03	1.23E-08	1.85E-03	2.48E-03	1.23E-08	8.99E-05	2.48E-03	1.23E-08	1.58E-03

Appendix 10. PHREEQC results of pH, alkalinity, Al, Fe, and Ca concentrations for simulations 4 to 8.

Leaching step	Description	pH					Alkalinity (mmol/l)					All simulations (mg/l)		
		S4	S5	S6	S7	S8	S4	S5	S6	S7	S8	Al	Fe	Ca
1	BR	12.18	9.34	7.61	9.41	7.56	37.87	31.30	31.30	37.87	37.88	134.58	0.00	72.66
	Açaí	12.17	9.34	7.65	9.40	7.54	32.70	21.97	21.98	32.70	32.71	100.86	0.77	59.58
	Soil	12.03	9.34	7.96	9.42	7.57	36.48	32.85	32.85	36.48	36.49	130.38	0.03	56.81
	Gypsum	12.49	9.60	7.41	9.56	7.77	57.03	1.59	1.59	57.02	57.03	0.23	0.25	509.73
2	BR	11.80	9.18	7.46	9.23	7.35	19.19	19.66	19.66	19.19	19.19	62.93	0.00	36.53
	Açaí	11.84	9.21	7.39	9.26	7.39	21.13	15.65	15.65	21.13	21.13	66.63	2.29	44.39
	Soil	11.78	9.17	7.79	9.20	7.33	17.17	16.79	16.79	17.17	17.17	50.04	0.89	40.75
	Gypsum	12.33	9.43	7.27	9.28	7.41	37.10	1.69	1.69	37.10	37.10	0.08	0.26	498.39
3	BR	11.66	9.07	7.29	9.08	7.22	12.39	13.00	13.00	12.39	12.39	34.02	0.07	38.65
	Açaí	11.69	9.09	7.28	9.10	7.24	13.32	9.18	9.18	13.32	13.32	36.35	10.01	39.38
	Soil	11.63	9.08	7.27	9.09	7.23	12.99	12.64	12.64	12.99	12.99	37.06	3.42	42.46
	Gypsum	11.75	9.10	7.15	8.92	7.13	9.96	5.13	5.13	9.96	9.96	4.30	0.04	99.63
4	BR	11.53	8.98	7.10	8.98	7.13	9.38	10.28	10.28	9.38	9.38	25.32	0.15	28.27
	Açaí	11.48	8.93	7.16	8.96	7.07	8.84	7.27	7.27	8.84	8.84	25.40	17.54	15.77
	Soil	11.51	8.99	7.08	8.99	7.14	9.53	7.93	7.93	9.53	9.53	26.00	3.39	26.60
	Gypsum	11.58	8.94	7.08	8.76	7.07	7.14	6.84	6.84	7.14	7.14	10.39	0.00	59.05
5	BR	11.43	8.92	7.05	8.94	7.05	7.89	8.88	8.88	7.89	7.89	22.37	0.49	18.03
	Açaí	11.38	8.88	7.10	8.91	7.02	7.70	6.60	6.60	7.70	7.70	21.56	19.31	16.03
	Soil	11.43	8.92	7.09	8.96	7.07	8.60	7.63	7.63	8.60	8.60	26.77	6.74	14.61
	Gypsum	11.52	8.93	7.09	8.67	7.04	7.53	6.99	6.99	7.53	7.53	13.13	0.00	74.28

Appendix 11. Results from Actlabs of minor elements XRF, BR: Bauxite residue, BRA: Bauxite residue with açaí, BRS: Bauxite Residue with soil, BRG: Bauxite Residue with gypsum and BRI: Bauxite residue initial with no batching test.

Report Number: A21-01861														
Report Date: 4/3/2021														
Analyte Symbol	Ba	Co	Cr	Cu	Ga	Nb	Ni	Pb	Rb	Sr	Sn	V	Y	Zn
Unit Symbol	ppm	ppm	ppm	ppm	ppm	ppm	ppm	ppm	ppm	ppm	ppm	ppm	ppm	ppm
Detection Limit	5	5	5	5	5	1	4	5	2	2	5	5	2	5
Analysis Method	PPXRF	PPXRF	PPXRF	PPXRF	PPXRF	PPXRF	PPXRF	PPXRF	PPXRF	PPXRF	PPXRF	PPXRF	PPXRF	PPXRF
BR	46	11	306	< 5	64	95	24	93	26	55	89	560	136	31
BRA	46	8	290	< 5	65	96	23	91	24	52	90	534	123	30
BRS	40	5	273	< 5	60	84	20	86	23	48	76	501	119	24
BRG	48	7	285	< 5	65	91	22	92	23	146	86	538	123	25
BRI	46	< 5	296	< 5	68	92	21	90	22	51	90	548	122	30

Appendix 12. PHREEQC input file code for Simulation 1 (phreeqc.dat).

```
USER_PUNCH 1
headings Sample_Ref   EC_(uS/cm) TDS_g/kg-solution alk_mg/L
start
10 PUNCH Description
25 PUNCH SC
32 PUNCH (RHO * SOLN_VOL - TOT("water")) * 1000 / (RHO * SOLN_VOL)
40 PUNCH alk * ((50.05) / 1000)
end
SELECTED_OUTPUT 1
file simulation1.txt
charge_balance
ionic_strength
temp
percent_error
alkalinity
totals                  Na          K          Mg          Ca          F          Cl          S(+6)       Br          N(+5)       P(5)        Al          V           Cr          Mn          Fe          Cu          Zn          Ga          As          Si
-saturation_indices  Fe(OH)2 Fe(OH)3 Gibbsite Goethite Pyrolusite Kaolinite Diaspore Magnetite Boehmite Cuprite
# Simulation 1 using PHREEQC.dat based on the pH measured in the lab to compare EC
END
SOLUTION_SPREAD
units mg/l
```

Number	Description	pH	pe	Temp	Na	K	Mg	Ca	F	Cl	S(+6)	Br	N(+5)	P(5)	Al	V	Cr	Mn	Fe	Cu	Zn	Ga	As	Si
1	1WBR1	11.98	4	25.6	4.47E+02	1.02E+00	2.99E-04	7.26E+01	1.18E+00	3.26E+00	0.00E+00	0.00E+00	7.15E-01	0.00E+00	1.35E+02	5.04E-01	5.78E-02	6.18E-03	3.16E-05	1.26E-01	7.54E-02	1.85E-01	1.19E-02	2.13E-01
2	1WBRA2	11.76	4	25.6	4.31E+02	3.91E+00	2.99E-04	5.96E+01	5.42E-01	9.86E+00	0.00E+00	0.00E+00	7.42E-01	0.00E+00	1.01E+02	8.03E-01	8.43E-02	4.60E-05	7.71E-01	3.65E-02	1.11E-02	1.55E-01	3.15E-02	1.26E+01
3	1WBRS1	11.93	4	29.3	4.48E+02	9.76E-01	2.99E-04	5.68E+01	1.49E+00	3.11E+00	0.00E+00	0.00E+00	3.20E+00	0.00E+00	1.30E+02	8.85E-01	4.98E-02	4.60E-05	2.60E-02	6.33E-03	9.08E-03	1.93E-01	3.11E-02	1.69E+01
4	1WBRG2	10.92	4	30.2	7.32E+02	1.53E+00	3.78E-02	5.09E+02	4.67E-01	4.19E+00	7.59E+00	0.00E+00	7.13E-01	0.00E+00	2.31E-01	1.40E-01	4.52E-02	4.60E-05	2.47E-01	2.25E-02	1.79E-02	2.14E-02	3.15E-05	1.05E+00
5	2WBR1	11.82	4	29.8	2.41E+02	5.53E-01	2.99E-04	3.65E+01	6.39E-01	2.06E+00	0.00E+00	0.00E+00	7.03E-01	0.00E+00	6.29E+01	3.54E-01	2.39E-02	4.60E-05	3.16E-05	4.63E-03	9.59E-03	5.92E-02	9.29E-03	2.00E+00
6	2WBRA1	11.54	4	30.1	2.70E+02	2.43E+00	2.99E-04	4.44E+01	3.15E+00	2.97E+00	0.00E+00	3.37E+00	7.44E-01	0.00E+00	6.66E+01	5.57E-01	4.85E-02	6.02E-03	2.29E+00	9.68E-02	5.03E-02	6.95E-02	2.42E-02	8.96E+00
7	2WBRS1	11.76	4	30.1	2.22E+02	6.03E-01	3.07E-02	4.07E+01	6.61E-01	2.21E+00	0.00E+00	0.00E+00	7.06E-01	0.00E+00	5.00E+01	5.88E-01	1.41E-02	4.60E-05	8.93E-01	4.00E-03	6.70E-03	4.20E-02	2.75E-02	1.08E+01
8	2WBRG1	10.94	4	29.6	2.86E+02	6.87E-01	3.60E-02	4.98E+02	5.38E-01	2.06E+00	5.15E+00	0.00E+00	7.05E-01	0.00E+00	8.08E-02	1.40E-01	1.16E-02	4.60E-05	2.62E-01	6.77E-03	1.59E-02	1.26E-02	3.15E-05	1.03E+01
9	3WBR2	11.69	4	30.2	1.56E+02	4.37E-01	2.99E-04	3.87E+01	3.71E-01	1.77E+00	0.00E+00	0.00E+00	7.68E-01	0.00E+00	3.40E+01	3.29E-01	2.51E-02	6.99E-03	6.82E-02	1.29E-01	7.04E-02	1.84E-02	3.15E-05	1.15E+01
10	3WBRA2	11.33	4	29.6	1.67E+02	1.43E+00	4.05E-02	3.94E+01	4.71E-01	2.15E+00	0.00E+00	3.51E+00	9.94E-01	0.00E+00	3.63E+01	3.90E-01	4.03E-02	6.62E-03	1.00E+01	1.03E-02	2.07E-02	3.03E-02	1.75E-02	1.23E+01
11	3WBRS2	11.61	4	31.4	1.57E+02	4.93E-01	5.96E-02	4.25E+01	3.54E-01	2.56E+00	0.00E+00	0.00E+00	7.92E-01	0.00E+00	3.71E+01	3.46E-01	2.25E-02	4.60E-05	3.43E+00	7.80E-03	1.50E-02	1.90E-02	1.69E-02	1.51E-01
12	3WBRG3	11.41	4	29.7	1.12E+02	3.46E-01	2.99E-04	9.96E+01	4.34E-01	9.53E+00	5.07E-01	0.00E+00	8.02E-01	1.71E+00	4.30E+00	1.30E-01	4.96E-03	4.60E-05	4.37E-02	4.81E-03	1.23E-02	2.32E-02	3.15E-05	2.24E+01
13	4WBR2	11.6	4	29.9	1.21E+02	3.83E-01	2.99E-04	2.83E+01	3.40E-01	1.81E+00	0.00E+00	0.00E+00	7.68E-01	0.00E+00	2.53E+01	2.74E-01	6.60E-03	4.82E-03	1.47E-01	9.54E-02	5.28E-02	1.03E-02	9.15E-03	2.50E+01
14	4WBRA2	11.29	4	29.3	1.16E+02	1.09E+00	1.65E-01	1.58E+01	3.90E-01	2.05E+00	0.00E+00	3.44E+00	7.98E-01	0.00E+00	2.54E+01	2.49E-01	4.26E-02	1.71E-02	1.76E+01	3.14E-02	4.21E-02	2.21E-02	1.74E-02	3.29E+00
15	4WBRS1	11.35	4	30.7	1.23E+02	3.78E-01	2.99E-04	2.66E+01	2.96E-01	1.81E+00	0.00E+00	0.00E+00	7.70E-01	0.00E+00	2.60E+01	2.12E-01	1.24E-02	4.60E-05	3.39E+00	2.78E-02	2.11E-02	9.91E-03	9.74E-03	2.11E+01
16	4WBRG2	11.55	4	28.1	7.20E+01	2.51E-01	2.99E-04	5.91E+01	2.75E-01	1.53E+00	0.00E+00	0.00E+00	7.65E-01	2.66E+00	1.04E+01	9.97E-02	3.73E-05	6.58E-03	3.16E-05	9.46E-02	6.48E-02	1.97E-02	3.15E-05	1.61E+01
17	5WBR2	11.52	4	30.4	1.06E+02	3.47E-01	2.99E-04	1.80E+01	3.90E-01	1.61E+00	0.00E+00	3.26E+00	0.00E+00	0.00E+00	2.24E+01	2.35E-01	5.35E-03	4.60E-05	4.89E-01	3.90E-03	9.88E-03	7.87E-03	1.63E-02	2.07E+01
18	5WBRA2	11.23	4	30.2	9.75E+01	2.80E+00	1.05E-01	1.60E+01	4.32E-01	1.78E+00	0.00E+00	3.28E+00	7.79E-01	0.00E+00	2.16E+01	1.81E-01	4.23E-02	1.70E-02	1.93E+01	9.74E-03	1.22E-01	1.99E-02	1.15E-02	6.74E+00
19	5WBRS2	11.32	4	30.9	1.13E+02	2.91E-01	4.36E-02	1.46E+01	4.90E-01	1.82E+00	0.00E+00	3.39E+00	7.77E-01	0.00E+00	2.68E+01	1.51E-01	1.46E-02	4.60E-05	6.75E+00	4.46E-03	2.07E-02	1.11E-02	8.85E-03	2.53E+00
20	5WBRG2	11.47	4	30.3	5.70E+01	2.18E-01	2.99E-04	7.43E+01	4.99E-01	1.47E+00	0.00E+00	0.00E+00	7.95E-01	3.94E+00	1.31E+01	7.38E-02	3.73E-05	4.60E-05	3.16E-05	4.84E-03	7.88E-03	1.51E-02	3.15E-05	6.90E-01

```
END
```

Appendix 13. PHREEQC input file code for Simulation 2 (phreeqc.dat).

```
USER_PUNCH 1
headings Sample_R‹EC_(uS/cm) TDS_g/kg-solution alk_mg/L
start
10 PUNCH Description
25 PUNCH SC
32 PUNCH (RHO * SOLN_VOL - TOT("water")) * 1000 / (RHO * SOLN_VOL)
40 PUNCH alk * ((50.05) / 1000)
end
SELECTED_OUTPUT 1
file simulation2.txt
charge_balance
ionic_strength
temp
percent_error
alkalinity
totals Na K Mg Ca F Cl S(+6) Br N(+5) P(5) Al V Cr Mn Fe Cu Zn Ga As
-molalities OH- HCO3- # add here other aqueous species of interest
-saturation_indices Fe(OH)2 Fe(OH)3 Gibbsite Goethite Pyrolusite Kaolinite Diaspore Magnetite Boehmite Cuprite
# Simulation 2 using phreeqc.dat based on the pH charge command of PHREEQC (compare EC with the one measured in the lab and find the differences)
END
SOLUTION_SPREAD
units mg/l
```

Number	Description	pH	pe	Temp	Na	K	Mg	Ca	F	Cl	S(+6)	Br	N(+5)	P(5)	Al	V	Cr	Mn	Fe
1	1WBR1	11.98 charge	4	25.6	4.47E+02	1.02E+00	2.99E-04	7.26E+01	1.18E+00	3.26E+00	0.00E+00	0.00E+00	7.15E-01	0.00E+00	1.35E+02	5.04E-01	5.78E-02	6.18E-03	3.16E-05
2	1WBRA2	11.76 charge	4	25.6	4.31E+02	3.91E+00	2.99E-04	5.96E+01	5.42E-01	9.86E+00	0.00E+00	0.00E+00	7.42E-01	0.00E+00	1.01E+02	8.03E-01	8.43E-02	4.60E-05	7.71E-01
3	1WBRS1	11.93 charge	4	29.3	4.48E+02	9.76E-01	2.99E-04	5.68E+01	1.49E+00	3.11E+00	0.00E+00	0.00E+00	3.20E+00	0.00E+00	1.30E+02	8.85E-01	4.98E-02	4.60E-05	2.60E-02
4	1WBRG2	10.92 charge	4	30.2	7.32E+02	1.53E+00	3.78E-02	5.09E+02	4.67E-01	4.19E+00	7.59E+00	0.00E+00	7.13E-01	0.00E+00	2.31E-01	1.40E-01	4.52E-02	4.60E-05	2.47E-01
5	2WBR1	11.82 charge	4	29.8	2.41E+02	5.53E-01	2.99E-04	3.65E+01	6.39E-01	2.06E+00	0.00E+00	0.00E+00	7.03E-01	0.00E+00	6.29E+01	3.54E-01	2.39E-02	4.60E-05	3.16E-05
6	2WBRA1	11.54 charge	4	30.1	2.70E+02	2.43E+00	2.99E-04	4.44E+01	3.15E+00	2.97E+00	0.00E+00	3.37E+00	7.44E-01	0.00E+00	6.66E+01	5.57E-01	4.85E-02	6.02E-03	2.29E+00
7	2WBRS1	11.76 charge	4	30.1	2.22E+02	6.03E-01	3.07E-02	4.07E+01	6.61E-01	2.21E+00	0.00E+00	0.00E+00	7.06E-01	0.00E+00	5.00E+01	5.88E-01	1.41E-02	4.60E-05	8.93E-01
8	2WBRG1	10.94 charge	4	29.6	2.86E+02	6.87E-01	3.60E-02	4.98E+02	5.38E-01	2.06E+00	5.15E+00	0.00E+00	7.05E-01	0.00E+00	8.08E-02	1.40E-01	1.16E-02	4.60E-05	2.62E-01
9	3WBR2	11.69 charge	4	30.2	1.56E+02	4.37E-01	2.99E-04	3.87E+01	3.71E-01	1.77E+00	0.00E+00	0.00E+00	7.68E-01	0.00E+00	3.40E+01	3.29E-01	2.51E-02	6.99E-03	6.82E-02
10	3WBRA2	11.33 charge	4	29.6	1.67E+02	1.43E+00	4.05E-02	3.94E+01	4.71E-01	2.15E+00	0.00E+00	3.51E+00	9.94E-01	0.00E+00	3.63E+01	3.90E-01	4.03E-02	6.62E-03	1.00E+01
11	3WBRS2	11.61 charge	4	31.4	1.57E+02	4.93E-01	5.96E-02	4.25E+01	3.54E-01	2.56E+00	0.00E+00	0.00E+00	7.92E-01	0.00E+00	3.71E+01	3.46E-01	2.25E-02	4.60E-05	3.43E+00
12	3WBRG3	11.41 charge	4	29.7	1.12E+02	3.46E-01	2.99E-04	9.96E+01	4.34E-01	9.53E+00	5.07E-01	0.00E+00	8.02E-01	1.71E+00	4.30E+00	1.30E-01	4.96E-03	4.60E-05	4.37E-02
13	4WBR2	11.60 charge	4	29.9	1.21E+02	3.83E-01	2.99E-04	2.83E+01	3.40E-01	1.81E+00	0.00E+00	0.00E+00	7.68E-01	0.00E+00	2.53E+01	2.74E-01	6.60E-03	4.82E-03	1.47E-01
14	4WBRA2	11.29 charge	4	29.3	1.16E+02	1.09E+00	1.65E-01	1.58E+01	3.90E-01	2.05E+00	0.00E+00	3.44E+00	7.98E-01	0.00E+00	2.54E+01	2.49E-01	4.26E-02	1.71E-02	1.76E+01
15	4WBRS1	11.35 charge	4	30.7	1.23E+02	3.78E-01	2.99E-04	2.66E+01	2.96E-01	1.81E+00	0.00E+00	0.00E+00	7.70E-01	0.00E+00	2.60E+01	2.12E-01	1.24E-02	4.60E-05	3.39E+00
16	4WBRG2	11.55 charge	4	28.1	7.20E+01	2.51E-01	2.99E-04	5.91E+01	2.75E-01	1.53E+00	0.00E+00	0.00E+00	7.65E-01	2.66E+00	1.04E+01	9.97E-02	3.73E-05	6.58E-03	3.16E-05
17	5WBR2	11.52 charge	4	30.4	1.06E+02	3.47E-01	2.99E-04	1.80E+01	3.90E-01	1.61E+00	0.00E+00	3.26E+00	0.00E+00	0.00E+00	2.24E+01	2.35E-01	5.35E-03	4.60E-05	4.89E-01
18	5WBRA2	11.23 charge	4	30.2	9.75E+01	2.80E+00	1.05E-01	1.60E+01	4.32E-01	1.78E+00	0.00E+00	3.28E+00	7.79E-01	0.00E+00	2.16E+01	1.81E-01	4.23E-02	1.70E-02	1.93E+01
19	5WBRS2	11.32 charge	4	30.9	1.13E+02	2.91E-01	4.36E-02	1.46E+01	4.90E-01	1.82E+00	0.00E+00	3.39E+00	7.77E-01	0.00E+00	2.68E+01	1.51E-01	1.46E-02	4.60E-05	6.75E+00
20	5WBRG2	11.47 charge	4	30.3	5.70E+01	2.18E-01	2.99E-04	7.43E+01	4.99E-01	1.47E+00	0.00E+00	0.00E+00	7.95E-01	3.94E+00	1.31E+01	7.38E-02	3.73E-05	4.60E-05	3.16E-05

```
END
```

Appendix 14. PHREEQC input file code for Simulation 3 (llndl.dat).

```
USER_PUNCH 1
headings  EC_(uS/cm) TDS_g/kg-solution alk_mg/L
start
10 PUNCH Description
25 PUNCH SC
32 PUNCH (RHO * SOLN_VOL - TOT("water")) * 1000 / (RHO * SOLN_VOL)
40 PUNCH alk * ((50.05) / 1000)
end
SELECTED_OUTPUT 1
file simulation3.txt
charge_balance
ionic_strength
temp
percent_error
alkalinity
totals      Na              K          Mg          Ca          F           Cl          S(+6)       Br          N(+5)       P(5)        Al          V           Cr          Mn          Fe          Cu          Zn          Ga          As          Si
-molalities OH- HCO3- # add here other aqueous species of interest
-saturation_indices Fe(OH)2 Fe(OH)3 Gibbsite Goethite Pyrolusite Kaolinite Diaspore Magnetite Boehmite Cuprite
# Simulation 3 using llnl.dat based on the pH measured in the lab to compare alk, charge balance, and S.I
END
SOLUTION_SPREAD
units mg/l
```

Number	Description	pH	pe	Temp	Na	K	Mg	Ca	F	Cl	S(+6)	Br	N(+5)	P(5)	Al	V	Cr	Mn	Fe	Cu	Zn	Ga	As	Si
1	1WBR1	11.98	4	25.6	4.47E+02	1.02E+00	2.99E-04	7.26E+01	1.18E+00	3.26E+00	0.00E+00	0.00E+00	7.15E-01	0.00E+00	1.35E+02	5.04E-01	5.78E-02	6.18E-03	3.16E-05	1.26E-01	7.54E-02	1.85E-01	1.19E-02	2.13E-01
2	1WBRA2	11.76	4	25.6	4.31E+02	3.91E+00	2.99E-04	5.96E+01	5.42E-01	9.86E+00	0.00E+00	0.00E+00	7.42E-01	0.00E+00	1.01E+02	8.03E-01	8.43E-02	4.60E-05	7.71E-01	3.65E-02	1.11E-02	1.55E-01	3.15E-02	1.26E+01
3	1WBRS1	11.93	4	29.3	4.48E+02	9.76E-01	2.99E-04	5.68E+01	1.49E+00	3.11E+00	0.00E+00	0.00E+00	3.20E+00	0.00E+00	1.30E+02	8.85E-01	4.98E-02	4.60E-05	2.60E-02	6.33E-03	9.08E-03	1.93E-01	3.11E-02	1.69E+01
4	1WBRG2	10.92	4	30.2	7.32E+02	1.53E+00	3.78E-02	5.09E+02	4.67E-01	4.19E+00	7.59E+00	0.00E+00	7.13E-01	0.00E+00	2.31E-01	1.40E-01	4.52E-02	4.60E-05	2.47E-01	2.25E-02	1.79E-02	2.14E-02	3.15E-05	1.05E+00
5	2WBR1	11.82	4	29.8	2.41E+02	5.53E-01	2.99E-04	3.65E+01	6.39E-01	2.06E+00	0.00E+00	0.00E+00	7.03E-01	0.00E+00	6.29E+01	3.54E-01	2.39E-02	4.60E-05	3.16E-05	4.63E-03	9.59E-03	5.92E-02	9.29E-03	2.00E+00
6	2WBRA1	11.54	4	30.1	2.70E+02	2.43E+00	2.99E-04	4.44E+01	3.15E+00	2.97E+00	0.00E+00	3.37E+00	7.44E-01	0.00E+00	6.66E+01	5.57E-01	4.85E-02	6.02E-03	2.29E+00	9.68E-02	5.03E-02	6.95E-02	2.42E-02	8.96E+00
7	2WBRS1	11.76	4	30.1	2.22E+02	6.03E-01	3.07E-02	4.07E+01	6.61E-01	2.21E+00	0.00E+00	0.00E+00	7.06E-01	0.00E+00	5.00E+01	5.88E-01	1.41E-02	4.60E-05	8.93E-01	4.00E-03	6.70E-03	4.20E-02	2.75E-02	1.08E+01
8	2WBRG1	10.94	4	29.6	2.86E+02	6.87E-01	3.60E-02	4.98E+02	5.38E-01	2.06E+00	5.15E+00	0.00E+00	7.05E-01	0.00E+00	8.08E-02	1.40E-01	1.16E-02	4.60E-05	2.62E-01	6.77E-03	1.59E-02	1.26E-02	3.15E-05	1.03E+01
9	3WBR2	11.69	4	30.2	1.56E+02	4.37E-01	2.99E-04	3.87E+01	3.71E-01	1.77E+00	0.00E+00	0.00E+00	7.68E-01	0.00E+00	3.40E+01	3.29E-01	2.51E-02	6.99E-03	6.82E-02	1.29E-01	7.04E-02	1.84E-02	3.15E-05	1.15E+01
10	3WBRA2	11.33	4	29.6	1.67E+02	1.43E+00	4.05E-02	3.94E+01	4.71E-01	2.15E+00	0.00E+00	3.51E+00	9.94E-01	0.00E+00	3.63E+01	3.90E-01	4.03E-02	6.62E-03	1.00E+01	1.03E-02	2.07E-02	3.03E-02	1.75E-02	1.23E+01
11	3WBRS2	11.61	4	31.4	1.57E+02	4.93E-01	5.96E-02	4.25E+01	3.54E-01	2.56E+00	0.00E+00	0.00E+00	7.92E-01	0.00E+00	3.71E+01	3.46E-01	2.25E-02	4.60E-05	3.43E+00	7.80E-03	1.50E-02	1.90E-02	1.69E-02	1.51E-01
12	3WBRG3	11.41	4	29.7	1.12E+02	3.46E-01	2.99E-04	9.96E+01	4.34E-01	9.53E+00	5.07E-01	0.00E+00	8.02E-01	1.71E+00	4.30E+00	1.30E-01	4.96E-03	4.60E-05	4.37E-02	4.81E-03	1.23E-02	2.32E-02	3.15E-05	2.24E+01
13	4WBR2	11.6	4	29.9	1.21E+02	3.83E-01	2.99E-04	2.83E+01	3.40E-01	1.81E+00	0.00E+00	0.00E+00	7.68E-01	0.00E+00	2.53E+01	2.74E-01	6.60E-03	4.82E-03	1.47E-01	9.54E-02	5.28E-02	1.03E-02	9.15E-03	2.50E+01
14	4WBRA2	11.29	4	29.3	1.16E+02	1.09E+00	1.65E-01	1.58E+01	3.90E-01	2.05E+00	0.00E+00	3.44E+00	7.98E-01	0.00E+00	2.54E+01	2.49E-01	4.26E-02	1.71E-02	1.76E+01	3.14E-02	4.21E-02	2.21E-02	1.74E-02	3.29E+00
15	4WBRS1	11.35	4	30.7	1.23E+02	3.78E-01	2.99E-04	2.66E+01	2.96E-01	1.81E+00	0.00E+00	0.00E+00	7.70E-01	0.00E+00	2.60E+01	2.12E-01	1.24E-02	4.60E-05	3.39E+00	2.78E-02	2.11E-02	9.91E-03	9.74E-03	2.11E+01
16	4WBRG2	11.55	4	28.1	7.20E+01	2.51E-01	2.99E-04	5.91E+01	2.75E-01	1.53E+00	0.00E+00	0.00E+00	7.65E-01	2.66E+00	1.04E+01	9.97E-02	3.73E-05	6.58E-03	3.16E-05	9.46E-02	6.48E-02	1.97E-02	3.15E-05	1.61E+01
17	5WBR2	11.52	4	30.4	1.06E+02	3.47E-01	2.99E-04	1.80E+01	3.90E-01	1.61E+00	0.00E+00	3.26E+00	0.00E+00	0.00E+00	2.24E+01	2.35E-01	5.35E-03	4.60E-05	4.89E-01	3.90E-03	9.88E-03	7.87E-03	1.63E-02	2.07E+01
18	5WBRA2	11.23	4	30.2	9.75E+01	2.80E+00	1.05E-01	1.60E+01	4.32E-01	1.78E+00	0.00E+00	3.28E+00	7.79E-01	0.00E+00	2.16E+01	1.81E-01	4.23E-02	1.70E-02	1.93E+01	9.74E-03	1.22E-01	1.99E-02	1.15E-02	6.74E+00
19	5WBRS2	11.32	4	30.9	1.13E+02	2.91E-01	4.36E-02	1.46E+01	4.90E-01	1.82E+00	0.00E+00	3.39E+00	7.77E-01	0.00E+00	2.68E+01	1.51E-01	1.46E-02	4.60E-05	6.75E+00	4.46E-03	2.07E-02	1.11E-02	8.85E-03	2.53E+00
20	5WBRG2	11.47	4	30.3	5.70E+01	2.18E-01	2.99E-04	7.43E+01	4.99E-01	1.47E+00	0.00E+00	0.00E+00	7.95E-01	3.94E+00	1.31E+01	7.38E-02	3.73E-05	4.60E-05	3.16E-05	4.84E-03	7.88E-03	1.51E-02	3.15E-05	6.90E-01

```
END
```

Appendix 15. PHREEQC input file code for Simulation 4 (llnl.dat).

```
USER_PUNCH 1
headings  EC_(uS/cm) TDS_g/kg-solution alk_mg/L
start
10 PUNCH Description
25 PUNCH SC
32 PUNCH (RHO * SOLN_VOL - TOT("water")) * 1000 / (RHO * SOLN_VOL)
40 PUNCH alk * ((50.05) / 1000)
end
SELECTED_OUTPUT 1
file simulation4.txt
charge_balance
ionic_strength
temp
percent_error
alkalinity
totals      Na          K           Mg          Ca          F           Cl          S(+6)       Br          N(+5)       P(5)        Al          V           Cr          Mn          Fe          Cu          Zn          Ga          As          Si
-molalities OH- HCO3- # add here other aqueous species of interest
-saturation_indices Fe(OH)2 Fe(OH)3 Gibbsite Goethite Pyrolusite Kaolinite Diaspore Magnetite Boehmite Cuprite
# Simulation 4 using llnl.dat based on the pH charge command of PHREEQC (compare alk, charge balance, and S.I)
END
SOLUTION_SPREAD
units mg/l
```

Number	Description	pH	pe	Temp	Na	K	Mg	Ca	F	Cl	S(+6)	Br	N(+5)	P(5)	Al	V	Cr	Mn	Fe	Cu	Zn	Ga	As	Si
1	1WBR1	11.98 charge	4	25.6	4.47E+02	1.02E+00	2.99E-04	7.26E+01	1.18E+00	3.26E+00	0.00E+00	0.00E+00	7.15E-01	0.00E+00	1.35E+02	5.04E-01	5.78E-02	6.18E-03	3.16E-05	1.26E-01	7.54E-02	1.85E-01	1.19E-02	2.13E-01
2	1WBRA2	11.76 charge	4	25.6	4.31E+02	3.91E+00	2.99E-04	5.96E+01	5.42E-01	9.86E+00	0.00E+00	0.00E+00	7.42E-01	0.00E+00	1.01E+02	8.03E-01	8.43E-02	4.60E-05	7.71E-01	3.65E-02	1.11E-02	1.55E-01	3.15E-02	1.26E+01
3	1WBRS1	11.93 charge	4	29.3	4.48E+02	9.76E-01	2.99E-04	5.68E+01	1.49E+00	3.11E+00	0.00E+00	0.00E+00	3.20E+00	0.00E+00	1.30E+02	8.85E-01	4.98E-02	4.60E-05	2.60E-02	6.33E-03	9.08E-03	1.93E-01	3.11E-02	1.69E+01
4	1WBRG2	10.92 charge	4	30.2	7.32E+02	1.53E+00	3.78E-02	5.09E+02	4.67E-01	4.19E+00	7.59E+00	0.00E+00	7.13E-01	0.00E+00	2.31E-01	1.40E-01	4.52E-02	4.60E-05	2.47E-01	2.25E-02	1.79E-02	2.14E-02	3.15E-05	1.05E+00
5	2WBR1	11.82 charge	4	29.8	2.41E+02	5.53E-01	2.99E-04	3.65E+01	6.39E-01	2.06E+00	0.00E+00	0.00E+00	7.03E-01	0.00E+00	6.29E+01	3.54E-01	2.39E-02	4.60E-05	3.16E-05	4.63E-03	9.59E-03	5.92E-02	9.29E-03	2.00E+00
6	2WBRA1	11.54 charge	4	30.1	2.70E+02	2.43E+00	2.99E-04	4.44E+01	3.15E+00	2.97E+00	0.00E+00	3.37E+00	7.44E-01	0.00E+00	6.66E+01	5.57E-01	4.85E-02	6.02E-03	2.29E+00	9.68E-02	5.03E-02	6.95E-02	2.42E-02	8.96E+00
7	2WBRS1	11.76 charge	4	30.1	2.22E+02	6.03E-01	3.07E-02	4.07E+01	6.61E-01	2.21E+00	0.00E+00	0.00E+00	7.06E-01	0.00E+00	5.00E+01	5.88E-01	1.41E-02	4.60E-05	8.93E-01	4.00E-03	6.70E-03	4.20E-02	2.75E-02	1.08E+01
8	2WBRG1	10.94 charge	4	29.6	2.86E+02	6.87E-01	3.60E-02	4.98E+02	5.38E-01	2.06E+00	5.15E+00	0.00E+00	7.05E-01	0.00E+00	8.08E-02	1.40E-01	1.16E-02	4.60E-05	2.62E-01	6.77E-03	1.59E-02	1.26E-02	3.15E-05	1.03E+01
9	3WBR2	11.69 charge	4	30.2	1.56E+02	4.37E-01	2.99E-04	3.87E+01	3.71E-01	1.77E+00	0.00E+00	0.00E+00	7.68E-01	0.00E+00	3.40E+01	3.29E-01	2.51E-02	6.99E-03	6.82E-02	1.29E-01	7.04E-02	1.84E-02	3.15E-05	1.15E+01
10	3WBRA2	11.33 charge	4	29.6	1.67E+02	1.43E+00	4.05E-02	3.94E+01	4.71E-01	2.15E+00	0.00E+00	3.51E+00	9.94E-01	0.00E+00	3.63E+01	3.90E-01	4.03E-02	6.62E-03	1.00E+01	1.03E-02	2.07E-02	3.03E-02	1.75E-02	1.23E+01
11	3WBRS2	11.61 charge	4	31.4	1.57E+02	4.93E-01	5.96E-02	4.25E+01	3.54E-01	2.56E+00	0.00E+00	0.00E+00	7.92E-01	0.00E+00	3.71E+01	3.46E-01	2.25E-02	4.60E-05	3.43E+00	7.80E-03	1.50E-02	1.90E-02	1.69E-02	1.51E-01
12	3WBRG3	11.41 charge	4	29.7	1.12E+02	3.46E-01	2.99E-04	9.96E+01	4.34E-01	9.53E+00	5.07E-01	0.00E+00	8.02E-01	1.71E+00	4.30E+00	1.30E-01	4.96E-03	4.60E-05	4.37E-02	4.81E-03	1.23E-02	2.32E-02	3.15E-05	2.24E+01
13	4WBR2	11.60 charge	4	29.9	1.21E+02	3.83E-01	2.99E-04	2.83E+01	3.40E-01	1.81E+00	0.00E+00	0.00E+00	7.68E-01	0.00E+00	2.53E+01	2.74E-01	6.60E-03	4.82E-03	1.47E-01	9.54E-02	5.28E-02	1.03E-02	9.15E-03	2.50E+01
14	4WBRA2	11.29 charge	4	29.3	1.16E+02	1.09E+00	1.65E-01	1.58E+01	3.90E-01	2.05E+00	0.00E+00	3.44E+00	7.98E-01	0.00E+00	2.54E+01	2.49E-01	4.26E-02	1.71E-02	1.76E+01	3.14E-02	4.21E-02	2.21E-02	1.74E-02	3.29E+00
15	4WBRS1	11.35 charge	4	30.7	1.23E+02	3.78E-01	2.99E-04	2.66E+01	2.96E-01	1.81E+00	0.00E+00	0.00E+00	7.70E-01	0.00E+00	2.60E+01	2.12E-01	1.24E-02	4.60E-05	3.39E+00	2.78E-02	2.11E-02	9.91E-03	9.74E-03	2.11E+01
16	4WBRG2	11.55 charge	4	28.1	7.20E+01	2.51E-01	2.99E-04	5.91E+01	2.75E-01	1.53E+00	0.00E+00	0.00E+00	7.65E-01	2.66E+00	1.04E+01	9.97E-02	3.73E-05	6.58E-03	3.16E-05	9.46E-02	6.48E-02	1.97E-02	3.15E-05	1.61E+01
17	5WBR2	11.52 charge	4	30.4	1.06E+02	3.47E-01	2.99E-04	1.80E+01	3.90E-01	1.61E+00	0.00E+00	3.26E+00	0.00E+00	0.00E+00	2.24E+01	2.35E-01	5.35E-03	4.60E-05	4.89E-01	3.90E-03	9.88E-03	7.87E-03	1.63E-02	2.07E+01
18	5WBRA2	11.23 charge	4	30.2	9.75E+01	2.80E+00	1.05E-01	1.60E+01	4.32E-01	1.78E+00	0.00E+00	3.28E+00	7.79E-01	0.00E+00	2.16E+01	1.81E-01	4.23E-02	1.70E-02	1.93E+01	9.74E-03	1.22E-01	1.99E-02	1.15E-02	6.74E+00
19	5WBRS2	11.32 charge	4	30.9	1.13E+02	2.91E-01	4.36E-02	1.46E+01	4.90E-01	1.82E+00	0.00E+00	3.39E+00	7.77E-01	0.00E+00	2.68E+01	1.51E-01	1.46E-02	4.60E-05	6.75E+00	4.46E-03	2.07E-02	1.11E-02	8.85E-03	2.53E+00
20	5WBRG2	11.47 charge	4	30.3	5.70E+01	2.18E-01	2.99E-04	7.43E+01	4.99E-01	1.47E+00	0.00E+00	0.00E+00	7.95E-01	3.94E+00	1.31E+01	7.38E-02	3.73E-05	4.60E-05	3.16E-05	4.84E-03	7.88E-03	1.51E-02	3.15E-05	6.90E-01

```
END
```

Appendix 16. PHREEQC input file code for Simulation 5 (llnl.dat).

```
USER_PUNCH 1
headings  EC_(uS/cm) TDS_g/kg-solution alk_mg/L
start
10 PUNCH Description
25 PUNCH SC
32 PUNCH (RHO * SOLN_VOL - TOT("water")) * 1000 / (RHO * SOLN_VOL)
40 PUNCH alk * ((50.05) / 1000)
end
SELECTED_OUTPUT 1
file simulation5.txt
charge_balance
ionic_strength
temp
percent_error
alkalinity
totals      Na              K               Mg      Ca      F       Cl      S(+6)   Br      N(+5)   P(5)    Al      V       Cr      Mn      Fe      Cu      Zn      Ga      As      Si
-molalities OH- HCO3- CO3-2 # add here other aqueous species of interest
-saturation_indices Fe(OH)2 Fe(OH)3 Gibbsite Goethite Pyrolusite Kaolinite Diaspore Magnetite Boehmite Cuprite Calcite Monohydrocalcite Dolomite Magnesite Aragonite Dawsonite Hydrozincite Rhodochrosite Siderite  CO2(g)
# Simulation 5 using llnl.dat based on the pH measured in the lab to compare alk, charge balance, S.I, and equilibrium phases(equilibrate with the partial pressure of CO2 in the atm)
#check if the carbonate pahses are closest to equilibrium under normal atm conditions.
# why ? because carbonate phases might precipitate in the BRDA. This will mitigate the mobility of trace elements wich are toxic to plant growth and groundwater
END
SOLUTION_SPREAD
units mg/l
```

Number	Description	pH	pe	Temp	Na	K	Mg	Ca	F	Cl	S(+6)	Br	N(+5)	P(5)	Al	V	Cr	Mn	Fe	Cu	Zn	Ga	As	Si
1	1WBR1	11.98 charge	4	25.6	4.47E+02	1.02E+00	2.99E-04	7.26E+01	1.18E+00	3.26E+00	0.00E+00	0.00E+00	7.15E-01	0.00E+00	1.35E+02	5.04E-01	5.78E-02	6.18E-03	3.16E-05	1.26E-01	7.54E-02	1.85E-01	1.19E-02	2.13E-01
2	1WBRA2	11.76 charge	4	25.6	4.31E+02	3.91E+00	2.99E-04	5.96E+01	5.42E-01	9.86E+00	0.00E+00	0.00E+00	7.42E-01	0.00E+00	1.01E+02	8.03E-01	8.43E-02	4.60E-05	7.71E-01	3.65E-02	1.11E-02	1.55E-01	3.15E-02	1.26E+01
3	1WBRS1	11.93 charge	4	29.3	4.48E+02	9.76E-01	2.99E-04	5.68E+01	1.49E+00	3.11E+00	0.00E+00	0.00E+00	3.20E+00	0.00E+00	1.30E+02	8.85E-01	4.98E-02	4.60E-05	2.60E-02	6.33E-03	9.08E-03	1.93E-01	3.11E-02	1.69E+01
4	1WBRG2	10.92 charge	4	30.2	7.32E+02	1.53E+00	3.78E-02	5.09E+02	4.67E-01	4.19E+00	7.59E+00	0.00E+00	7.13E-01	0.00E+00	2.31E-01	1.40E-01	4.52E-02	4.60E-05	2.47E-01	2.25E-02	1.79E-02	2.14E-02	3.15E-05	1.05E+00
5	2WBR1	11.82 charge	4	29.8	2.41E+02	5.53E-01	2.99E-04	3.65E+01	6.39E-01	2.06E+00	0.00E+00	0.00E+00	7.03E-01	0.00E+00	6.29E+01	3.54E-01	2.39E-02	4.60E-05	3.16E-05	4.63E-03	9.59E-03	5.92E-02	9.29E-03	2.00E+00
6	2WBRA1	11.54 charge	4	30.1	2.70E+02	2.43E+00	2.99E-04	4.44E+01	3.15E+00	2.97E+00	0.00E+00	3.37E+00	7.44E-01	0.00E+00	6.66E+01	5.57E-01	4.85E-02	6.02E-03	2.29E+00	9.68E-02	5.03E-02	6.95E-02	2.42E-02	8.96E+00
7	2WBRS1	11.76 charge	4	30.1	2.22E+02	6.03E-01	3.07E-02	4.07E+01	6.61E-01	2.21E+00	0.00E+00	0.00E+00	7.06E-01	0.00E+00	5.00E+01	5.88E-01	1.41E-02	4.60E-05	8.93E-01	4.00E-03	6.70E-03	4.20E-02	2.75E-02	1.08E+01
8	2WBRG1	10.94 charge	4	29.6	2.86E+02	6.87E-01	3.60E-02	4.98E+02	5.38E-01	2.06E+00	5.15E+00	0.00E+00	7.05E-01	0.00E+00	8.08E-02	1.40E-01	1.16E-02	4.60E-05	2.62E-01	6.77E-03	1.59E-02	1.26E-02	3.15E-05	1.03E+01
9	3WBR2	11.69 charge	4	30.2	1.56E+02	4.37E-01	2.99E-04	3.87E+01	3.71E-01	1.77E+00	0.00E+00	0.00E+00	7.68E-01	0.00E+00	3.40E+01	3.29E-01	2.51E-02	6.99E-03	6.82E-02	1.29E-01	7.04E-02	1.84E-02	3.15E-05	1.15E+01
10	3WBRA2	11.33 charge	4	29.6	1.67E+02	1.43E+00	4.05E-02	3.94E+01	4.71E-01	2.15E+00	0.00E+00	3.51E+00	9.94E-01	0.00E+00	3.63E+01	3.90E-01	4.03E-02	6.62E-03	1.00E+01	1.03E-02	2.07E-02	3.03E-02	1.75E-02	1.23E+01
11	3WBRS2	11.61 charge	4	31.4	1.57E+02	4.93E-01	5.96E-02	4.25E+01	3.54E-01	2.56E+00	0.00E+00	0.00E+00	7.92E-01	0.00E+00	3.71E+01	3.46E-01	2.25E-02	4.60E-05	3.43E+00	7.80E-03	1.50E-02	1.90E-02	1.69E-02	1.51E-01
12	3WBRG3	11.41 charge	4	29.7	1.12E+02	3.46E-01	2.99E-04	9.96E+01	4.34E-01	9.53E+00	5.07E-01	0.00E+00	8.02E-01	1.71E+00	4.30E+00	1.30E-01	4.96E-03	4.60E-05	4.37E-02	4.81E-03	1.23E-02	2.32E-02	3.15E-05	2.24E+01
13	4WBR2	11.60 charge	4	29.9	1.21E+02	3.83E-01	2.99E-04	2.83E+01	3.40E-01	1.81E+00	0.00E+00	0.00E+00	7.68E-01	0.00E+00	2.53E+01	2.74E-01	6.60E-03	4.82E-03	1.47E-01	9.54E-02	5.28E-02	1.03E-02	9.15E-03	2.50E+01
14	4WBRA2	11.29 charge	4	29.3	1.16E+02	1.09E+00	1.65E-01	1.58E+01	3.90E-01	2.05E+00	0.00E+00	3.44E+00	7.98E-01	0.00E+00	2.54E+01	2.49E-01	4.26E-02	1.71E-02	1.76E+01	3.14E-02	4.21E-02	2.21E-02	1.74E-02	3.29E+00
15	4WBRS1	11.35 charge	4	30.7	1.23E+02	3.78E-01	2.99E-04	2.66E+01	2.96E-01	1.81E+00	0.00E+00	0.00E+00	7.70E-01	0.00E+00	2.60E+01	2.12E-01	1.24E-02	4.60E-05	3.39E+00	2.78E-02	2.11E-02	9.91E-03	9.74E-03	2.11E+01
16	4WBRG2	11.55 charge	4	28.1	7.20E+01	2.51E-01	2.99E-04	5.91E+01	2.75E-01	1.53E+00	0.00E+00	0.00E+00	7.65E-01	2.66E+00	1.04E+01	9.97E-02	3.73E-05	6.58E-03	3.16E-05	9.46E-02	6.48E-02	1.97E-02	3.15E-05	1.61E+01
17	5WBR2	11.52 charge	4	30.4	1.06E+02	3.47E-01	2.99E-04	1.80E+01	3.90E-01	1.61E+00	0.00E+00	3.26E+00	0.00E+00	0.00E+00	2.24E+01	2.35E-01	5.35E-03	4.60E-05	4.89E-01	3.90E-03	9.88E-03	7.87E-03	1.63E-02	2.07E+01
18	5WBRA2	11.23 charge	4	30.2	9.75E+01	2.80E+00	1.05E-01	1.60E+01	4.32E-01	1.78E+00	0.00E+00	3.28E+00	7.79E-01	0.00E+00	2.16E+01	1.81E-01	4.23E-02	1.70E-02	1.93E+01	9.74E-03	1.22E-01	1.99E-02	1.15E-02	6.74E+00
19	5WBRS2	11.32 charge	4	30.9	1.13E+02	2.91E-01	4.36E-02	1.46E+01	4.90E-01	1.82E+00	0.00E+00	3.39E+00	7.77E-01	0.00E+00	2.68E+01	1.51E-01	1.46E-02	4.60E-05	6.75E+00	4.46E-03	2.07E-02	1.11E-02	8.85E-03	2.53E+00
20	5WBRG2	11.47 charge	4	30.3	5.70E+01	2.18E-01	2.99E-04	7.43E+01	4.99E-01	1.47E+00	0.00E+00	0.00E+00	7.95E-01	3.94E+00	1.31E+01	7.38E-02	3.73E-05	4.60E-05	3.16E-05	4.84E-03	7.88E-03	1.51E-02	3.15E-05	6.90E-01

```
EQUILIBRIUM_PHASES 1-20
CO2(g) -3.5 10
END
RUN_CELLS
-cells 1-20
```

Appendix 17. PHREEQC input file code for Simulation 6 (llnl.dat).

```
USER_PUNCH 1
headings EC_(uS/cm) TDS_g/kg-solution alk_mg/L Ca_mg/l Mg_mg/l Na_mg/l
start
10 PUNCH Description
25 PUNCH SC
32 PUNCH (RHO * SOLN_VOL - TOT("water")) * 1000 / (RHO * SOLN_VOL)
40 PUNCH alk * ((50.05) / 1000)
50 PUNCH Ca * ((40.078) / 1000)
60 PUNCH Mg * ((24.305) / 1000)
70 PUNCH Na * ((22.9898) / 1000)
end
SELECTED_OUTPUT 1
file simulation6.txt
charge_balance
ionic_strength
temp
percent_error
alkalinity
totals Na K Mg Ca F Cl S(+6) Br N(+5) P(5) Al V Cr Mn Fe Cu Zn Ga As Si
-molalities OH- HCO3- CO3-2 CO2
-saturation_indices Fe(OH)2 Fe(OH)3 Gibbsite Goethite Pyrolusite Kaolinite Diaspore Magnetite Boehmite Cuprite Calcite Monohydrocalcite Dolomite Magnesite Aragonite Dawsonite Hydrozincite Rhodochrosite Siderite CO2 HCO3-(g)
# Simulation 6 using llnl.dat based on the pH measured in the lab to compare alk, charge balance and S.I and equilibrium phases(equilibrated with the partial pressure of CO2 in the atm)
#check if the carbonate pahses are near to equilibrium under normal soil conditions.
# why ? because carbonate phases might precipitate in the BRDA. This will mitigate the mobility of trace elements wich are toxic to plant growth and groundwater
END
SOLUTION_SPREAD
units mg/l
```

Number	Description	pH	pe	Temp	Na	K	Mg	Ca	F	Cl	S(+6)	Br	N(+5)	P(5)	Al	V	Cr	Mn	Fe	Cu	Zn	Ga	As	Si
1	1WBR1	11.98 charge	4	25.6	4.47E+02	1.02E+00	2.99E-04	7.26E+01	1.18E+00	3.26E+00	0.00E+00	0.00E+00	7.15E-01	0.00E+00	1.35E+02	5.04E-01	5.78E-02	6.18E-03	3.16E-05	1.26E-01	7.54E-02	1.85E-01	1.19E-02	2.13E-01
2	1WBRA2	11.76 charge	4	25.6	4.31E+02	3.91E+00	2.99E-04	5.96E+01	5.42E-01	9.86E+00	0.00E+00	0.00E+00	7.42E-01	0.00E+00	1.01E+02	8.03E-01	8.43E-02	4.60E-05	7.71E-01	3.65E-02	1.11E-02	1.55E-01	3.15E-02	1.26E+01
3	1WBRS1	11.93 charge	4	29.3	4.48E+02	9.76E-01	2.99E-04	5.68E+01	1.49E+00	3.11E+00	0.00E+00	0.00E+00	3.20E+00	0.00E+00	1.30E+02	8.85E-01	4.98E-02	4.60E-05	2.60E-02	6.33E-03	9.08E-03	1.93E-01	3.11E-02	1.69E+01
4	1WBRG2	10.92 charge	4	30.2	7.32E+02	1.53E+00	3.78E-02	5.09E+02	4.67E-01	4.19E+00	7.59E+00	0.00E+00	7.13E-01	0.00E+00	2.31E-01	1.40E-01	4.52E-02	4.60E-05	2.47E-01	2.25E-02	1.79E-02	2.14E-02	3.15E-05	1.05E+00
5	2WBR1	11.82 charge	4	29.8	2.41E+02	5.53E-01	2.99E-04	3.65E+01	6.39E-01	2.06E+00	0.00E+00	0.00E+00	7.03E-01	0.00E+00	6.29E+01	3.54E-01	2.39E-02	4.60E-05	3.16E-05	4.63E-03	9.59E-03	5.92E-02	9.29E-03	2.00E+00
6	2WBRA1	11.54 charge	4	30.1	2.70E+02	2.43E+00	2.99E-04	4.44E+01	3.15E+00	2.97E+00	0.00E+00	3.37E+00	7.44E-01	0.00E+00	6.66E+01	5.57E-01	4.85E-02	6.02E-03	2.29E+00	9.68E-02	5.03E-02	6.95E-02	2.42E-02	8.96E+00
7	2WBRS1	11.76 charge	4	30.1	2.22E+02	6.03E-01	3.07E-02	4.07E+01	6.61E-01	2.21E+00	0.00E+00	0.00E+00	7.06E-01	0.00E+00	5.00E+01	5.88E-01	1.41E-02	4.60E-05	8.93E-01	4.00E-03	6.70E-03	4.20E-02	2.75E-02	1.08E+01
8	2WBRG1	10.94 charge	4	29.6	2.86E+02	6.87E-01	3.60E-02	4.98E+02	5.38E-01	2.06E+00	5.15E+00	0.00E+00	7.05E-01	0.00E+00	8.08E-02	1.40E-01	1.16E-02	4.60E-05	2.62E-01	6.77E-03	1.59E-02	1.26E-02	3.15E-05	1.03E+01
9	3WBR2	11.69 charge	4	30.2	1.56E+02	4.37E-01	2.99E-04	3.87E+01	3.71E-01	1.77E+00	0.00E+00	0.00E+00	7.68E-01	0.00E+00	3.40E+01	3.29E-01	2.51E-02	6.99E-03	6.82E-02	1.29E-01	7.04E-02	1.84E-02	3.15E-05	1.15E+01
10	3WBRA2	11.33 charge	4	29.6	1.67E+02	1.43E+00	4.05E-02	3.94E+01	4.71E-01	2.15E+00	0.00E+00	3.51E+00	9.94E-01	0.00E+00	3.63E+01	3.90E-01	4.03E-02	6.62E-03	1.00E+01	1.03E-02	2.07E-02	3.03E-02	1.75E-02	1.23E+01
11	3WBRS2	11.61 charge	4	31.4	1.57E+02	4.93E-01	5.96E-02	4.25E+01	3.54E-01	2.56E+00	0.00E+00	0.00E+00	7.92E-01	0.00E+00	3.71E+01	3.46E-01	2.25E-02	4.60E-05	3.43E+00	7.80E-03	1.50E-02	1.90E-02	1.69E-02	1.51E-01
12	3WBRG3	11.41 charge	4	29.7	1.12E+02	3.46E-01	2.99E-04	9.96E+01	4.34E-01	9.53E+00	5.07E-01	0.00E+00	8.02E-01	1.71E+00	4.30E+00	1.30E-01	4.96E-03	4.60E-05	4.37E-02	4.81E-03	1.23E-02	2.32E-02	3.15E-05	2.24E+01
13	4WBR2	11.60 charge	4	29.9	1.21E+02	3.83E-01	2.99E-04	2.83E+01	3.40E-01	1.81E+00	0.00E+00	0.00E+00	7.68E-01	0.00E+00	2.53E+01	2.74E-01	6.60E-03	4.82E-03	1.47E-01	9.54E-02	5.28E-02	1.03E-02	9.15E-03	2.50E+01
14	4WBRA2	11.29 charge	4	29.3	1.16E+02	1.09E+00	1.65E-01	1.58E+01	3.90E-01	2.05E+00	0.00E+00	3.44E+00	7.98E-01	0.00E+00	2.54E+01	2.49E-01	4.26E-02	1.71E-02	1.76E+01	3.14E-02	4.21E-02	2.21E-02	1.74E-02	3.29E+00
15	4WBRS1	11.35 charge	4	30.7	1.23E+02	3.78E-01	2.99E-04	2.66E+01	2.96E-01	1.81E+00	0.00E+00	0.00E+00	7.70E-01	0.00E+00	2.60E+01	2.12E-01	1.24E-02	4.60E-05	3.39E+00	2.78E-02	2.11E-02	9.91E-03	9.74E-03	2.11E+01
16	4WBRG2	11.55 charge	4	28.1	7.20E+01	2.51E-01	2.99E-04	5.91E+01	2.75E-01	1.53E+00	0.00E+00	0.00E+00	7.65E-01	2.66E+00	1.04E+01	9.97E-02	3.73E-05	6.58E-03	3.16E-05	9.46E-02	6.48E-02	1.97E-02	3.15E-05	1.61E+01
17	5WBR2	11.52 charge	4	30.4	1.06E+02	3.47E-01	2.99E-04	1.80E+01	3.90E-01	1.61E+00	0.00E+00	3.26E+00	0.00E+00	0.00E+00	2.24E+01	2.35E-01	5.35E-03	4.60E-05	4.89E-01	3.90E-03	9.88E-03	7.87E-03	1.63E-02	2.07E+01
18	5WBRA2	11.23 charge	4	30.2	9.75E+01	2.80E+00	1.05E-01	1.60E+01	4.32E-01	1.78E+00	0.00E+00	3.28E+00	7.79E-01	0.00E+00	2.16E+01	1.81E-01	4.23E-02	1.70E-02	1.93E+01	9.74E-03	1.22E-01	1.99E-02	1.15E-02	6.74E+00
19	5WBRS2	11.32 charge	4	30.9	1.13E+02	2.91E-01	4.36E-02	1.46E+01	4.90E-01	1.82E+00	0.00E+00	3.39E+00	7.77E-01	0.00E+00	2.68E+01	1.51E-01	1.46E-02	4.60E-05	6.75E+00	4.46E-03	2.07E-02	1.11E-02	8.85E-03	2.53E+00
20	5WBRG2	11.47 charge	4	30.3	5.70E+01	2.18E-01	2.99E-04	7.43E+01	4.99E-01	1.47E+00	0.00E+00	0.00E+00	7.95E-01	3.94E+00	1.31E+01	7.38E-02	3.73E-05	4.60E-05	3.16E-05	4.84E-03	7.88E-03	1.51E-02	3.15E-05	6.90E-01

```
EQUILIBRIUM_PHASES 1-20
CO2(g) -1.5 10
END
RUN_CELLS
-cells 1-20
```

Appendix 18. PHREEQC input file code for Simulation 7 (llnl.dat).

```
USER_PUNCH 1
headings  EC_(uS/cm) TDS_g/kg-solution alk_mg/L
start
10 PUNCH Description
25 PUNCH SC
32 PUNCH (RHO * SOLN_VOL - TOT("water")) * 1000 / (RHO * SOLN_VOL)
40 PUNCH alk * ((50.05) / 1000)
end
SELECTED_OUTPUT 1
file simulation7allowing_precipitation_secondary_minerals_in_atm_CO2.txt
charge_balance
ionic_strength
temp
percent_error
alkalinity
totals      Na          K           Mg    Ca          F           Cl          S(+6)       Br          N(+5)       P(5)        Al          V           Cr          Mn          Fe          Cu          Zn          Ga          As          Si
-molalities OH- HCO3- CO3-2 # add here other aqueous species of interest
-saturation_indices Fe(OH)2 Fe(OH)3 Gibbsite Goethite Pyrolusite Kaolinite Diaspore Magnetite Boehmite Cuprite CO2(g)
-equilibrium_phases Fe(OH)3
equilibrium_phases Gibbsite
equilibrium_phases Goethite
equilibrium_phases Pyrolusite
equilibrium_phases Kaolinite
equilibrium_phases Diaspore
equilibrium_phases Magnetite
equilibrium_phases Boehmite
equilibrium_phases Cuprite
equilibrium_phases Calcite
equilibrium_phases Monohydrocalcite
equilibrium_phases Dolomite
equilibrium_phases Magnesite
equilibrium_phases Aragonite
equilibrium_phases Dawsonite
equilibrium_phases Hydrozincite
equilibrium_phases Rhodochrosite
equilibrium_phases Siderite
END
```

SOLUTION_SPREAD

units mg/l

Number	Description	pH	pe	Temp	Na	K	Mg	Ca	F	Cl	S(+6)	Br	N(+5)	P(5)	Al	V	Cr	Mn	Fe	Cu	Zn	Ga	As	Si
1	1WBR1	11.98 charge	4	25.6	4.47E+02	1.02E+00	2.99E-04	7.26E+01	1.18E+00	3.26E+00	0.00E+00	0.00E+00	7.15E-01	0.00E+00	1.35E+02	5.04E-01	5.78E-02	6.18E-03	3.16E-05	1.26E-01	7.54E-02	1.85E-01	1.19E-02	2.13E-01
2	1WBRA2	11.76 charge	4	25.6	4.31E+02	3.91E+00	2.99E-04	5.96E+01	5.42E-01	9.86E+00	0.00E+00	0.00E+00	7.42E-01	0.00E+00	1.01E+02	8.03E-01	8.43E-02	4.60E-05	7.71E-01	3.65E-02	1.11E-02	1.55E-01	3.15E-02	1.26E+01
3	1WBRS1	11.93 charge	4	29.3	4.48E+02	9.76E-01	2.99E-04	5.68E+01	1.49E+00	3.11E+00	0.00E+00	0.00E+00	3.20E+00	0.00E+00	1.30E+02	8.85E-01	4.98E-02	4.60E-05	2.60E-02	6.33E-03	9.08E-03	1.93E-01	3.11E-02	1.69E+01
4	1WBRG2	10.92 charge	4	30.2	7.32E+02	1.53E+00	3.78E-02	5.09E+02	4.67E-01	4.19E+00	7.59E+00	0.00E+00	7.13E-01	0.00E+00	2.31E-01	1.40E-01	4.52E-02	4.60E-05	2.47E-01	2.25E-02	1.79E-02	2.14E-02	3.15E-05	1.05E+00
5	2WBR1	11.82 charge	4	29.8	2.41E+02	5.53E-01	2.99E-04	3.65E+01	6.39E-01	2.06E+00	0.00E+00	0.00E+00	7.03E-01	0.00E+00	6.29E+01	3.54E-01	2.39E-02	4.60E-05	3.16E-05	4.63E-03	9.59E-03	5.92E-02	9.29E-03	2.00E+00
6	2WBRA1	11.54 charge	4	30.1	2.70E+02	2.43E+00	2.99E-04	4.44E+01	3.15E+00	2.97E+00	0.00E+00	3.37E+00	7.44E-01	0.00E+00	6.66E+01	5.57E-01	4.85E-02	6.02E-03	2.29E+00	9.68E-02	5.03E-02	6.95E-02	2.42E-02	8.96E+00
7	2WBRS1	11.76 charge	4	30.1	2.22E+02	6.03E-01	3.07E-02	4.07E+01	6.61E-01	2.21E+00	0.00E+00	0.00E+00	7.06E-01	0.00E+00	5.00E+01	5.88E-01	1.41E-02	4.60E-05	8.93E-01	4.00E-03	6.70E-03	4.20E-02	2.75E-02	1.08E+01
8	2WBRG1	10.94 charge	4	29.6	2.86E+02	6.87E-01	3.60E-02	4.98E+02	5.38E-01	2.06E+00	5.15E+00	0.00E+00	7.05E-01	0.00E+00	8.08E-02	1.40E-01	1.16E-02	4.60E-05	2.62E-01	6.77E-03	1.59E-02	1.26E-02	3.15E-05	1.03E+01
9	3WBR2	11.69 charge	4	30.2	1.56E+02	4.37E-01	2.99E-04	3.87E+01	3.71E-01	1.77E+00	0.00E+00	0.00E+00	7.68E-01	0.00E+00	3.40E+01	3.29E-01	2.51E-02	6.99E-03	6.82E-02	1.29E-01	7.04E-02	1.84E-02	3.15E-05	1.15E+01
10	3WBRA2	11.33 charge	4	29.6	1.67E+02	1.43E+00	4.05E-02	3.94E+01	4.71E-01	2.15E+00	0.00E+00	3.51E+00	9.94E-01	0.00E+00	3.63E+01	3.90E-01	4.03E-02	6.62E-03	1.00E+01	1.03E-02	2.07E-02	3.03E-02	1.75E-02	1.23E+01
11	3WBRS2	11.61 charge	4	31.4	1.57E+02	4.93E-01	5.96E-02	4.25E+01	3.54E-01	2.56E+00	0.00E+00	0.00E+00	7.92E-01	0.00E+00	3.71E+01	3.46E-01	2.25E-02	4.60E-05	3.43E+00	7.80E-03	1.50E-02	1.90E-02	1.69E-02	1.51E-01
12	3WBRG3	11.41 charge	4	29.7	1.12E+02	3.46E-01	2.99E-04	9.96E+01	4.34E-01	9.53E+00	5.07E-01	0.00E+00	8.02E-01	1.71E+00	4.30E+00	1.30E-01	4.96E-03	4.60E-05	4.37E-02	4.81E-03	1.23E-02	2.32E-02	3.15E-05	2.24E+01
13	4WBR2	11.60 charge	4	29.9	1.21E+02	3.83E-01	2.99E-04	2.83E+01	3.40E-01	1.81E+00	0.00E+00	0.00E+00	7.68E-01	0.00E+00	2.53E+01	2.74E-01	6.60E-03	4.82E-03	1.47E-01	9.54E-02	5.28E-02	1.03E-02	9.15E-03	2.50E+01
14	4WBRA2	11.29 charge	4	29.3	1.16E+02	1.09E+00	1.65E-01	1.58E+01	3.90E-01	2.05E+00	0.00E+00	3.44E+00	7.98E-01	0.00E+00	2.54E+01	2.49E-01	4.26E-02	1.71E-02	1.76E+01	3.14E-02	4.21E-02	2.21E-02	1.74E-02	3.29E+00
15	4WBRS1	11.35 charge	4	30.7	1.23E+02	3.78E-01	2.99E-04	2.66E+01	2.96E-01	1.81E+00	0.00E+00	0.00E+00	7.70E-01	0.00E+00	2.60E+01	2.12E-01	1.24E-02	4.60E-05	3.39E+00	2.78E-02	2.11E-02	9.91E-03	9.74E-03	2.11E+01
16	4WBRG2	11.55 charge	4	28.1	7.20E+01	2.51E-01	2.99E-04	5.91E+01	2.75E-01	1.53E+00	0.00E+00	0.00E+00	7.65E-01	2.66E+00	1.04E+01	9.97E-02	3.73E-05	6.58E-03	3.16E-05	9.46E-02	6.48E-02	1.97E-02	3.15E-05	1.61E+01
17	5WBR2	11.52 charge	4	30.4	1.06E+02	3.47E-01	2.99E-04	1.80E+01	3.90E-01	1.61E+00	0.00E+00	3.26E+00	0.00E+00	0.00E+00	2.24E+01	2.35E-01	5.35E-03	4.60E-05	4.89E-01	3.90E-03	9.88E-03	7.87E-03	1.63E-02	2.07E+01
18	5WBRA2	11.23 charge	4	30.2	9.75E+01	2.80E+00	1.05E-01	1.60E+01	4.32E-01	1.78E+00	0.00E+00	3.28E+00	7.79E-01	0.00E+00	2.16E+01	1.81E-01	4.23E-02	1.70E-02	1.93E+01	9.74E-03	1.22E-01	1.99E-02	1.15E-02	6.74E+00
19	5WBRS2	11.32 charge	4	30.9	1.13E+02	2.91E-01	4.36E-02	1.46E+01	4.90E-01	1.82E+00	0.00E+00	3.39E+00	7.77E-01	0.00E+00	2.68E+01	1.51E-01	1.46E-02	4.60E-05	6.75E+00	4.46E-03	2.07E-02	1.11E-02	8.85E-03	2.53E+00
20	5WBRG2	11.47 charge	4	30.3	5.70E+01	2.18E-01	2.99E-04	7.43E+01	4.99E-01	1.47E+00	0.00E+00	0.00E+00	7.95E-01	3.94E+00	1.31E+01	7.38E-02	3.73E-05	4.60E-05	3.16E-05	4.84E-03	7.88E-03	1.51E-02	3.15E-05	6.90E-01

EQUILIBRIUM_PHASES 1-20

CO2(g) -3.5 10

Fe(OH)3 0.0 0.0

Gibbsite 0.0 0.0

Goethite 0.0 0.0

Pyrolusite 0.0 0.0

Kaolinite 0.0 0.0

Diaspore 0.0 0.0

Magnetite 0.0 0.0

Boehmite 0.0 0.0

Cuprite 0.0 0.0

Calcite 0.0 0.0

Monohydrocalcite 0.0 0.0

Dolomite 0.0 0.0

Magnesite 0.0 0.0

Aragonite 0.0 0.0

Dawsonite 0.0 0.0

Hydrozincite 0.0 0.0

Rhodochrosite 0.0 0.0

Siderite 0.0 0.0

END

RUN_CELLS

-cells 1-20

Appendix 19. PHREEQC input file code for Simulation 8 (llnl.dat).

```
USER_PUNCH 1
headings  EC_(uS/cm) TDS_g/kg-solution alk_mg/L
start
10 PUNCH Description
25 PUNCH SC
32 PUNCH (RHO * SOLN_VOL - TOT("water")) * 1000 / (RHO * SOLN_VOL)
40 PUNCH alk * ((50.05) / 1000)
end
SELECTED_OUTPUT 1
file simulation8allowing_precipitationnotcarbonates_in_soil_CO2.txt
charge_balance
ionic_strength
temp
percent_error
alkalinity
totals      Na          K           Mg          Ca          F           Cl          S(+6)       Br          N(+5)       P(5)        Al          V           Cr          Mn          Fe          Cu          Zn          Ga          As          Si
-molalities OH- HCO3- CO3-2 # add here other aqueous species of interest
-saturation_indices Fe(OH)2 Fe(OH)3 Gibbsite Goethite Pyrolusite Kaolinite Diaspore Magnetite Boehmite Cuprite CO2(g)
equilibrium_phases Fe(OH)3
equilibrium_phases Gibbsite
equilibrium_phases Goethite
equilibrium_phases Pyrolusite
equilibrium_phases Kaolinite
equilibrium_phases Diaspore
equilibrium_phases Magnetite
equilibrium_phases Boehmite
equilibrium_phases Cuprite
equilibrium_phases Calcite
equilibrium_phases Monohydrocalcite
equilibrium_phases Dolomite
equilibrium_phases Magnesite
equilibrium_phases Aragonite
equilibrium_phases Dawsonite
equilibrium_phases Hydrozincite
equilibrium_phases Rhodochrosite
equilibrium_phases Siderite
END
```

SOLUTION_SPREAD
units mg/l

Number	Description	pH	pe	Temp	Na	K	Mg	Ca	F	Cl	S(+6)	Br	N(+5)	P(5)	Al	V	Cr	Mn	Fe	Cu	Zn	Ga	As	Si
1	1WBR1	11.98 charge	4	25.6	4.47E+02	1.02E+00	2.99E-04	7.26E+01	1.18E+00	3.26E+00	0.00E+00	0.00E+00	7.15E-01	0.00E+00	1.35E+02	5.04E-01	5.78E-02	6.18E-03	3.16E-05	1.26E-01	7.54E-02	1.85E-01	1.19E-02	2.13E-01
2	1WBRA2	11.76 charge	4	25.6	4.31E+02	3.91E+00	2.99E-04	5.96E+01	5.42E-01	9.86E+00	0.00E+00	0.00E+00	7.42E-01	0.00E+00	1.01E+02	8.03E-01	8.43E-02	4.60E-05	7.71E-01	3.65E-02	1.11E-02	1.55E-01	3.15E-02	1.26E+01
3	1WBRS1	11.93 charge	4	29.3	4.48E+02	9.76E-01	2.99E-04	5.68E+01	1.49E+00	3.11E+00	0.00E+00	0.00E+00	3.20E+00	0.00E+00	1.30E+02	8.85E-01	4.98E-02	4.60E-05	2.60E-02	6.33E-03	9.08E-03	1.93E-01	3.11E-02	1.69E+01
4	1WBRG2	10.92 charge	4	30.2	7.32E+02	1.53E+00	3.78E-02	5.09E+02	4.67E-01	4.19E+00	7.59E+00	0.00E+00	7.13E-01	0.00E+00	2.31E-01	1.40E-01	4.52E-02	4.60E-05	2.47E-01	2.25E-02	1.79E-02	2.14E-02	3.15E-05	1.05E+00
5	2WBR1	11.82 charge	4	29.8	2.41E+02	5.53E-01	2.99E-04	3.65E+01	6.39E-01	2.06E+00	0.00E+00	0.00E+00	7.03E-01	0.00E+00	6.29E+01	3.54E-01	2.39E-02	4.60E-05	3.16E-05	4.63E-03	9.59E-03	5.92E-02	9.29E-03	2.00E+00
6	2WBRA1	11.54 charge	4	30.1	2.70E+02	2.43E+00	2.99E-04	4.44E+01	3.15E+00	2.97E+00	0.00E+00	3.37E+00	7.44E-01	0.00E+00	6.66E+01	5.57E-01	4.85E-02	6.02E-03	2.29E+00	9.68E-02	5.03E-02	6.95E-02	2.42E-02	8.96E+00
7	2WBRS1	11.76 charge	4	30.1	2.22E+02	6.03E-01	3.07E-02	4.07E+01	6.61E-01	2.21E+00	0.00E+00	0.00E+00	7.06E-01	0.00E+00	5.00E+01	5.88E-01	1.41E-02	4.60E-05	8.93E-01	4.00E-03	6.70E-03	4.20E-02	2.75E-02	1.08E+01
8	2WBRG1	10.94 charge	4	29.6	2.86E+02	6.87E-01	3.60E-02	4.98E+02	5.38E-01	2.06E+00	5.15E+00	0.00E+00	7.05E-01	0.00E+00	8.08E-02	1.40E-01	1.16E-02	4.60E-05	2.62E-01	6.77E-03	1.59E-02	1.26E-02	3.15E-05	1.03E+01
9	3WBR2	11.69 charge	4	30.2	1.56E+02	4.37E-01	2.99E-04	3.87E+01	3.71E-01	1.77E+00	0.00E+00	0.00E+00	7.68E-01	0.00E+00	3.40E+01	3.29E-01	2.51E-02	6.99E-03	6.82E-02	1.29E-01	7.04E-02	1.84E-02	3.15E-05	1.15E+01
10	3WBRA2	11.33 charge	4	29.6	1.67E+02	1.43E+00	4.05E-02	3.94E+01	4.71E-01	2.15E+00	0.00E+00	3.51E+00	9.94E-01	0.00E+00	3.63E+01	3.90E-01	4.03E-02	6.62E-03	1.00E+01	1.03E-02	2.07E-02	3.03E-02	1.75E-02	1.23E+01
11	3WBRS2	11.61 charge	4	31.4	1.57E+02	4.93E-01	5.96E-02	4.25E+01	3.54E-01	2.56E+00	0.00E+00	0.00E+00	7.92E-01	0.00E+00	3.71E+01	3.46E-01	2.25E-02	4.60E-05	3.43E+00	7.80E-03	1.50E-02	1.90E-02	1.69E-02	1.51E-01
12	3WBRG3	11.41 charge	4	29.7	1.12E+02	3.46E-01	2.99E-04	9.96E+01	4.34E-01	9.53E+00	5.07E-01	0.00E+00	8.02E-01	1.71E+00	4.30E+00	1.30E-01	4.96E-03	4.60E-05	4.37E-02	4.81E-03	1.23E-02	2.32E-02	3.15E-05	2.24E+01
13	4WBR2	11.60 charge	4	29.9	1.21E+02	3.83E-01	2.99E-04	2.83E+01	3.40E-01	1.81E+00	0.00E+00	0.00E+00	7.68E-01	0.00E+00	2.53E+01	2.74E-01	6.60E-03	4.82E-03	1.47E-01	9.54E-02	5.28E-02	1.03E-02	9.15E-03	2.50E+01
14	4WBRA2	11.29 charge	4	29.3	1.16E+02	1.09E+00	1.65E-01	1.58E+01	3.90E-01	2.05E+00	0.00E+00	3.44E+00	7.98E-01	0.00E+00	2.54E+01	2.49E-01	4.26E-02	1.71E-02	1.76E+01	3.14E-02	4.21E-02	2.21E-02	1.74E-02	3.29E+00
15	4WBRS1	11.35 charge	4	30.7	1.23E+02	3.78E-01	2.99E-04	2.66E+01	2.96E-01	1.81E+00	0.00E+00	0.00E+00	7.70E-01	0.00E+00	2.60E+01	2.12E-01	1.24E-02	4.60E-05	3.39E+00	2.78E-02	2.11E-02	9.91E-03	9.74E-03	2.11E+01
16	4WBRG2	11.55 charge	4	28.1	7.20E+01	2.51E-01	2.99E-04	5.91E+01	2.75E-01	1.53E+00	0.00E+00	0.00E+00	7.65E-01	2.66E+00	1.04E+01	9.97E-02	3.73E-05	6.58E-03	3.16E-05	9.46E-02	6.48E-02	1.97E-02	3.15E-05	1.61E+01
17	5WBR2	11.52 charge	4	30.4	1.06E+02	3.47E-01	2.99E-04	1.80E+01	3.90E-01	1.61E+00	0.00E+00	3.26E+00	0.00E+00	0.00E+00	2.24E+01	2.35E-01	5.35E-03	4.60E-05	4.89E-01	3.90E-03	9.88E-03	7.87E-03	1.63E-02	2.07E+01
18	5WBRA2	11.23 charge	4	30.2	9.75E+01	2.80E+00	1.05E-01	1.60E+01	4.32E-01	1.78E+00	0.00E+00	3.28E+00	7.79E-01	0.00E+00	2.16E+01	1.81E-01	4.23E-02	1.70E-02	1.93E+01	9.74E-03	1.22E-01	1.99E-02	1.15E-02	6.74E+00
19	5WBRS2	11.32 charge	4	30.9	1.13E+02	2.91E-01	4.36E-02	1.46E+01	4.90E-01	1.82E+00	0.00E+00	3.39E+00	7.77E-01	0.00E+00	2.68E+01	1.51E-01	1.46E-02	4.60E-05	6.75E+00	4.46E-03	2.07E-02	1.11E-02	8.85E-03	2.53E+00
20	5WBRG2	11.47 charge	4	30.3	5.70E+01	2.18E-01	2.99E-04	7.43E+01	4.99E-01	1.47E+00	0.00E+00	0.00E+00	7.95E-01	3.94E+00	1.31E+01	7.38E-02	3.73E-05	4.60E-05	3.16E-05	4.84E-03	7.88E-03	1.51E-02	3.15E-05	6.90E-01

EQUILIBRIUM_PHASES 1-20
CO2(g) -1.5 10
Fe(OH)3 0.0 0.0
Gibbsite 0.0 0.0
Goethite 0.0 0.0
Pyrolusite 0.0 0.0
Kaolinite 0.0 0.0
Diaspore 0.0 0.0
Magnetite 0.0 0.0
Boehmite 0.0 0.0
Cuprite 0.0 0.0
Calcite 0.0 0.0
Monohydrocalcite 0.0 0.0
Dolomite 0.0 0.0
Magnesite 0.0 0.0
Aragonite 0.0 0.0
Dawsonite 0.0 0.0
Hydrozincite 0.0 0.0
Rhodochrosite 0.0 0.0
Siderite 0.0 0.0
END
RUN_CELLS
-cells 1-20

Additional information about this project can be found at:

https://github.com/jorgeft/Bauxite-Residue-Disposal-and-the-Envrionmental-Benefit-of-Acai-Soil-and-Gypsum-Amendments